Supplementary Information

Page Number	Figure
S6	The proportion of global plant species that are under threat of extinction
S6	Primary threats to plant life
S7	Selected commercially available drugs of plant origin
S8	Structures of selected anti-HCV and anti PTP1B active compounds
S9	Prevalence of chronic HCV infection from WHO International Travel Health (top) and cases of DM in 2000 and projections for 2030 (Millions)
S10	Selected species from the family Asteraceae
S11-S12	Isolation and purification of rhododendrosaponins **I-III**
S13	MS chromatogram of rhododendrosaponin **I**
S14-S15	Identification
S16-S17	^{1}H NMR of rhododendrosaponin **I**
S18	^{13}C NMR of rhododendrosaponin **I**
S19	135° DEPT of rhododendrosaponin **I**
S20	HSQC spectrum of rhododendrosaponin **I**

Supplementary Information

Page Number	Figure
S21	MS chromatogram of rhododendrosaponin **II**
S22	^{1}H NMR of rhododendrosaponin **II**
S23	^{13}C NMR of rhododendrosaponin **II**
S24	MS chromatogram of rhododendrosaponin **III**
S25	^{1}H NMR of rhododendrosaponin **III**
S26	^{13}C NMR of rhododendrosaponin **III**
S27	NOESY spectrum of rhododendrosaponin **III**
S28	Selected HMBC correlations of the aglycone triterpene
S29	GC/MS detection of 3-hydroxybutanoate in rhododendrosaponin **III**
S30	HMBC correlations of 3-hydroxybutanoate dimer in rhododendrosaponin **III**
S31	Identification and determination of the carbohydrate units
S32	The total carbohydrate content of the major glycoside rhododendrosaponin **III**
S33	Glycosyl linkage analysis
S34	NSI-MS^{n} fragmentation of rhododendrosaponin **III**
S35	The absolute configuration determination of the carbohydrate units

Supplementary Information

Page Number	Figure
S36	An investigational method for carbohydrate analysis
S37	L- and D- glucose, xylose, and fucose standards by the carbohydrate analysis method
S38	Carbohydrate analysis for rhododendrosaponin **III**
S39	Overlay of the carbohydrate analysis chromatograms of rhododendrosaponins **I** and **III**
S40	Overlaying 2D NMR experiments
S41	Overlaid HSQC spectra of rhododendrosaponins **I** and **III**
S42	The expanded HSQC spectrum of rhododendrosaponin **I**
S43	The expanded HMBC spectrum of rhododendrosaponin **I**
S44	The expanded ROESY spectrum of rhododendrosaponin **I**
S45	135° DEPT spectrum of rhododendrosaponin **I** shows the presence of (-CHO) for the acyclic intermediate
S47	Overlaid HSQC spectra of rhododendrosaponins **II** and **III**
S48	The ^{13}C NMR spectrum of rhododendrosaponin **II**
S49	Expanded HMBC spectrum of rhododendrosaponin **II**

Supplementary Information

Page Number	Figure
S50	Co-injection of rhododendrosaponins **II** and **III** on 250 × 4.6 mm NH_2 column
S52	GC chromatograms of (R) and (S)-methyl 3-hydroxybutanoate.
S53	GC chromatograms of rhododendrosaponins **I-III** after methanolysis
S54	The proposed structures of rhododendrosaponins **I-III**
S56	The minimized 3D structure surface generated for rhododendrosaponin **III**
S58	Anti-HCV activity of rhododendrosaponins **I-III** in Huh-7 replicon cells
S60	LC- HRESIMS Spectrum of Compound **IV**
S61	^{1}H NMR Spectrum of Compound **IV** in Pyridine-d_5 (400 MHz)
S62	^{13}C NMR Spectrum of Compound **IV** in Pyridine-d_5 (100 MHz)
S63	COSY Spectrum of Compound **IV** in Pyridine-d_5 (400 MHz)
S64	HMQC Spectrum of Compound **IV** in Pyridine-d_5 (400 MHz)
S65	HMBC Spectrum of Compound **IV** in Pyridine-d_5 (400 MHz)
S66	LC- HRESIMS Spectrum of Compound **V**

Supplementary Information

Page Number	Figure
S67	^{1}H NMR Spectrum of Compound **V** in Methanol-d_4 (400 MHz)
S68	^{13}C NMR Spectrum of Compound **V** in Methanol-d_4 (100 MHz)
S69	COSY Spectrum of Compound **V** in Methanol-d_4 (400 MHz)
S70	HMQC Spectrum of Compound **V** in Methanol-d_4 (400 MHz)
S71	HMBC Spectrum of Compound **V** in Methanol-d_4 (400 MHz)
S72	The proposed structures of **IV** and **V**
S73	Docking scores of compounds **IV** and **V**
S73	The structures of legends **A**, **B**, and **C**
S74	Additional references

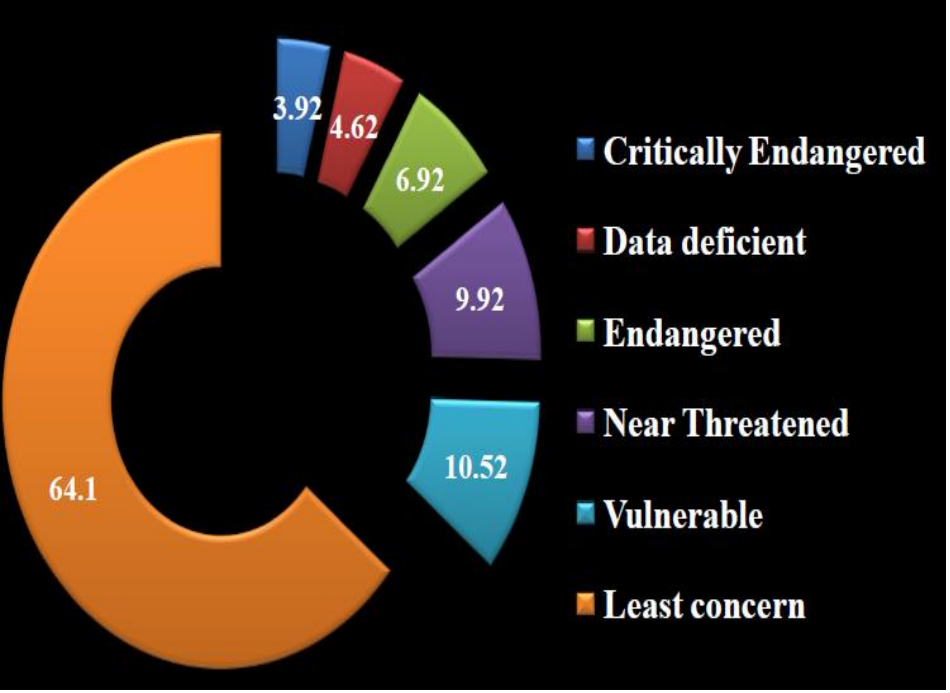

Supplementary Figure 1 | The proportion of global plant species that are under threat of extinction (data from Royal Botanic Gardens, Kew)

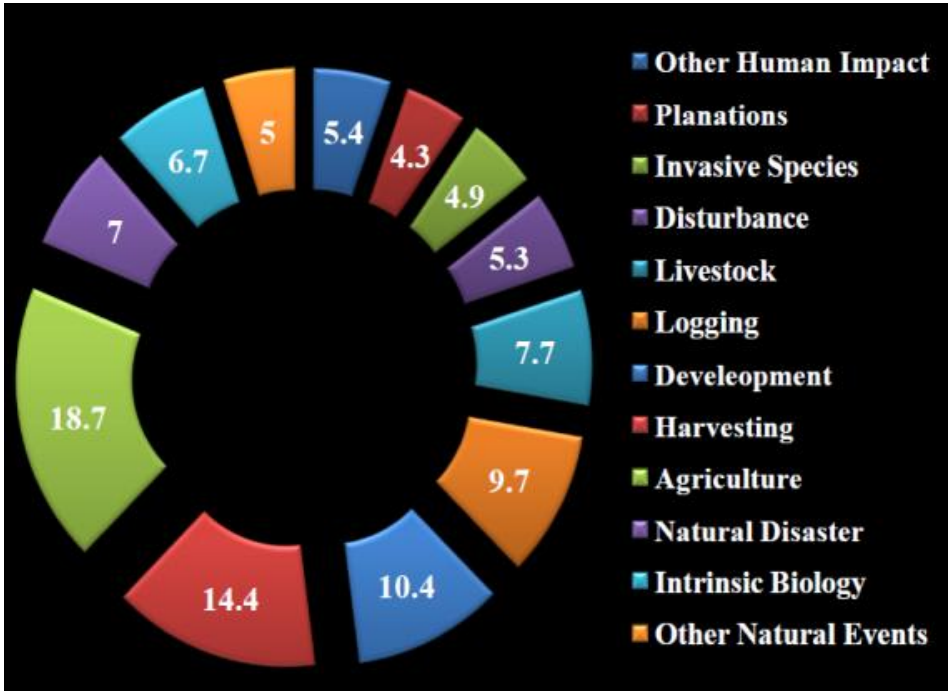

Supplementary Figure 2 | Primary threats to plant life (data from Royal Botanic Gardens, Kew)

- The Royal Botanic Gardens, founded in 1759, and declared a UNESCO World Heritage Site in 2003. The risk assessment, called the Sampled Red List Index for Plants, was conducted by plant scientists at the Royal Botanic Gardens, Kew, UK.

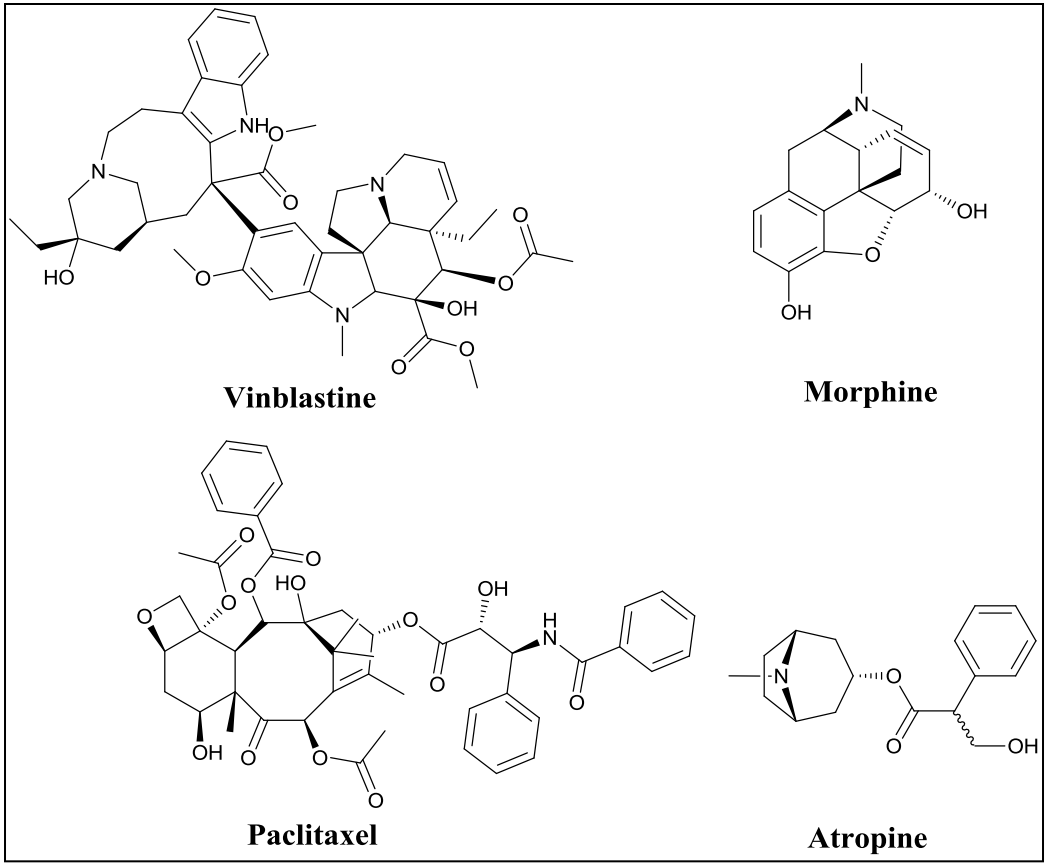

Supplementary Figure 3 | Selected commercially available drugs of plant origin

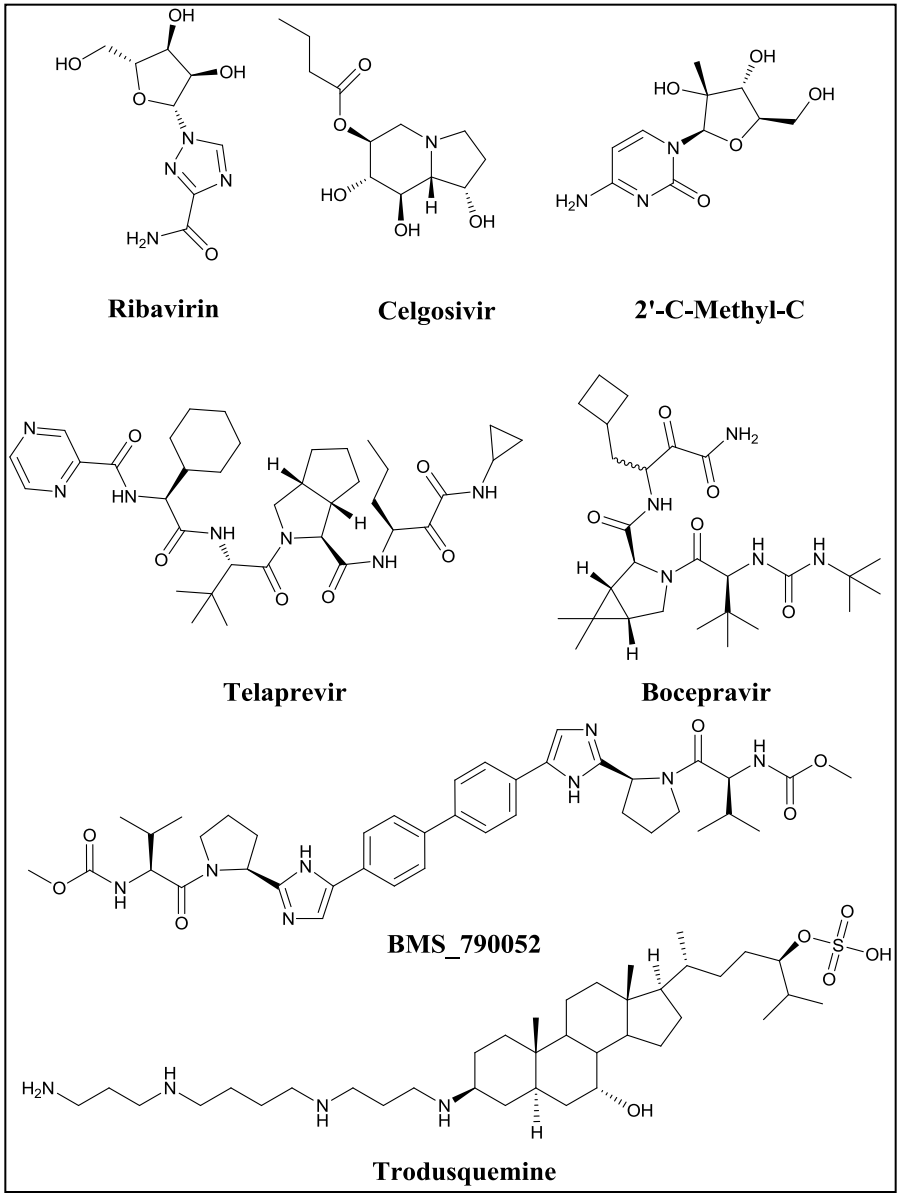

Supplementary Figure 4 | Structures of selected anti-HCV and anti PTP1B active compounds

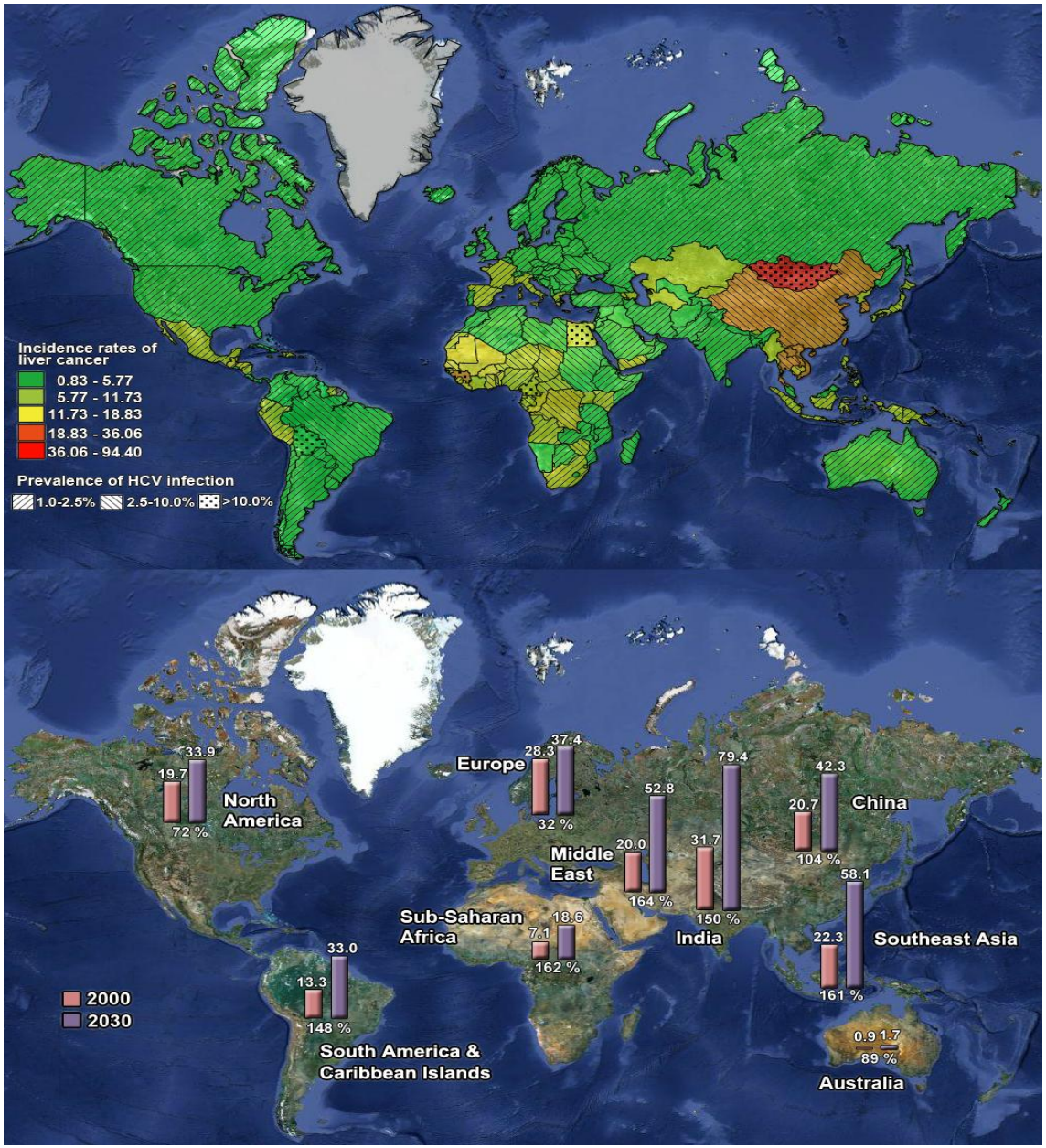

Supplementary Figure 5 | Estimated age-standardized incidence rate per 100,000 for liver cancer from GLOBOCAN 2008; prevalence of chronic HCV infection from WHO International Travel Health (top) and cases of DM in 2000 and projections for 2030 (Millions)

Supplementary Figure 6 | Selected species from the family Asteraceae; from the left above clockwise: *Echinacea purpurea, Kalimeris incise, Heliopsis helianthoides, and Liatris spicata*. (photo credit: M. A. Ibrahim)

Isolation

- The extraction started with a rapid solvent elution utilizing MeOH-DCM, where the active metabolites were extracted in DCM-MeOH (25:75), followed by HPLC on 250 × 21.2 mm C_{18} column with MeOH-H_2O, where the active material eluted off the column as a broad signal by the end of the elution. The material representing this broad signal was subjected to 250 × 21.2 mm NH_2 column with $CHCl_3$-MeOH to yield three UV inactive metabolites. The three resolved metabolites were further subjected to 250 × 4.6 mm NH_2 , and the co-injection of metabolites **2** and **3** on 250 × 4.6 mm NH_2 column was also completed.

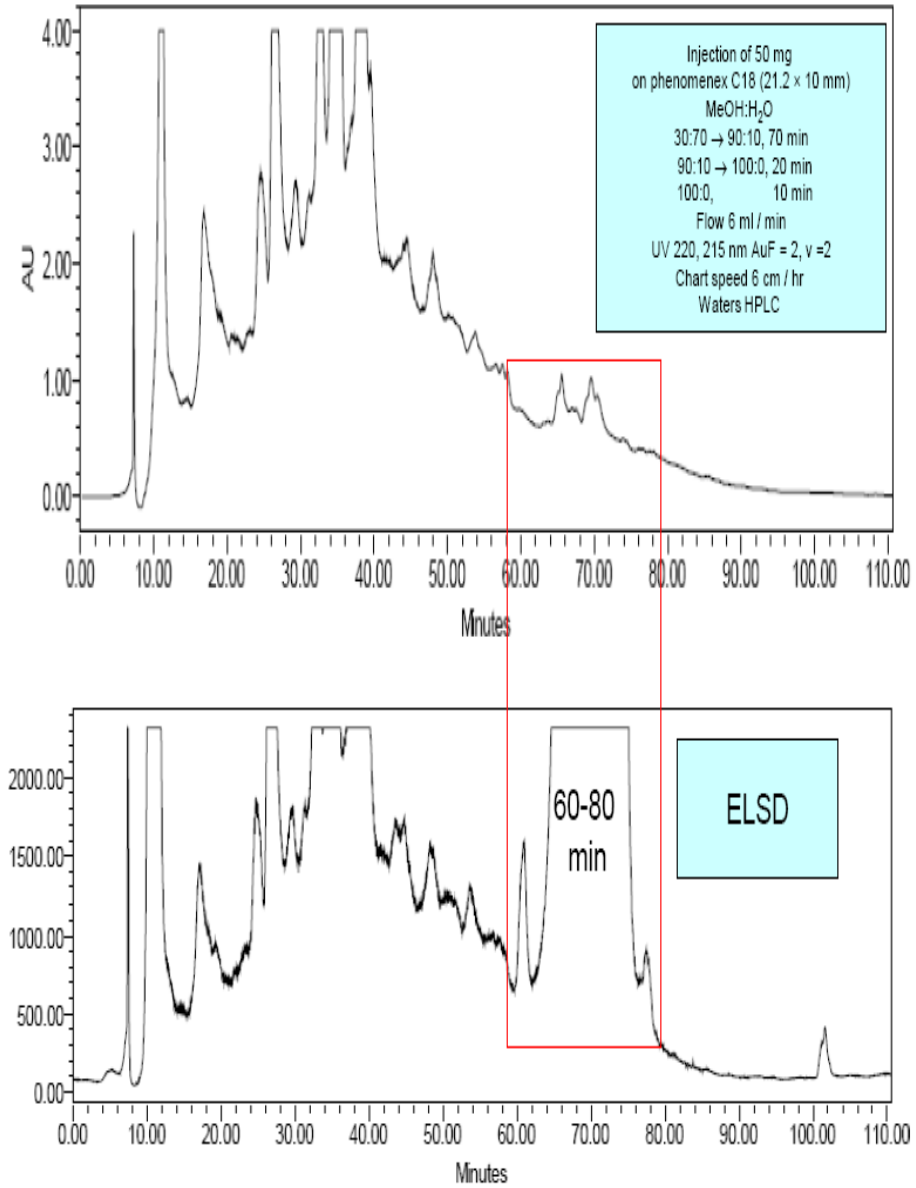

Supplementary Figure 7 | HPLC chromatogram for signal (DCM-MeOH); (25:75), on HPLC-C18 (21.2 × 250 mm)

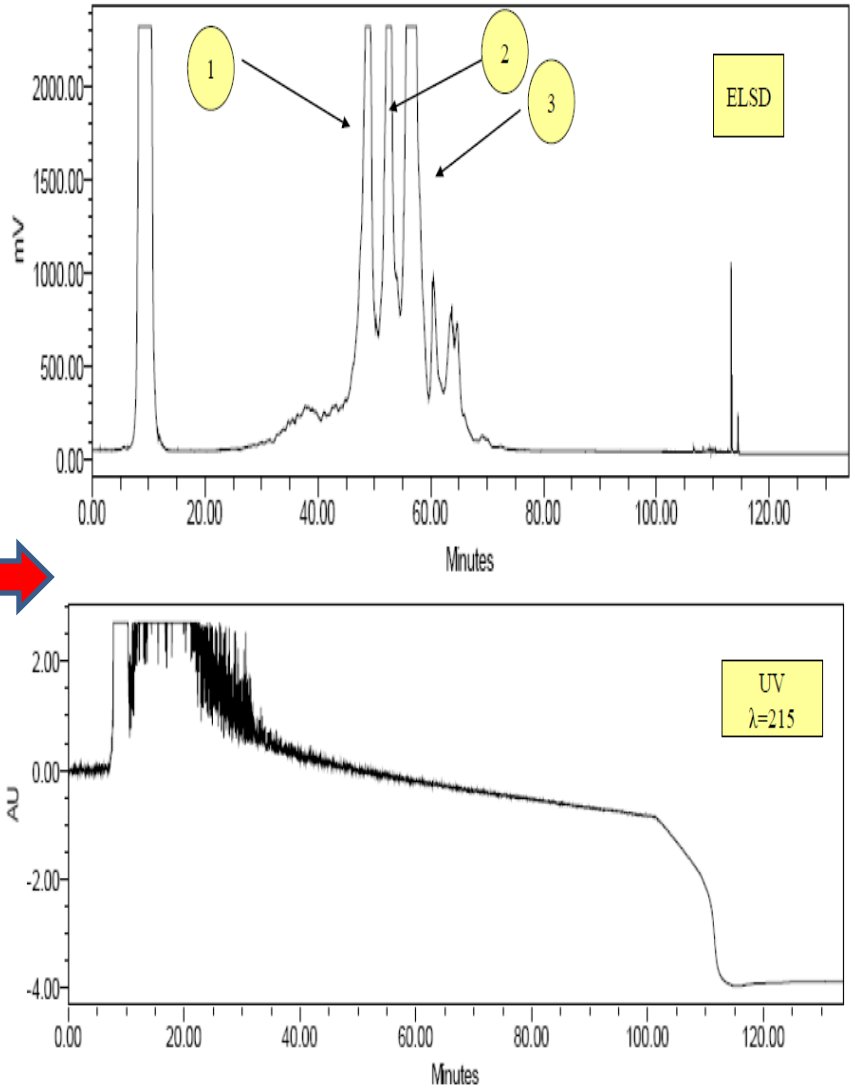

Supplementary Figure 8 | HPLC chromatogram of HPLC-C18 (21.2 × 250 mm), (signal 60-80 min) on HPLC-NH_2 (21.2 × 250 mm), signals 1-3 indicated the presence of the rhododendrosaponins I-III in similar order

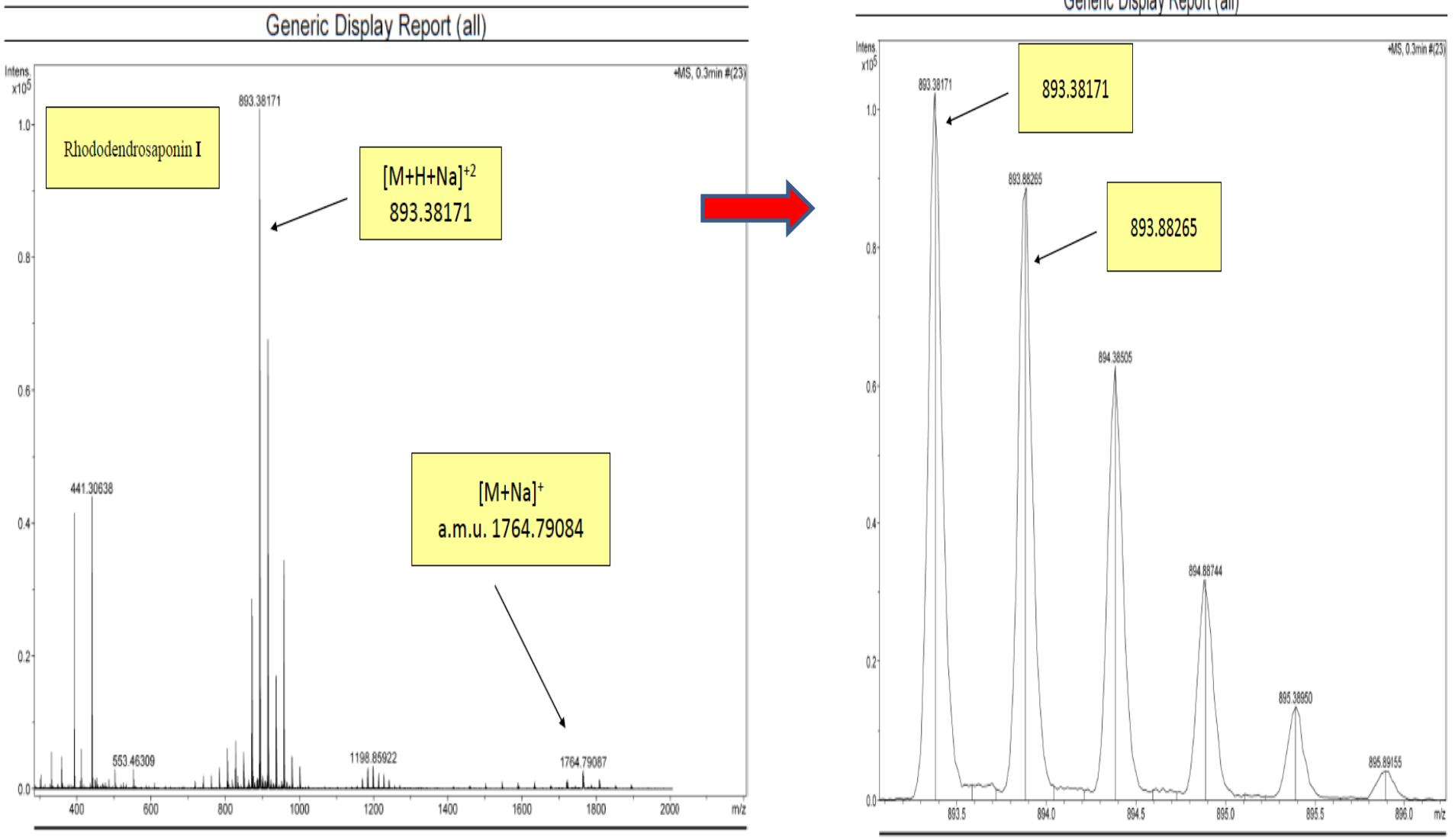

- Supplementary Figure 9 | MS chromatogram of rhododendrosaponin I

Identification

- The complete 1D and 2D NMR data sets of rhododendrosaponins **I-III** were gathered. Evaluation of ^{1}H and ^{13}C NMR data of the rhododendrosaponins **I-III**, permitted the validation of the basic skeletons of the oleanane-type triterpenes [polygalacic acid; (2β,3β,4α,16α)-2,3,16,23-tetrahydroxyolean-12-en-28-oic acid] with one characteristic double bond, where H-12 (5.34 Hz) shows an HMBC correlation to C-14 (40.9 Hz); H-23 shows HMBC correlations to C-3 (84.0 Hz), C-4 (43.1 Hz), C-5 (48.3 Hz) and C-24 (65.6 Hz);. H-25 (1.22 Hz) shows HMBC correlations to C-1 (44.4 Hz), C-5 (48.3 Hz), C-9 (48.2 Hz) and C-10 (37.6 Hz); H-26 (0.72 Hz) shows HMBC correlations to C-7 (33.8 Hz), C-8 (42.9 Hz), C-9 (48.2 Hz) and C-14 (40.9 Hz); H-27 (1.31 Hz) shows HMBC correlations to C-8 (42.9 Hz), C-13 (144.8 Hz), C-14 (40.9 Hz) and C-15 (36.4 Hz); H-30 (0.81 Hz) shows HMBC correlations to C-19 (48.2 Hz), C-21 (35.5 Hz) and C-29 (25.0 Hz).

- In addition mild hydrolysis using dioxane containing HCl followed by GC/MS analysis, showed the presence of 3-hydroxybutanoate, This was confirmed by HMBC correlations of the 3-hydroxybutanoate dimer, where H-2′ (2.83 Hz) shows HMBC correlations to C-1′ (171.5 Hz), C-3′ (68.8 Hz), and C-4′ (20.8 Hz), while H-2″ (2.52 Hz) shows HMBC correlations to C-1″ (172.6 Hz), C-3″ (65.6 Hz), and C-4″ (23.6 Hz).

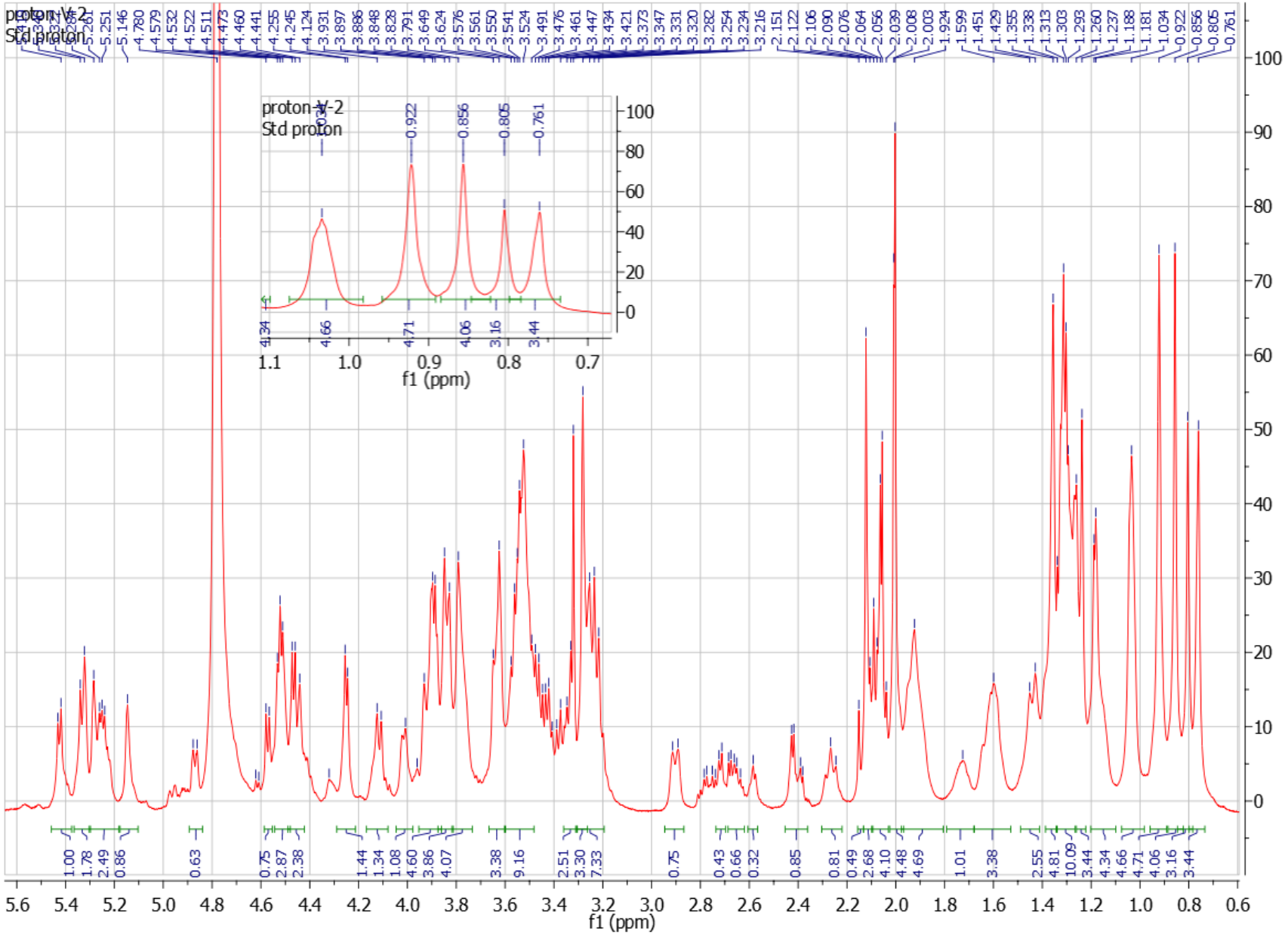

- Supplementary Figure 10 | ^{1}H NMR of rhododendrosaponin I

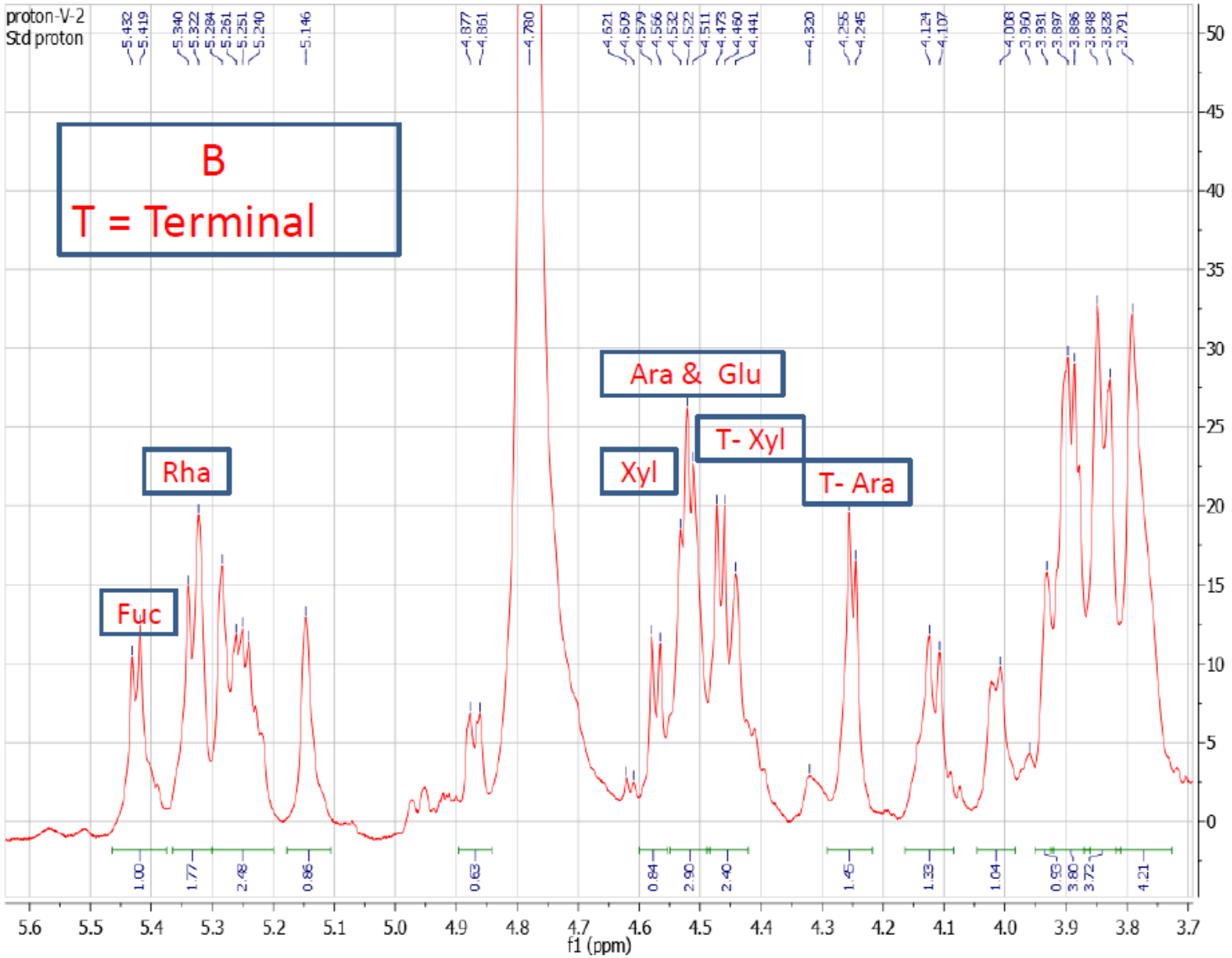

- Supplementary Figure 11 | ^{1}H NMR expansion of rhododendrosaponin I

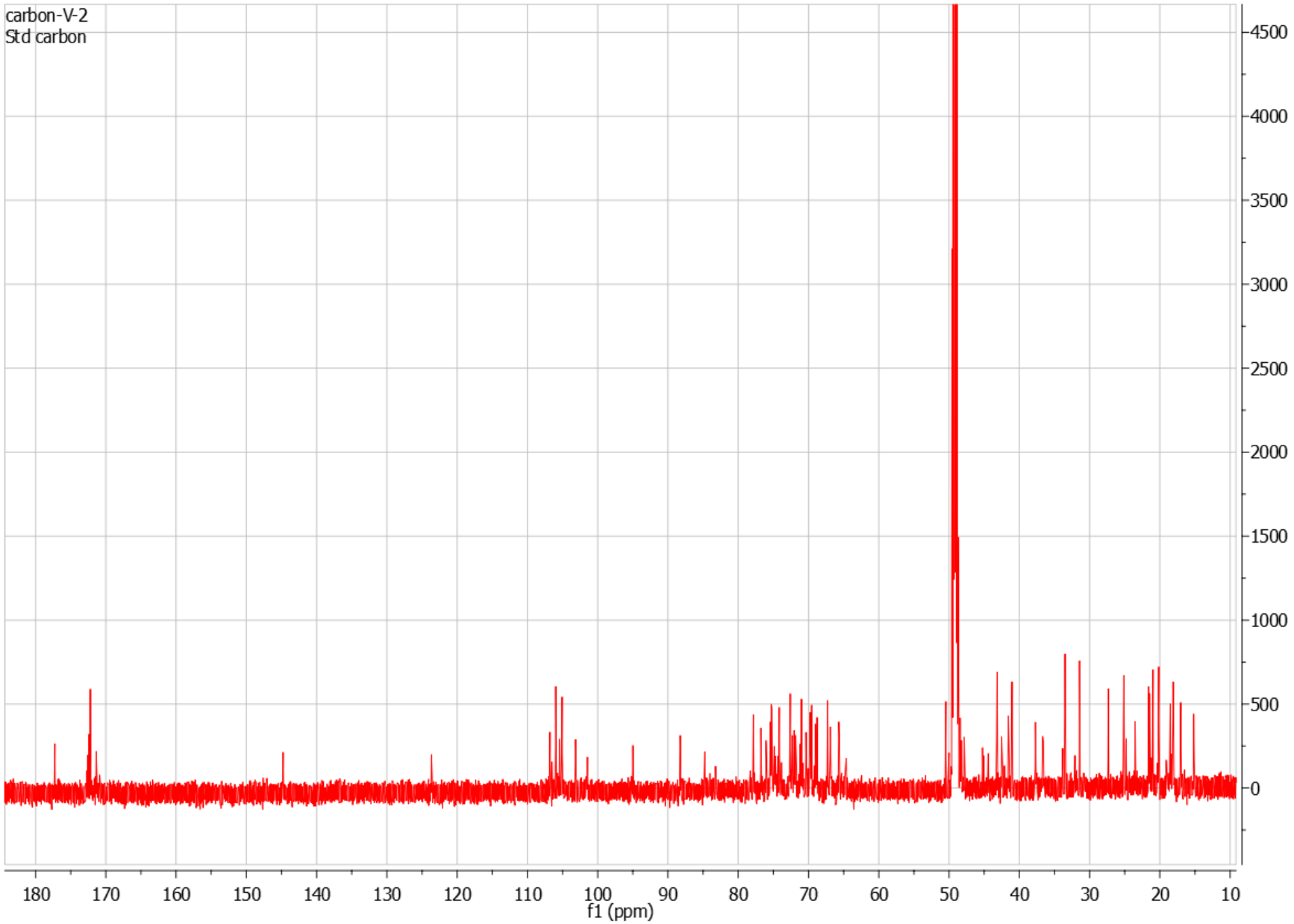

- Supplementary Figure 12 | ^{13}C NMR of rhododendrosaponin I

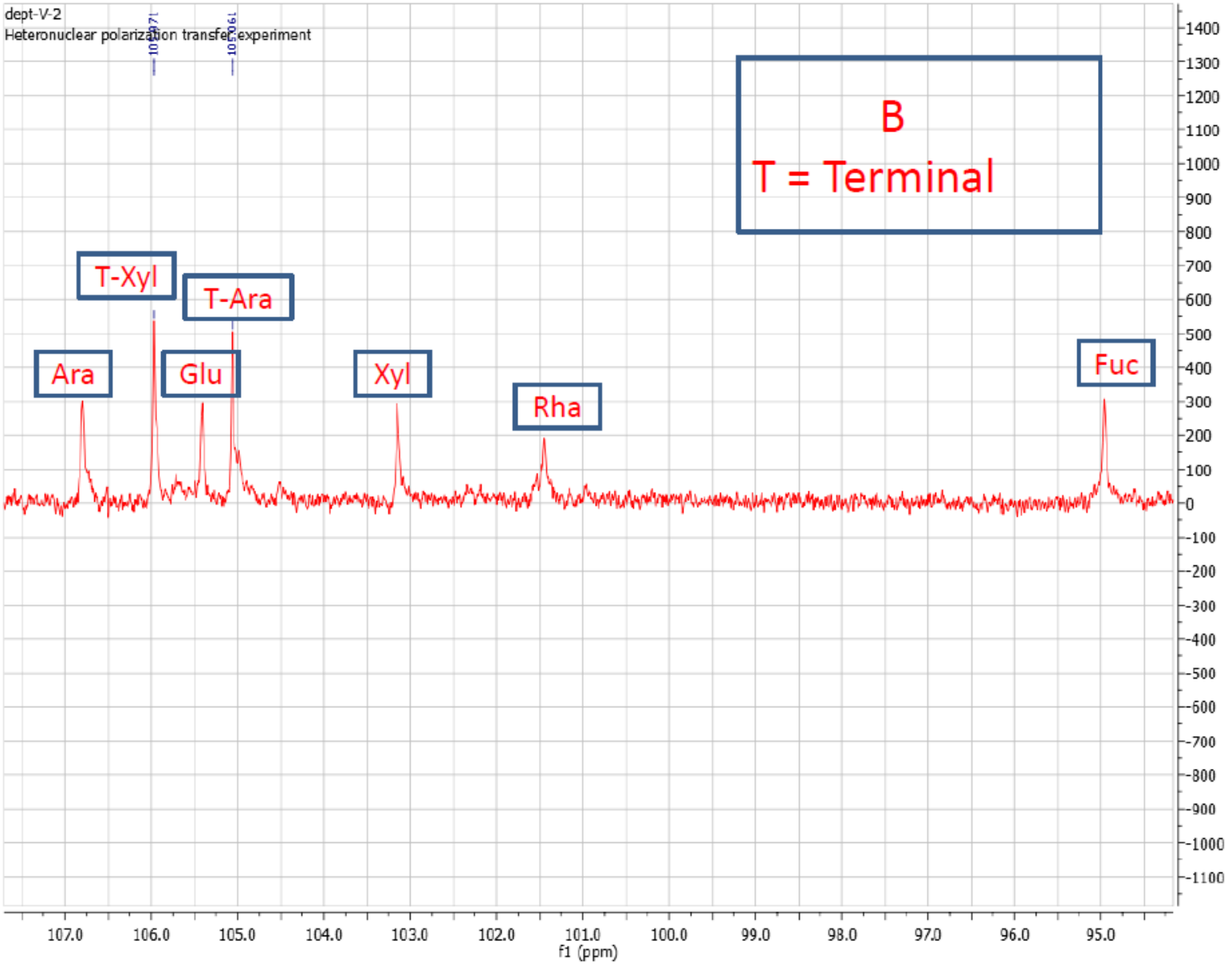

- Supplementary Figure 13 | 135° DEPT of rhododendrosaponin I (the downfield region)

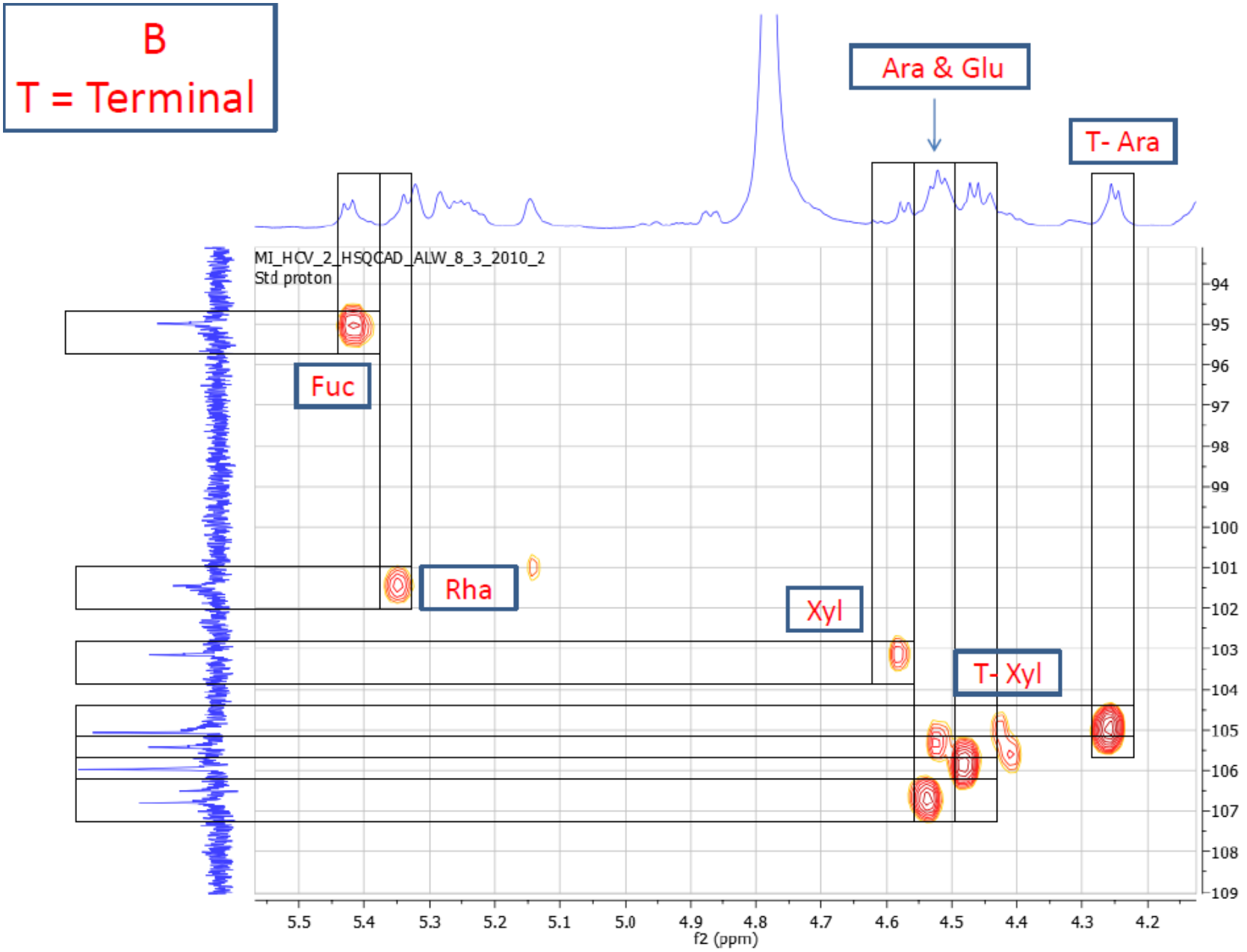

- Supplementary Figure 14 HSQC spectrum of rhododendrosaponin I in methanol-d_4 (600 MHz); (the downfield region)

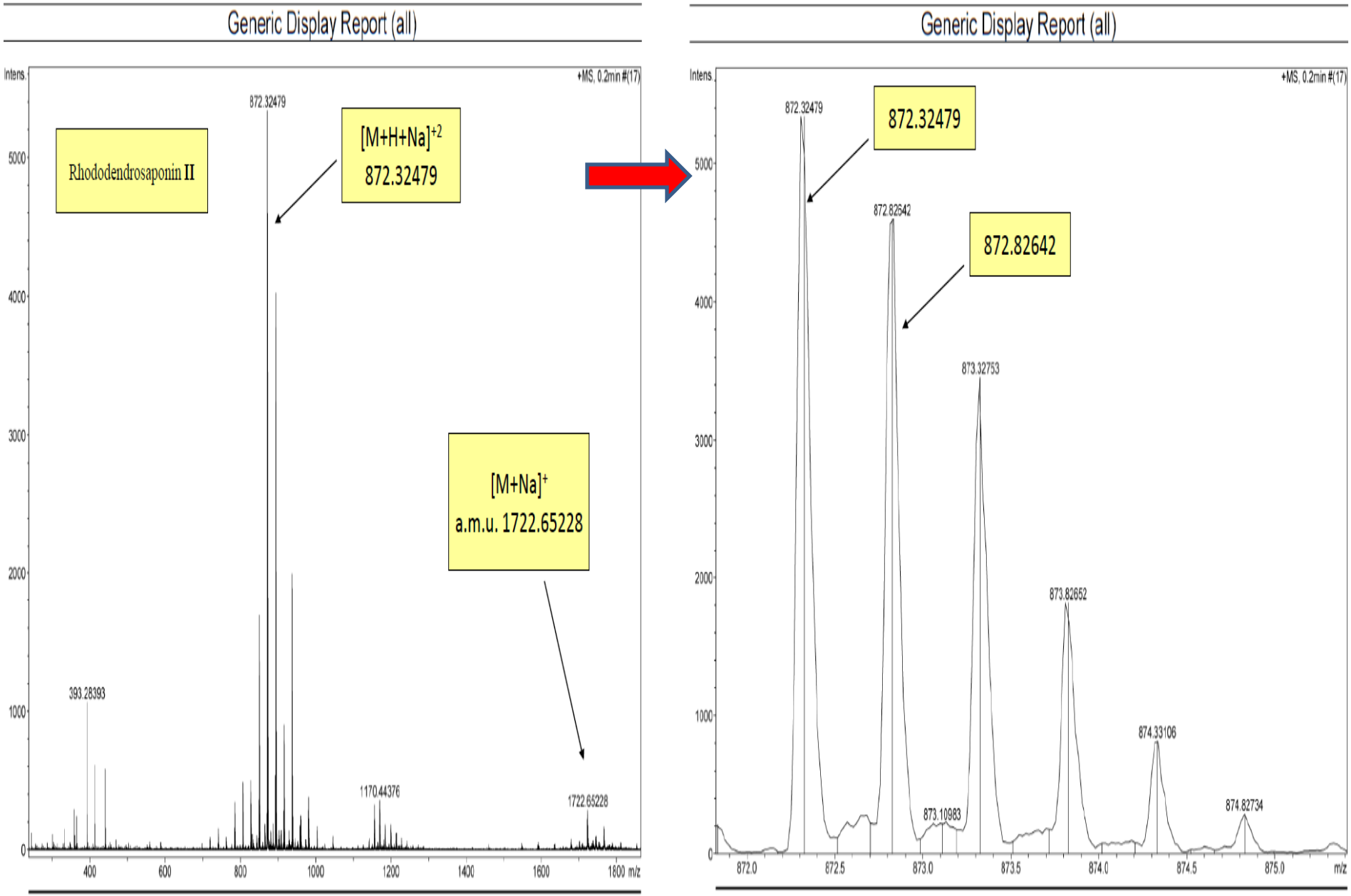

- Supplementary Figure 15 ıMS chromatogram of rhododendrosaponin II.

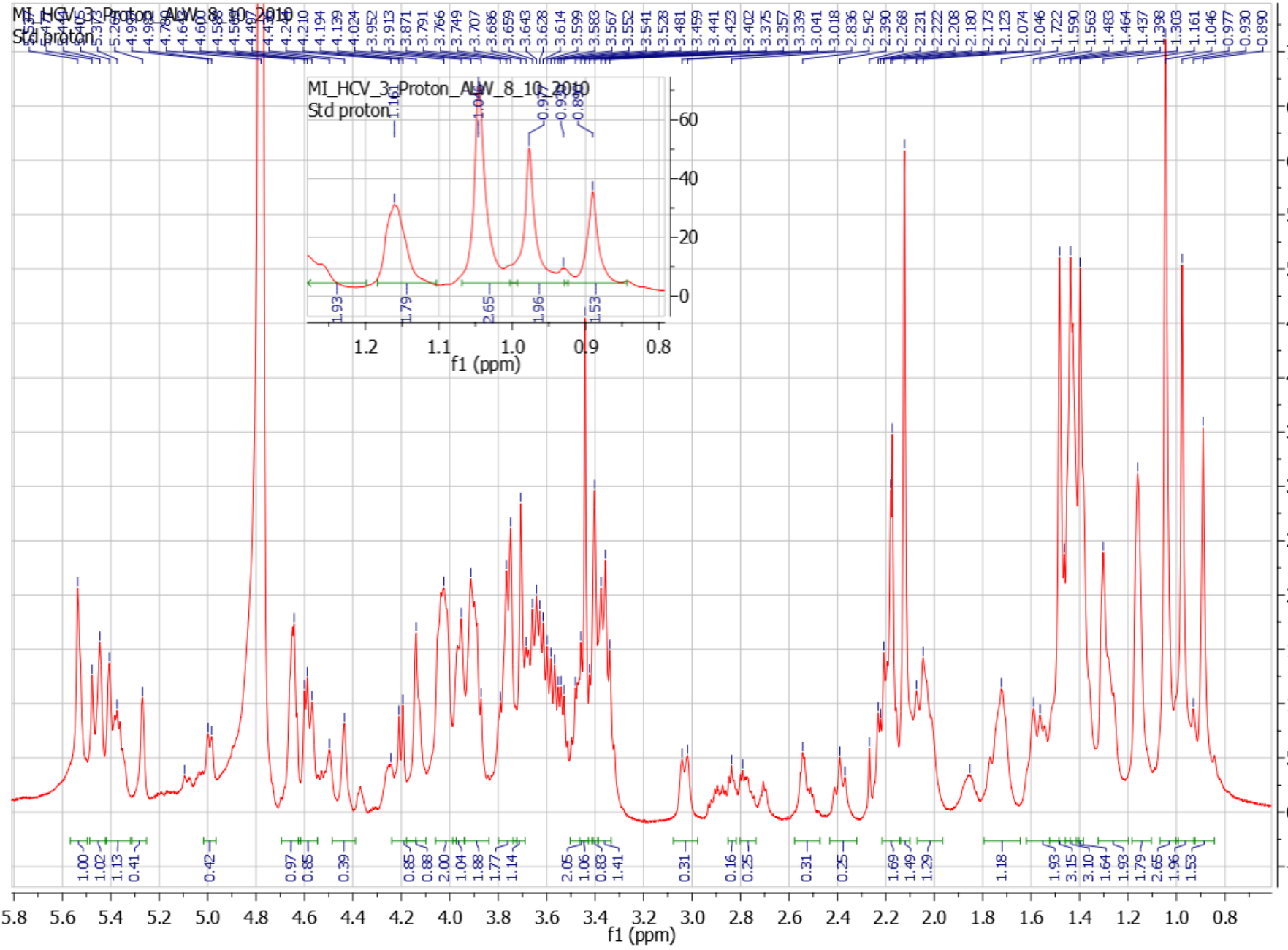

- **Supplementary Figure 16 | ^{1}H NMR of rhododendrosaponin II**

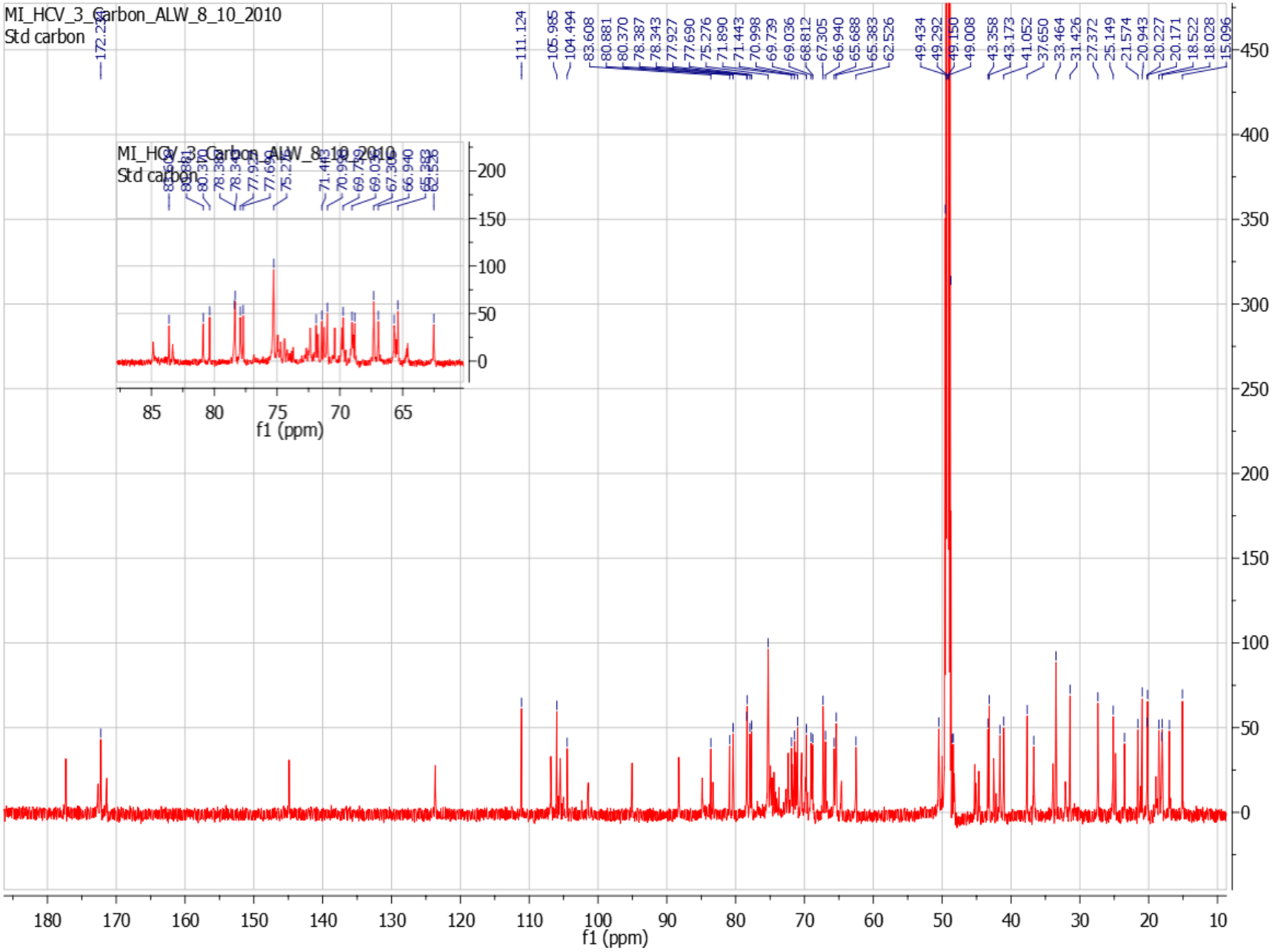

- **Supplementary Figure 17 | ^{13}C NMR of rhododendrosaponin II**

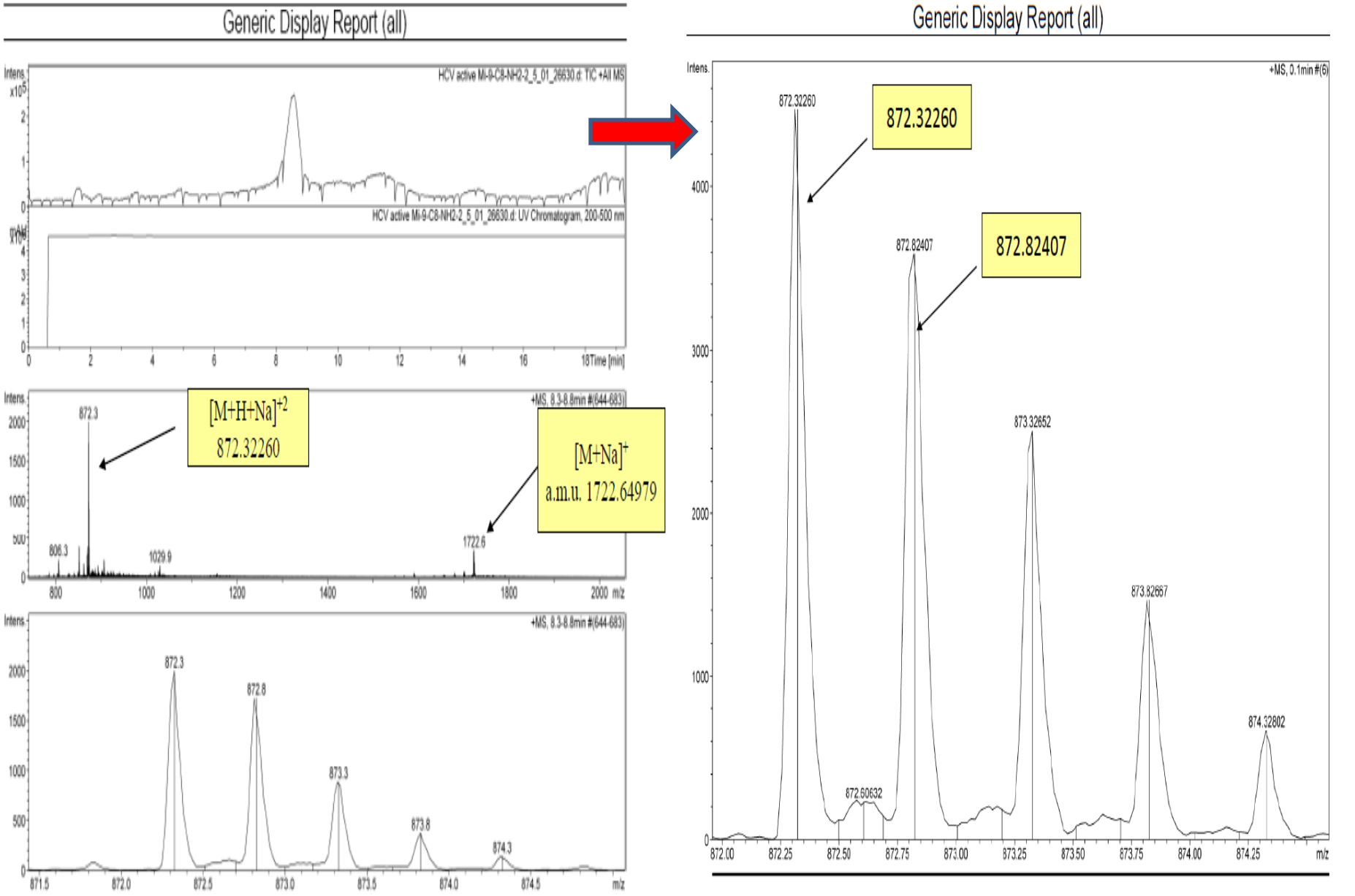

- **Supplementary Figure 18 | MS chromatogram of rhododendrosaponin III**

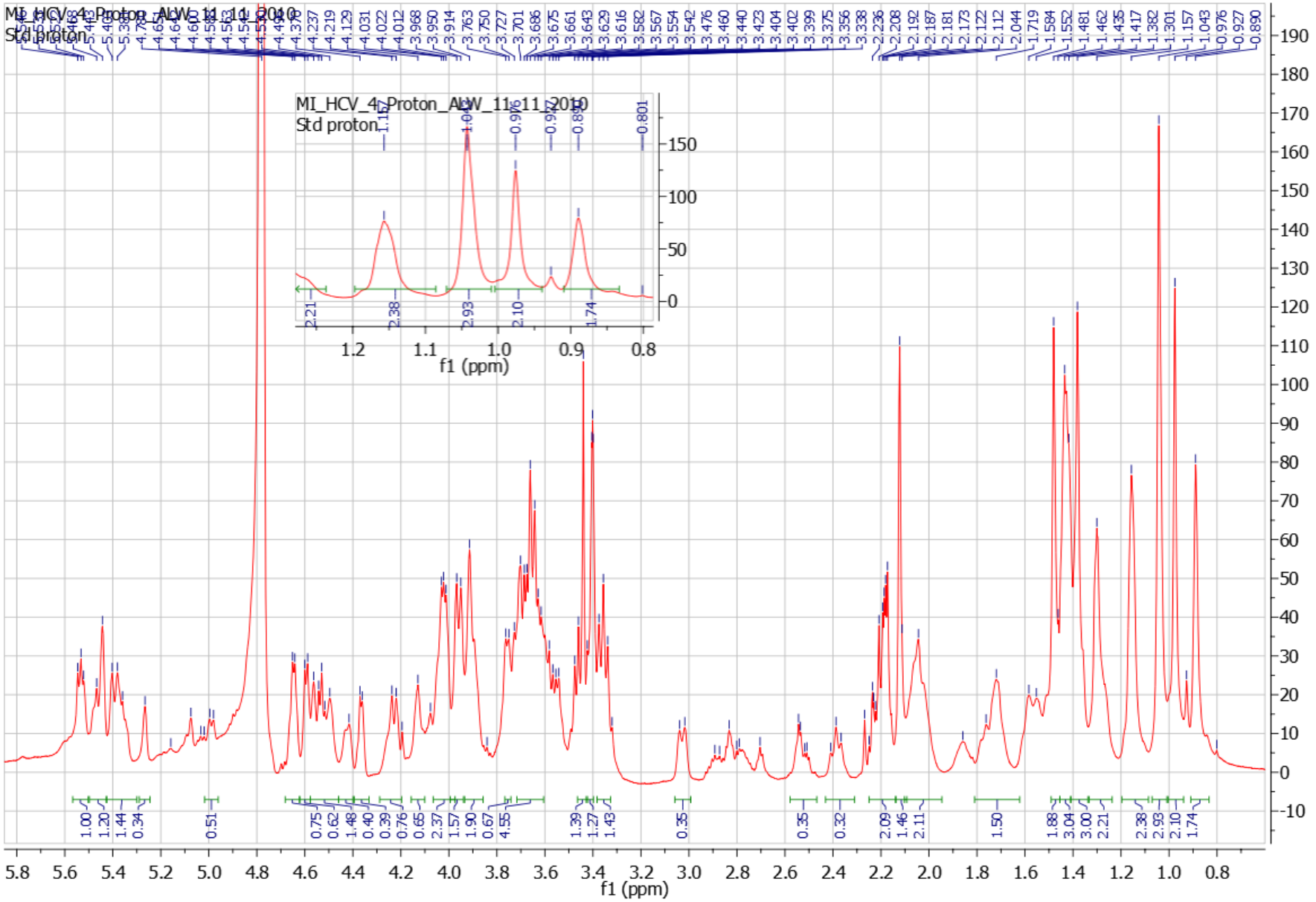

- Supplementary Figure 19 | ^{1}H NMR of rhododendrosaponin III

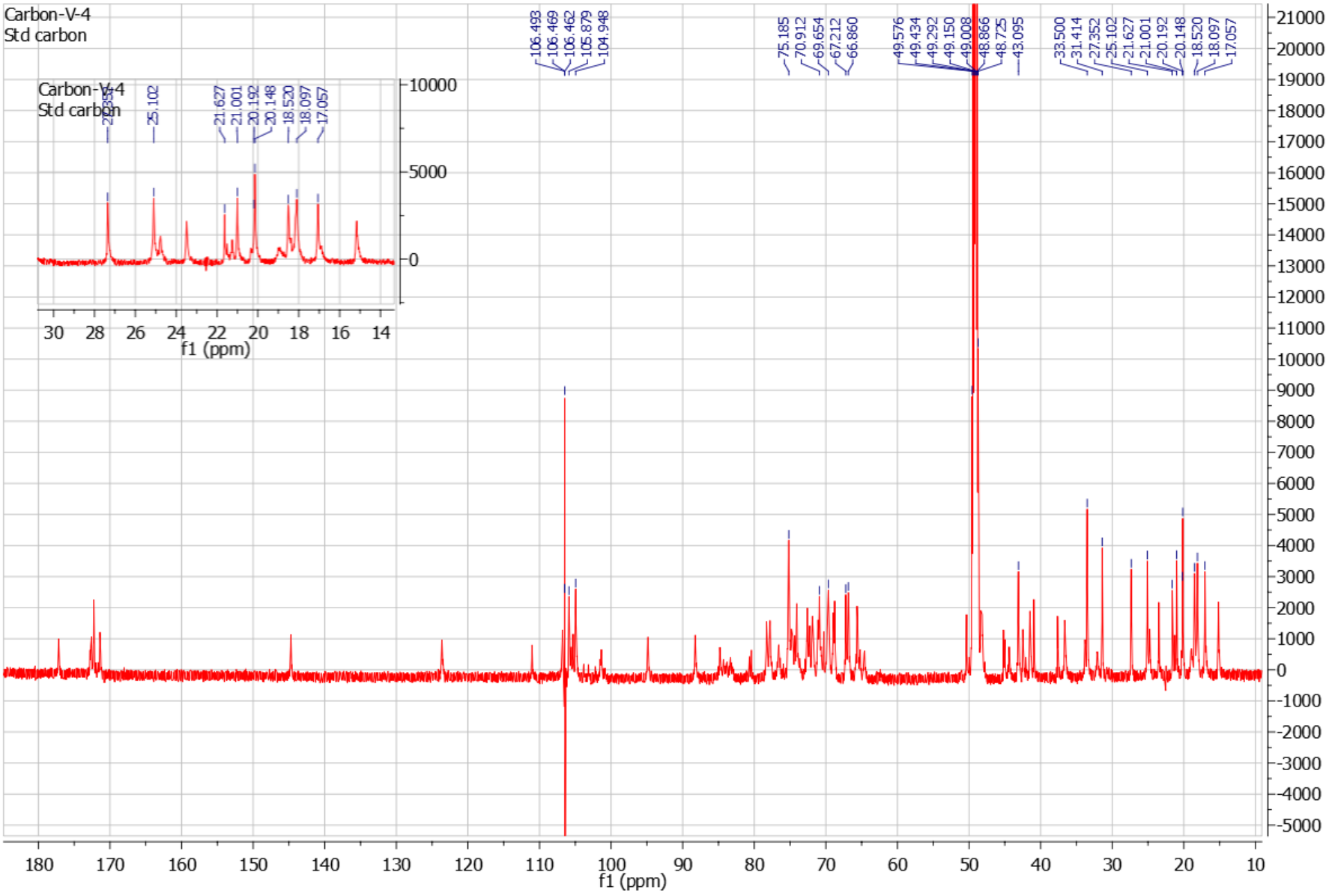

- **Supplementary Figure 20 |** ^{13}C NMR of rhododendrosaponin **III**

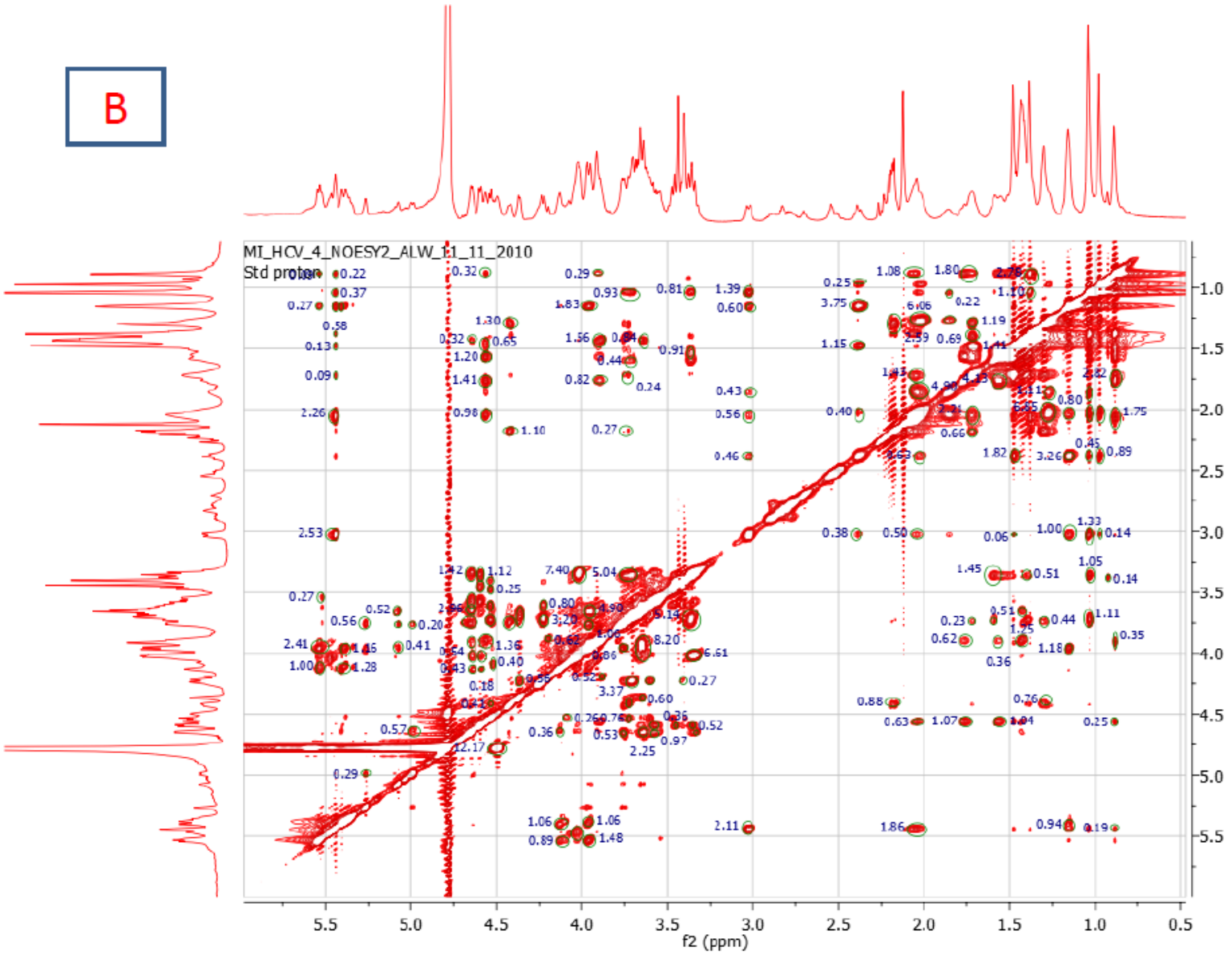

- Supplementary Figure 21 |NOESY spectrum of rhododendrosaponin III in methanol-d_4 (600 MHz)

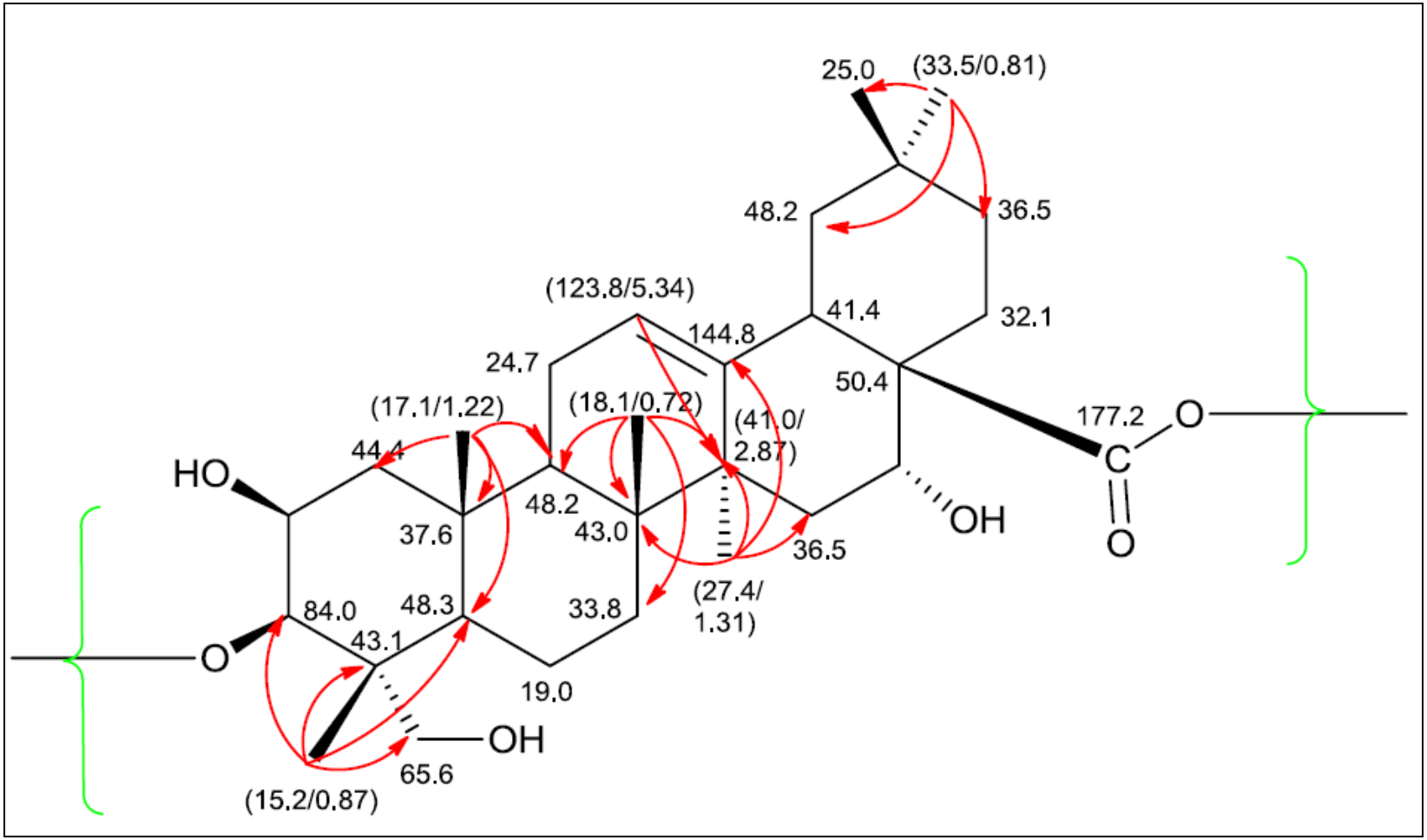

- Supplementary Figure 22 |Selected HMBC correlations of the aglycone triterpene

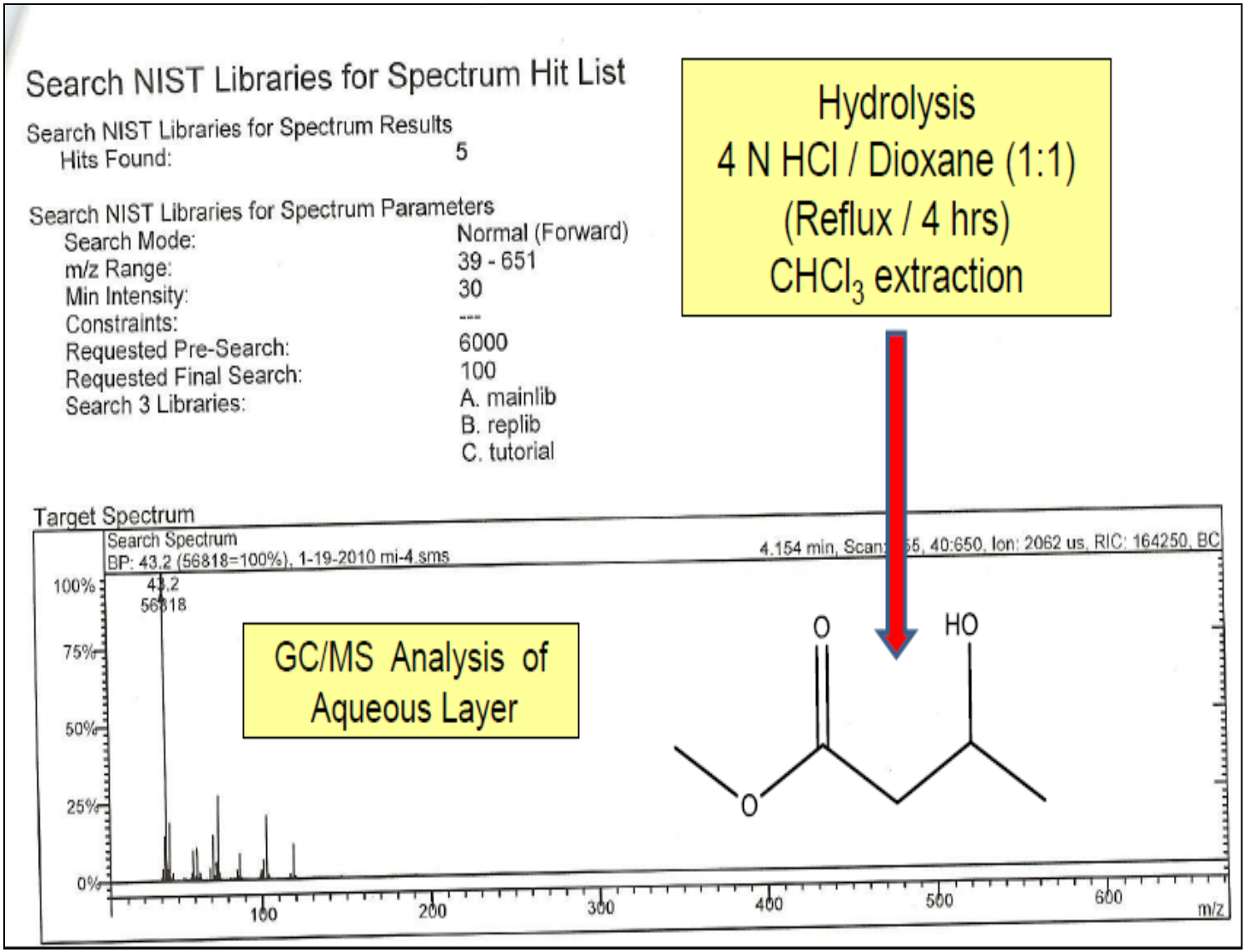

- Supplementary Figure 23 | GC/MS detection of 3-hydroxybutanoate in rhododendrosaponin III

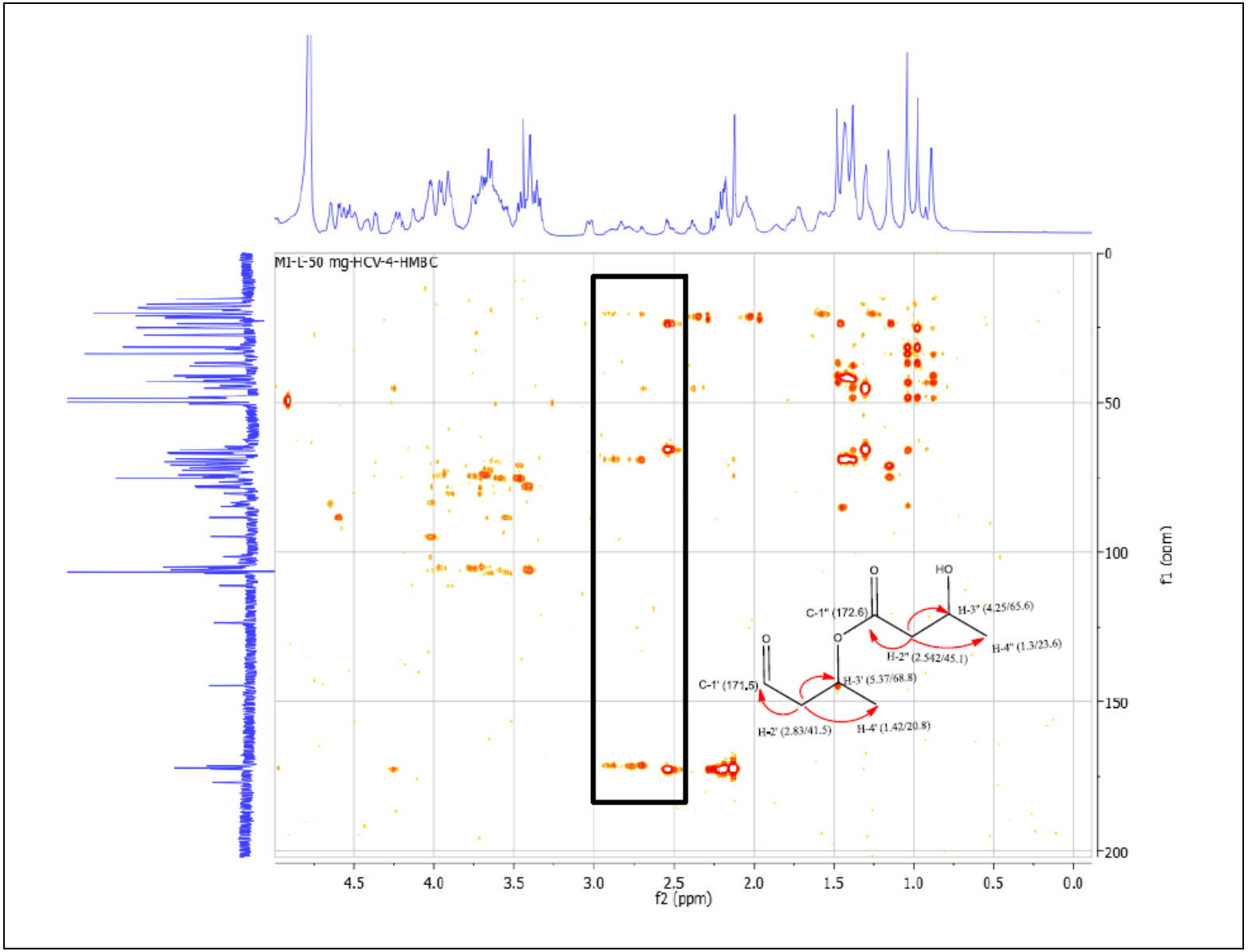

- **Supplementary Figure 24 |** HMBC correlations of 3-hydroxybutanoate dimmer in rhododendrosaponin **III**

Identification and determination of the carbohydrate units

- Identification and determination of the carbohydrate units were established using ^{13}C NMR and GC/MS/MS data while the determination of the sequence of oligosaccharides was completed through detailed MS studies including fragmentation by Nanospray Ionization-Linear Ion Trap Mass Spectrometry (NSI-MS^n) through collaboration with the Complex Carbohydrate Research Center at The University of Georgia. The total carbohydrate content of the major glycoside rhododendrosaponin **III** was shown by GC analysis to be 73.8% by weight. The processed data revealed the presence of a glucosyl, two arbinosyl, a rhamnosyl, a fucosyl, and two xylosyl units (Table 1). Inositol was added to the sample before derivatization as an internal standard (20 µg/sample) and the monosaccharides are identified by their retention times in comparison to standards and the carbohydrate character of these are authenticated by their mass spectra. The glycosyl linkages were summarized in (Table 2). The determination of the sequence of oligosaccharides was done via full MS and fragmentation by (NSI-MSn).

- Table 1 | The total carbohydrate content of the major glycoside rhododendrosaponin III

Residue	Weight (ug)[1]	mole%
Arabinose(Ara)	77.2	27.5
Ribose(Rib)	n.d.	n.d.
Rhamnose (Rha)	48.4	15.8
Fucose (Fuc)	43.7	14.2
Xylose (Xyl)	86.7	30.9
Glucuronic Acid(GlcUA)	n.d.	n.d.
Galacturonic acid (GalUA)	n.d.	n.d.
Mannose (Man)	n.d.	n.d.
Galactose (Gal)	n.d.	n.d.
Glucose (Glc)	39.2	11.6
N Acetyl Galactosamine (GalNAc)	n.d.	n.d.
N Acetyl Glucosamine (GlcNAc)	n.d.	n.d.
Heptose(Hep)	n.d.	n.d.
3 Deoxy-2-manno-2 Octulsonic acid (KDO)	n.d.	n.d.
Sum		100

- Table 2 | Glycosyl linkage analysis

MI021110	LK000042
Glycosyl Residue	Percentage Present
Terminally linked arabinofuranosyl residue (t-Araf)	2.6
Terminally linked arabinopyranosyl residue (t-Arap)	21.9
Terminally linked xylopyranosyl residue (t-Xylp)	9.2
4-linked rhamnopyranosyl residue (4-Rhap)	19.7
Terminally linked glucopyranosyl residue (t-Glcp)	2.2
2-linked fucopyranosyl residue (2-Fucp)	1.9
3-linked xylopyranosyl residue (3-Xylp)	12.0
2,3-linked fucopyranosyl residue (2,3-Fucp)	16.3
6-linked glucopyranosyl residue (6-Glcp)	8.8
4-linked glucopyranosyl residue (4-Glcp)	0.7
2,6-linked glucopyranosyl residue (2,6-Glcp)	4.7
Total	100

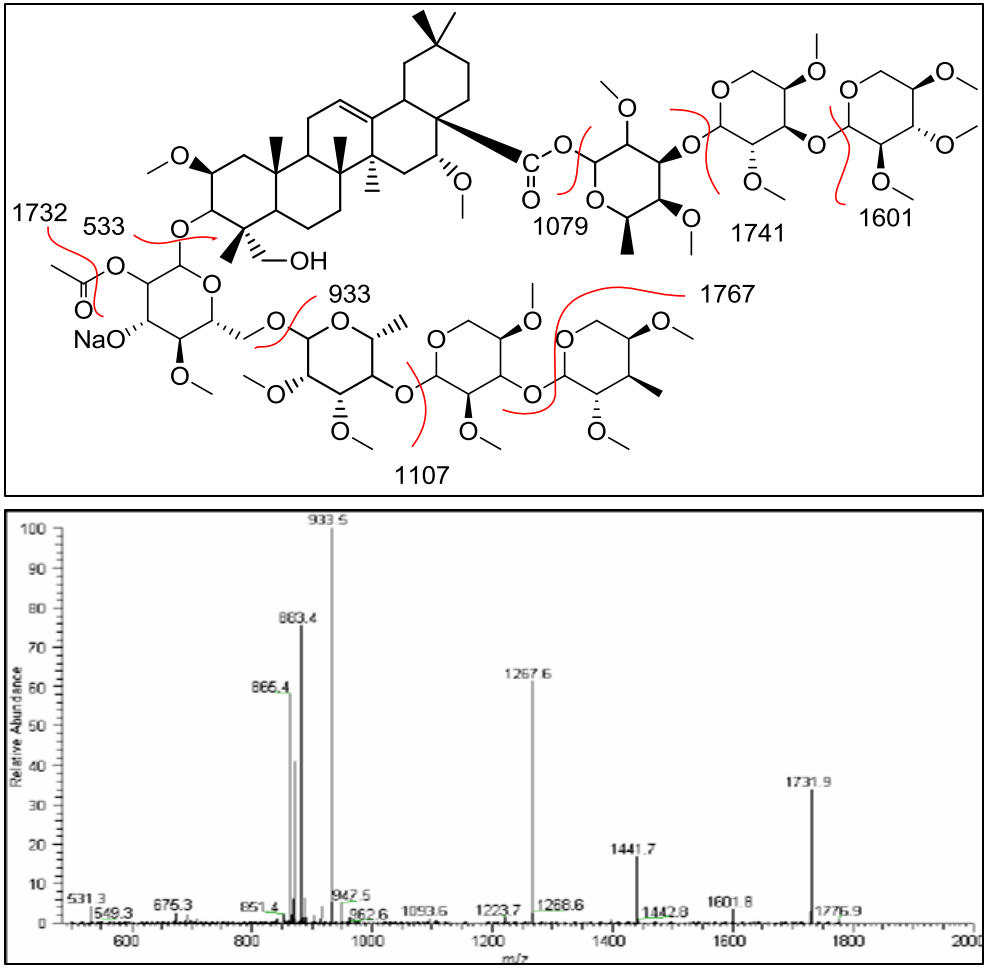

- Supplementary Figure 25 | NSI-MS^n fragmentation of rhododendrosaponin III

The absolute configuration determination of the carbohydrate units

- The absolute configuration determination of the carbohydrate units was completed using an HPLC method reported by Tanaka et al. First the compound is hydrolyzed via refluxing in 1 N HCl for 2-3 h followed by extraction with ethyl acetate. The aqueous layer is then neutralized with silver carbonate, centrifuged to remove the insoluble precipitate, dried, refluxed with L-cysteine methyl ester in pyridine for 1 hr at 60-70 °C, followed by the addition of phenylisothiocyanate with extended reflux for an additional 1 hr at 60-70 °C to form the thiazoline derivative that can be detected by UV. This method was tested using various standards, followed by application to the isolated metabolites.

- Tanaka, T., Naskashima, T., Ueda, T., Tomii, K., Kouno, I. Facile discrimination of aldose enantiomers by reversed-phase HPLC**.** *Chem. Pharm. Bull*. **2007**, *55*, 899-901.

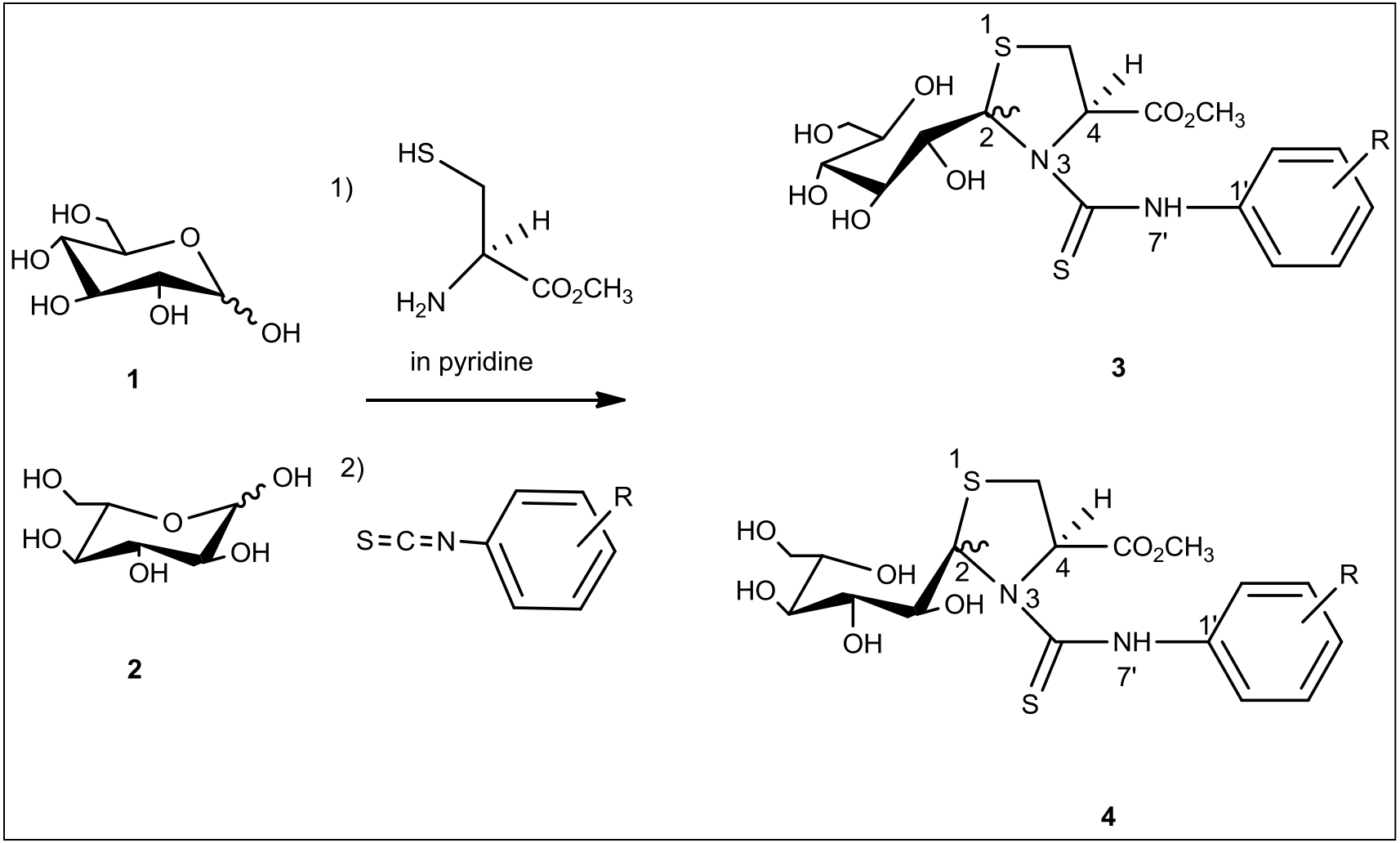

- Supplementary Figure 26 | An investigational method for carbohydrate analysis

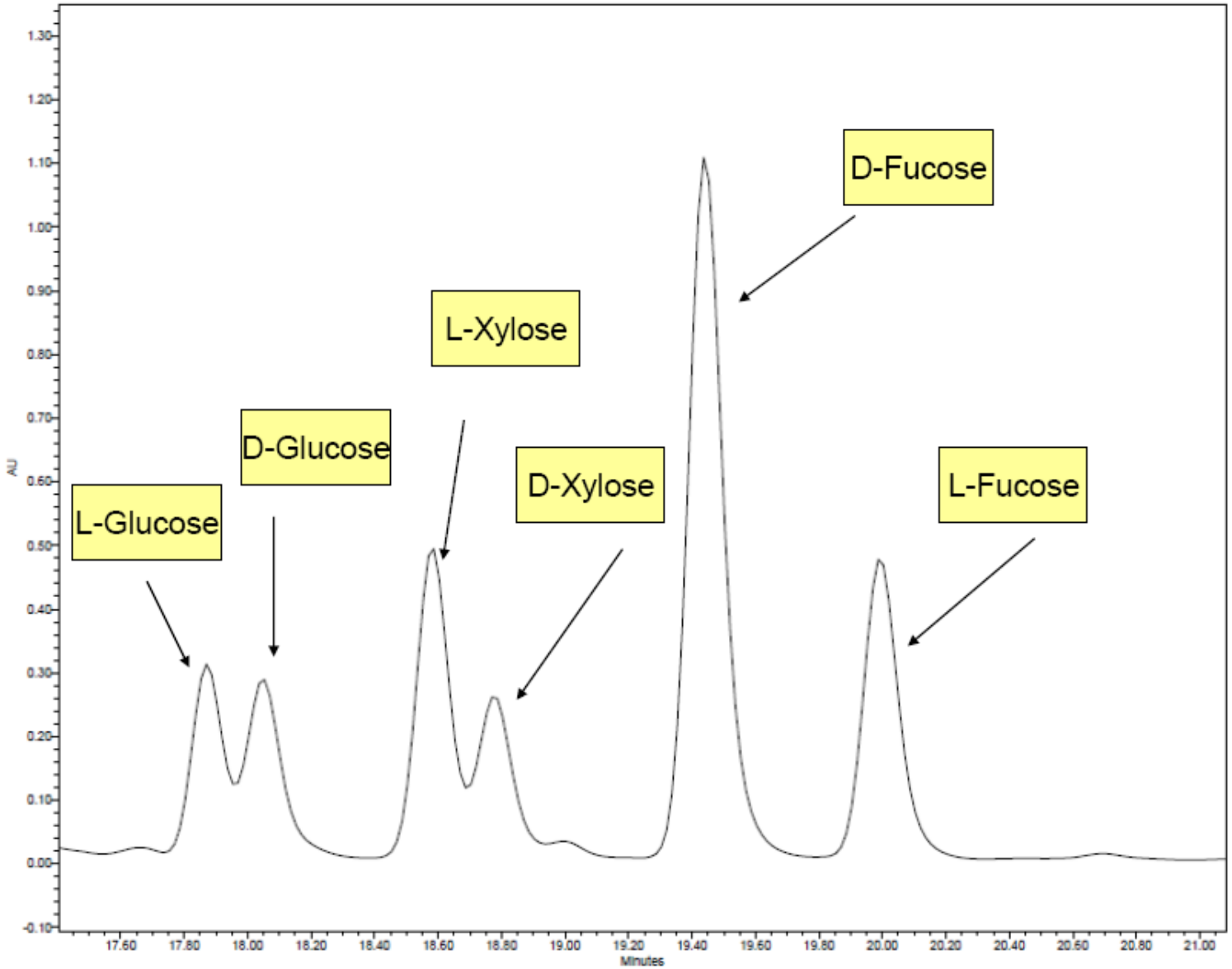

- Supplementary Figure 27 | L- and D- glucose, xylose, and fucose standards by the carbohydrate analysis method

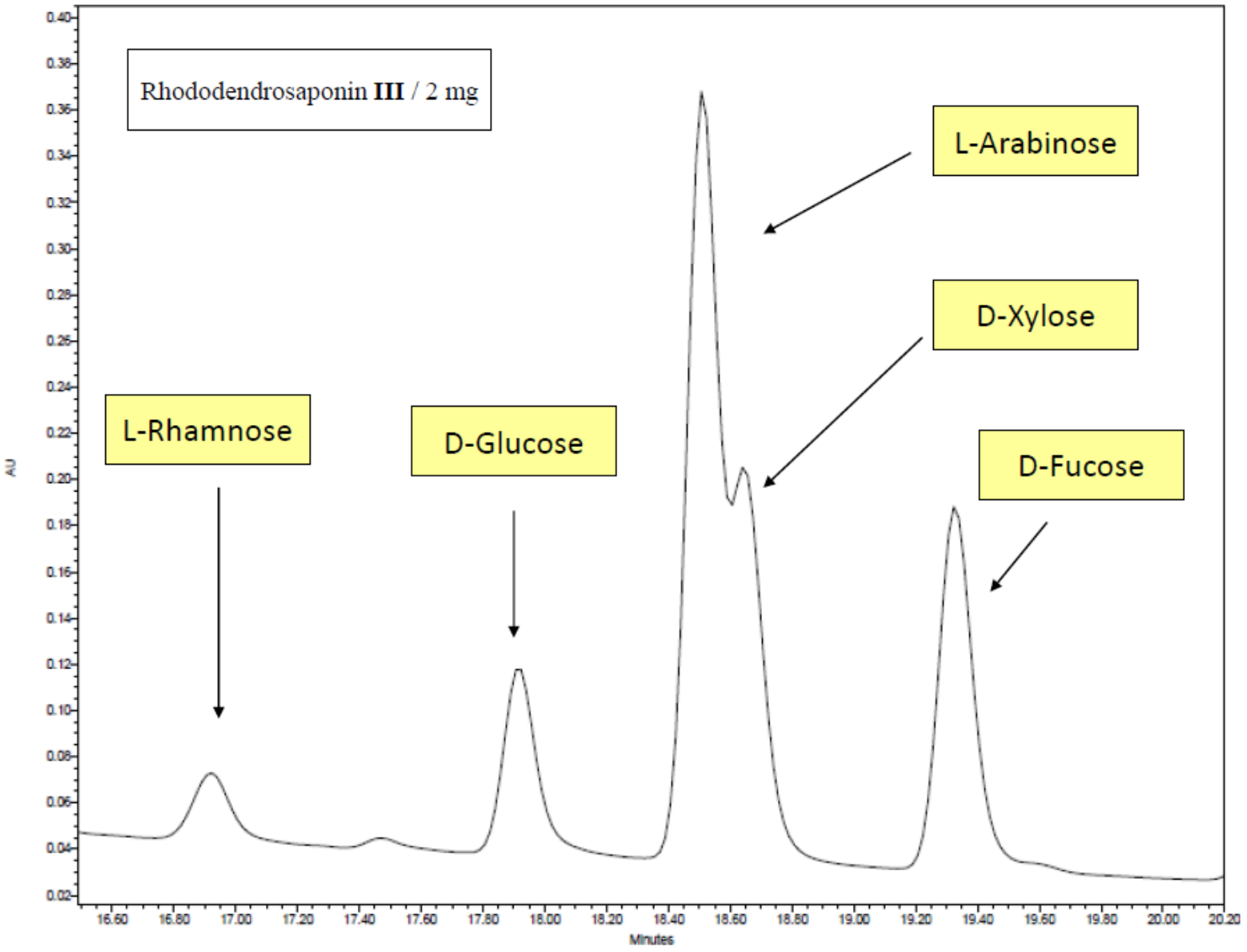

- Supplementary Figure 28 | Carbohydrate analysis for rhododendrosaponin III

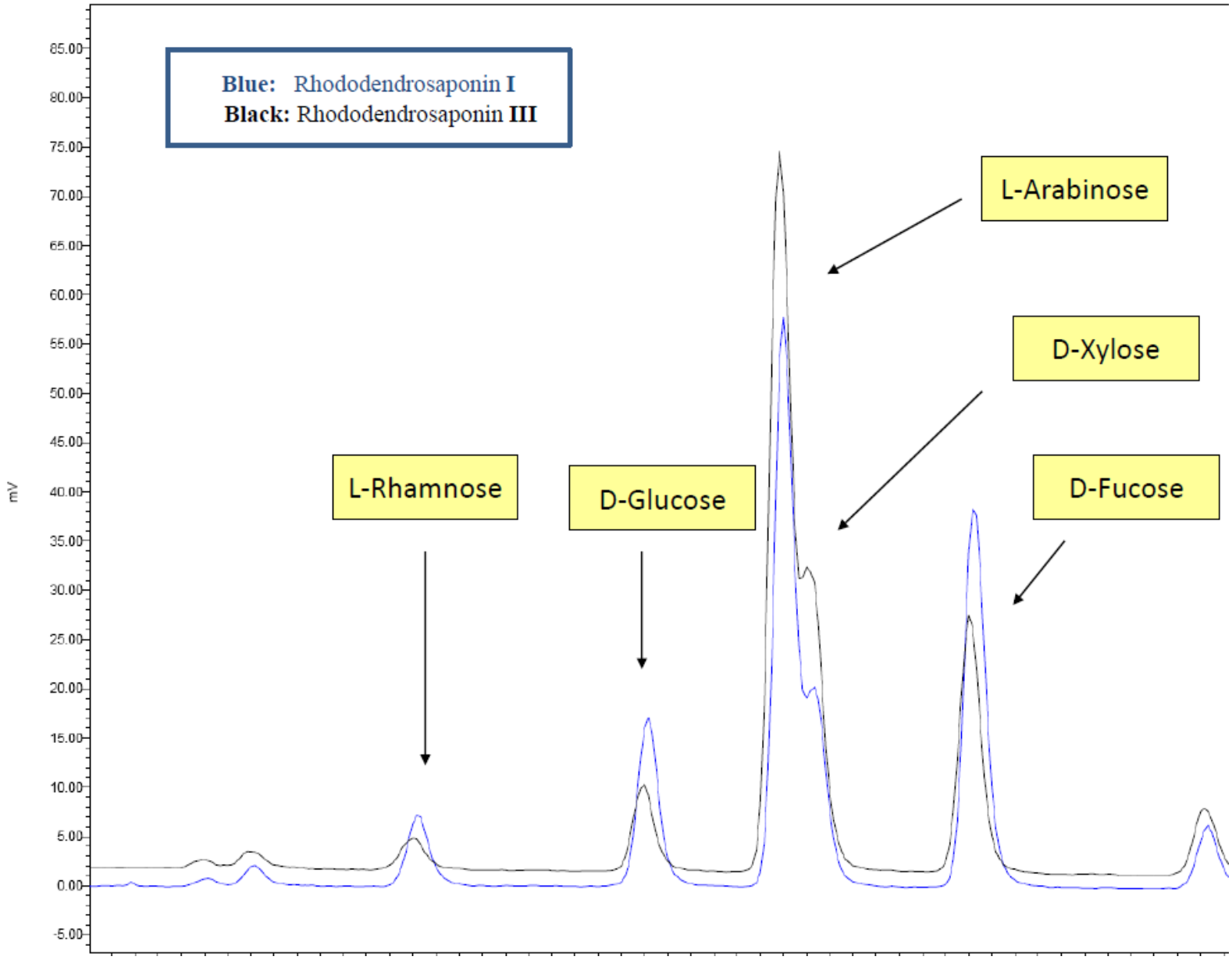

- Supplementary Figure 29 | Overlay of the carbohydrate analysis chromatograms of rhododendrosaponins I and III

Overlaying 2D NMR experiments

- Overlaying the most common 2D NMR experiments including ^{1}H-^{13}C) Heteronuclear Multiple Quantum Coherence Spectroscopy (HSQC), ^{1}H-^{13}C (2 and 3 bond) Heteronuclear Single bond Correlation Spectroscopy (HMBC) and ^{1}H -^{1}H Nuclear Overhauser Enhancement spectroscopy (NOESY/ROESY) helped to alleviate the extended time to quickly solve such considerably complex homologous series. Overlaid HSQC data for rhododendrosaponins **I** and **III** revealed a high level of homology with interchangeable α- and β- configuration at C-24 of rhododendrosaponins **I**. This was confirmed with the HSQC, HMBC, and ROESY spectra of rhododendrosaponins **I**. Interestingly, the superimposed data clearly demonstrated the presence of the uncommon Amadori-type pyranose-furanose isomerism of the terminal L-arbinosyl moiety. It was possible to monitor the presence of acyclic intermediate (-CHO) at 218.1 ppm. As further evidence, the glycosyl linkage analysis (Table 2) confirmed the presence of both forms. These data explainsthe complex NMR spectra for these compounds.

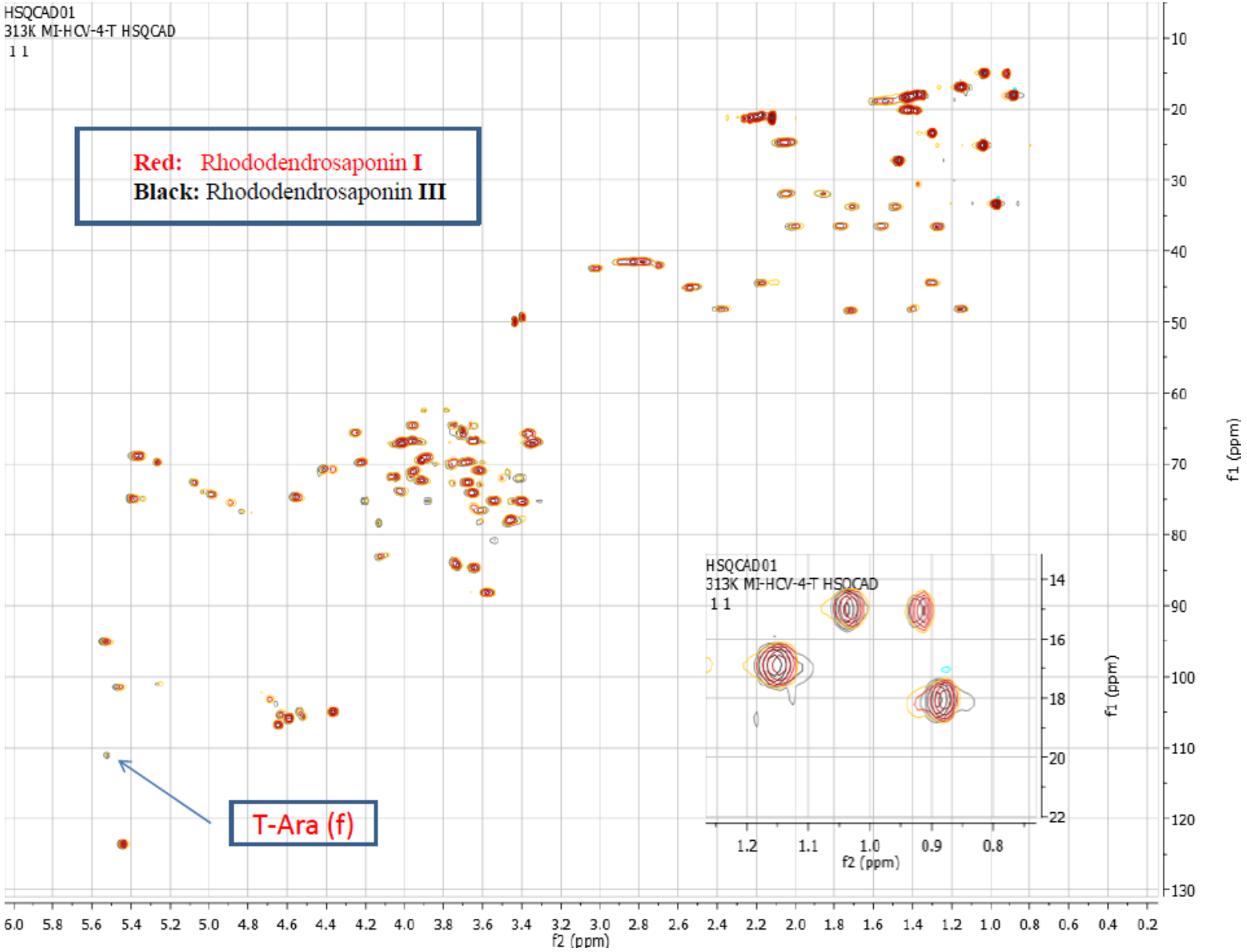

- Supplementary Figure 30 | Overlaid HSQC spectra of rhododendrosaponins I and III

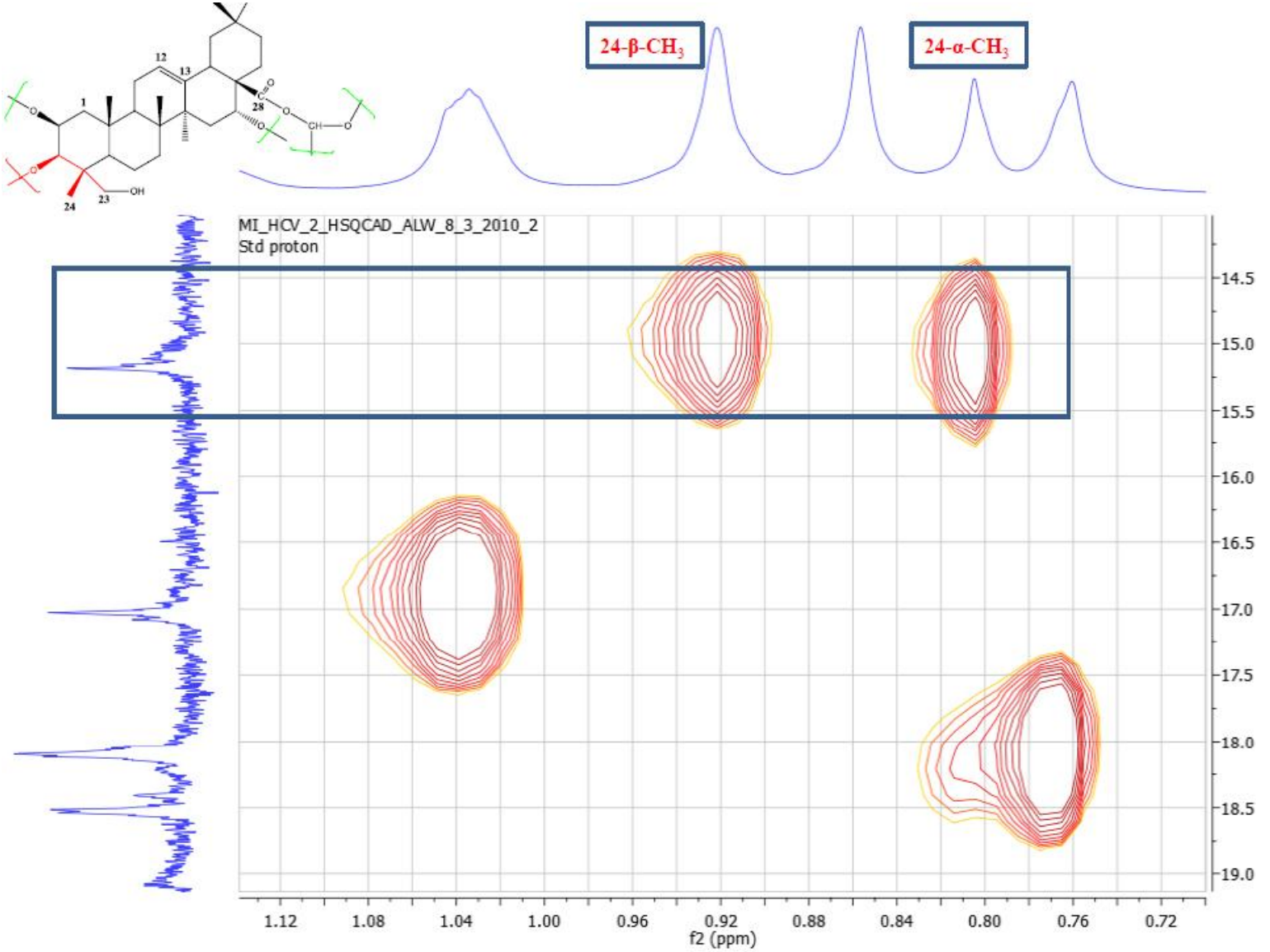

- Supplementary Figure 31 |The expanded HSQC spectrum of rhododendrosaponin I in methanol-d_4 (600 MHz) shows the presence of α and β isomers at C-24

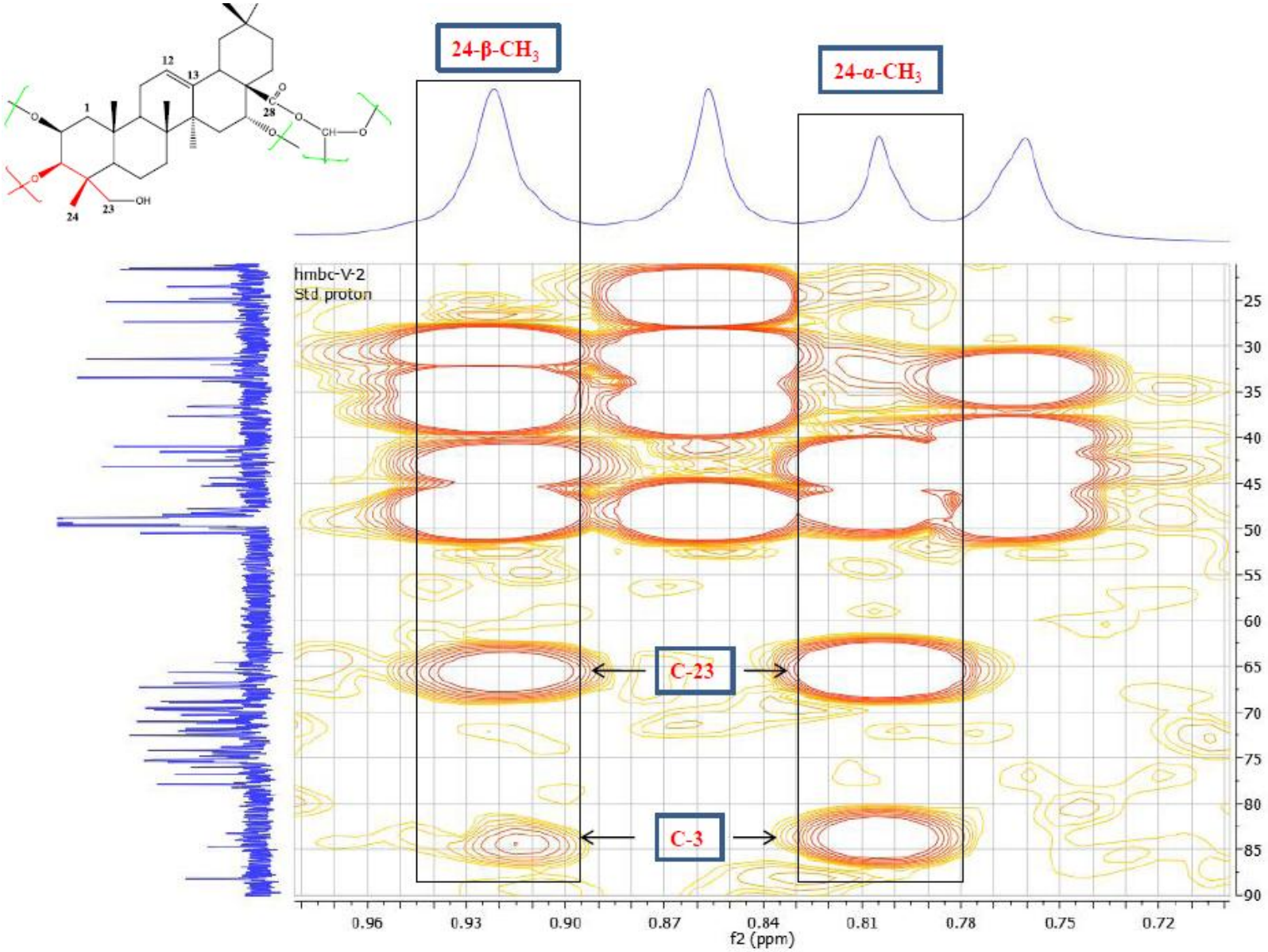

- Supplementary Figure 32 | The expanded HMBC spectrum of rhododendrosaponin I in methanol-d_4 (600 MHz) shows the presence of α and β isomers at C-24

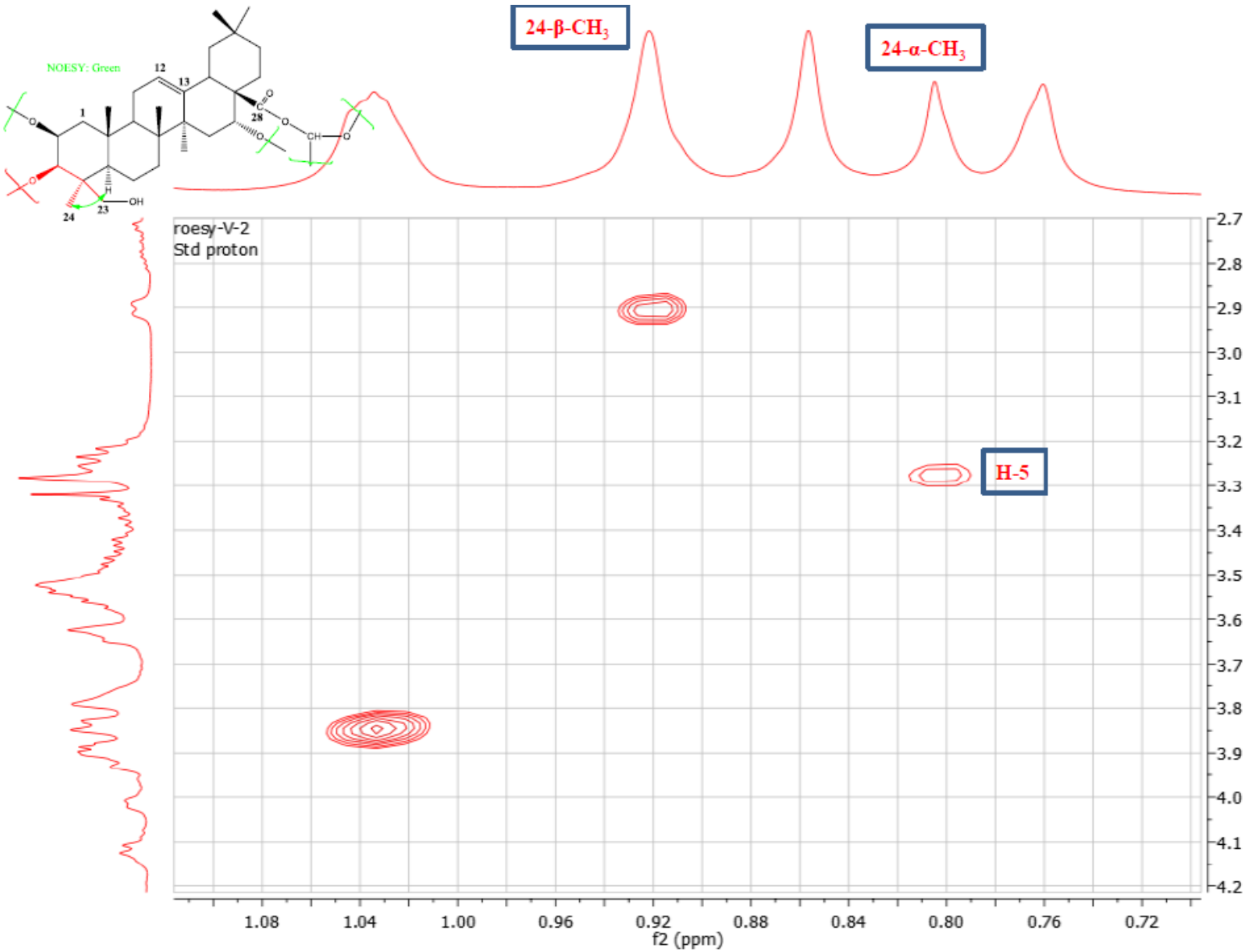

- Supplementary Figure 33 | The expanded ROESY spectrum of rhododendrosaponin I in methanol-d_4 (600 MHz) shows the presence of α and β isomers at C-24

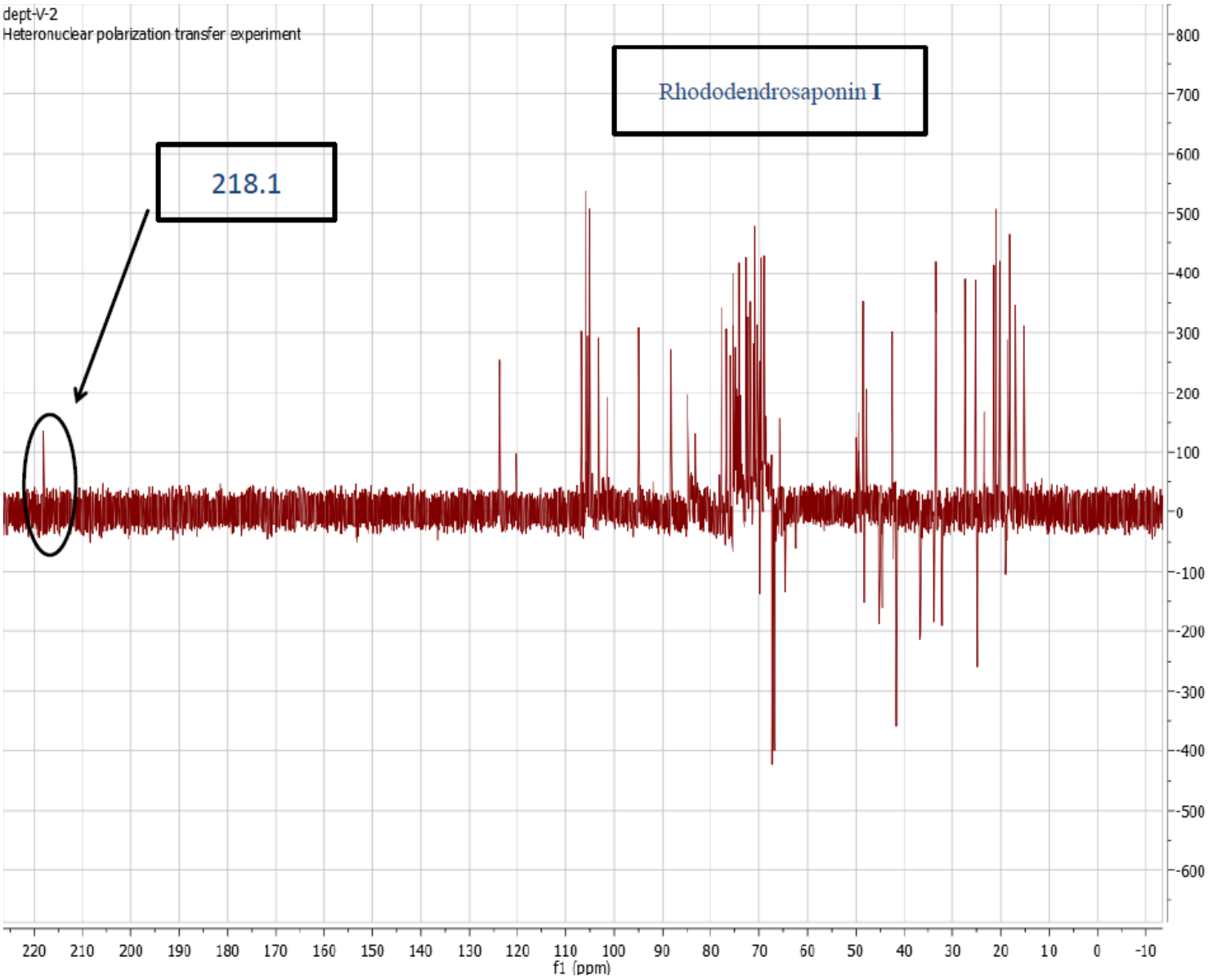

- Supplementary Figure 34 | 135° DEPT spectrum of rhododendrosaponin I in methanol-d_4 (600 MHz) shows the presence of (-CHO) for the acyclic intermediate

- In a similar manner stacked HSQC studies for rhododendrosaponins **II** and **III** revealed high level of similarity with pyranose-furanose isomerism. This was confirmed by monitoring the presence of the acyclic intermediate (-CHO) at 217.590 ppm, as well as the presence of arbinofuranosyl unit in rhododendrosaponin **II**. Further investigation through co-injection of rhododendrosaponins **II** and **III** on 250 × 21.2 mm NH_2 column with $CHCl_3$-MeOH confirms the isomerization.

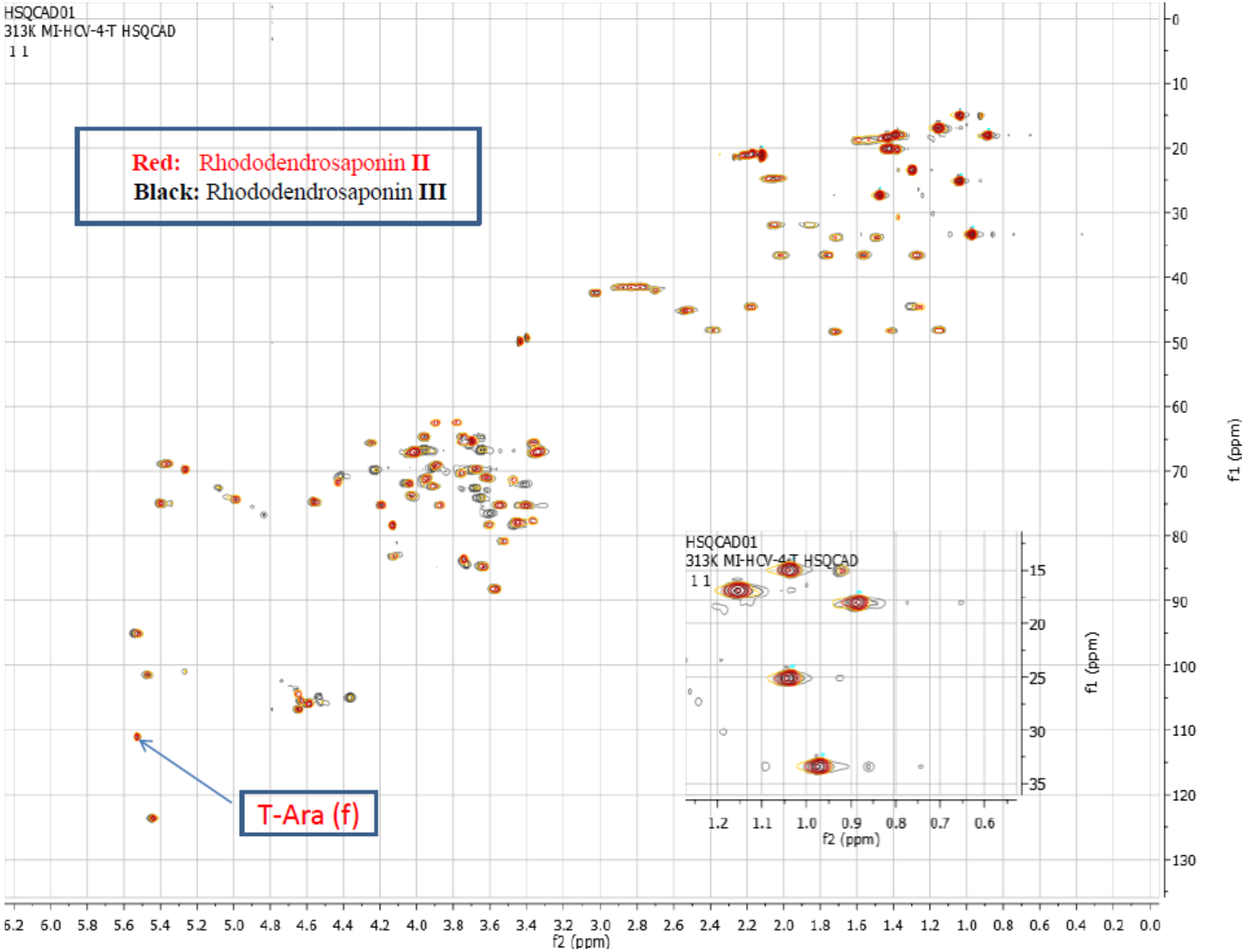

- Supplementary Figure 35 | Overlaid HSQC spectra of rhododendrosaponins II and III

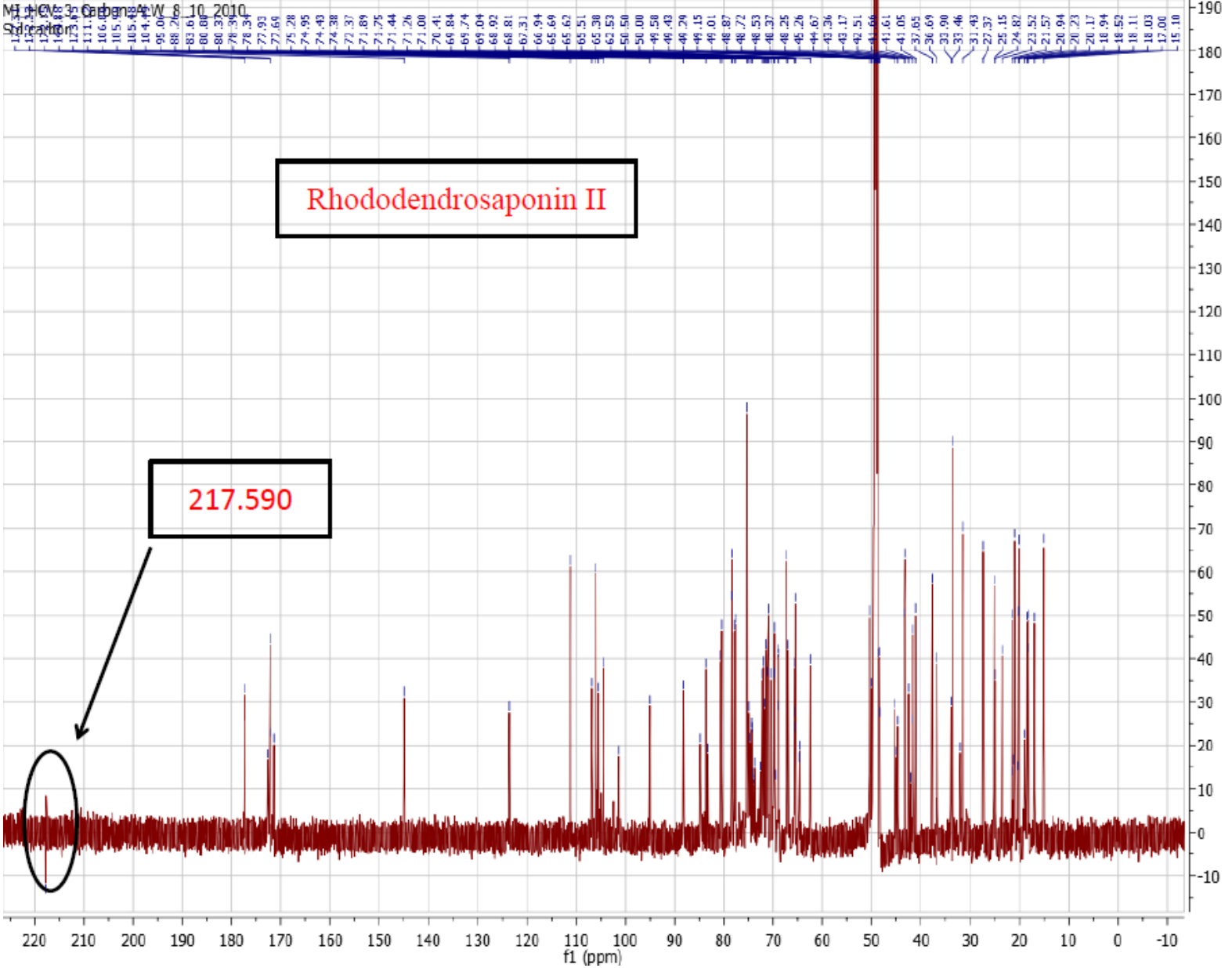

- Supplementary Figure 36 | The ^{13}C NMR spectrum of rhododendrosaponin II in methanol-d_4 (600 MHz) shows the presence of (-CHO) for the acyclic intermediate

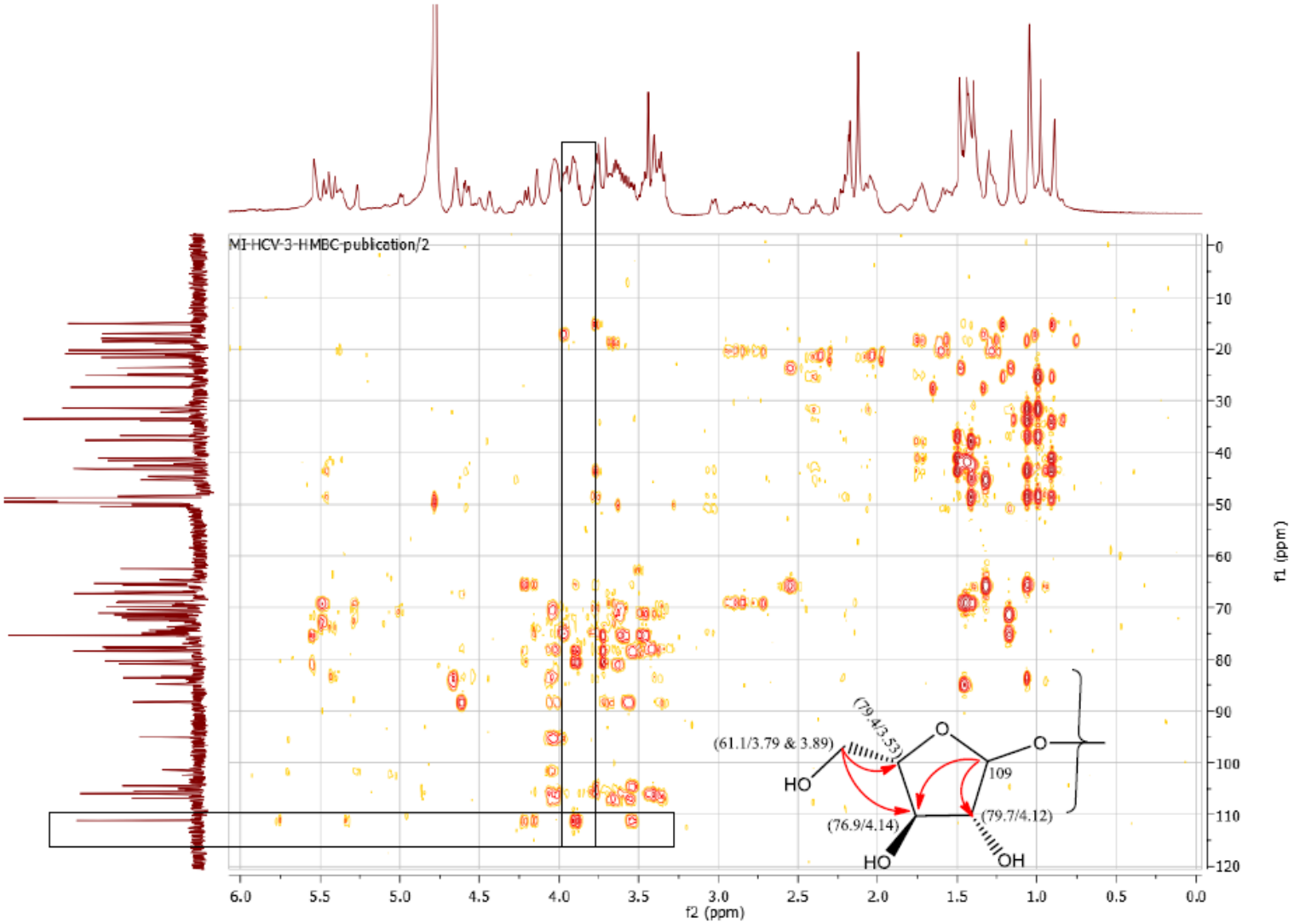

- Supplementary Figure 37 | Expanded HMBC spectrum of rhododendrosaponin II in methanol-d_4 (600 MHz) shows the presence of arbinofuranosyl moiety

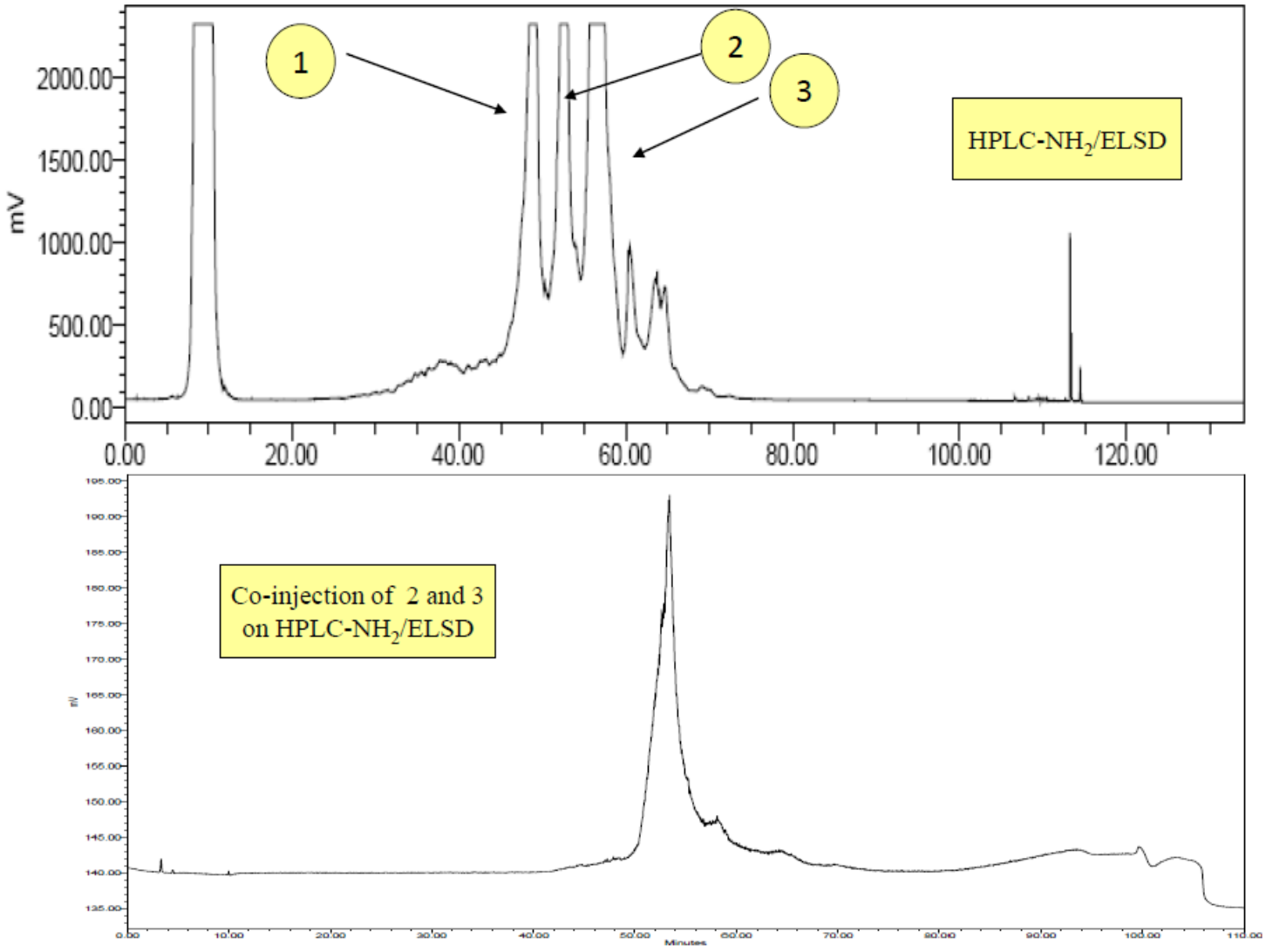

- Supplementary Figure 38 | Co-injection of rhododendrosaponins II and III on 250 × 4.6 mm NH_2 column

- ^{1}H NMR data for rhododendrosaponins **I** established the β-configuration of the following glycosyl groups: fucosyl (5.42 d, 7.8 Hz), glucosyl (4.57, 7.8 Hz), terminal xylosyl (4.24 d, 6.0 Hz), inner xylosyl (4.52 d, 6.0 Hz), terminal arabinosyl (4.48 d, 7.8 Hz), and inner arabinosyl (4.54 d, 6.6 Hz), while α-configuration of rhamnosyl (5.35, s). The 3β absolute configuration of 3-hydroxybutanoate was determined by acid-catalyzed methanolysis. This was followed by comparison with (R) and (S) standards using a chiral GC column [RESTEK capillary column: St-βDEXsa (30 m x 0.32 mm x 0.25 µm)].

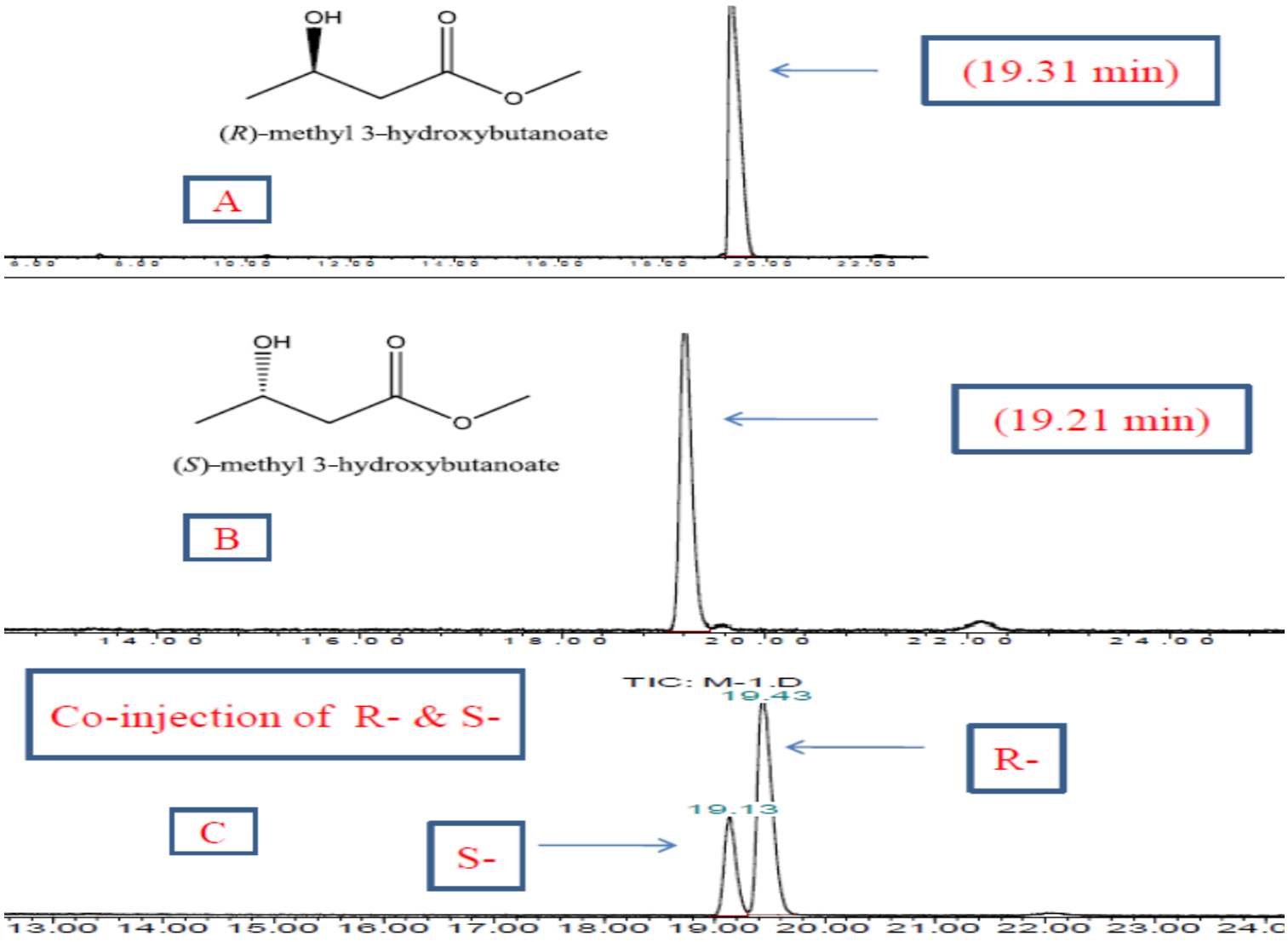

- Supplementary Figure 39 ı GC chromatograms of: A) (R)-methyl 3-hydroxybutanoate, B) (S)-methyl 3-hydroxybutanoate, C) Co-injection of (R) and (S)-methyl 3-hydroxybutanoate

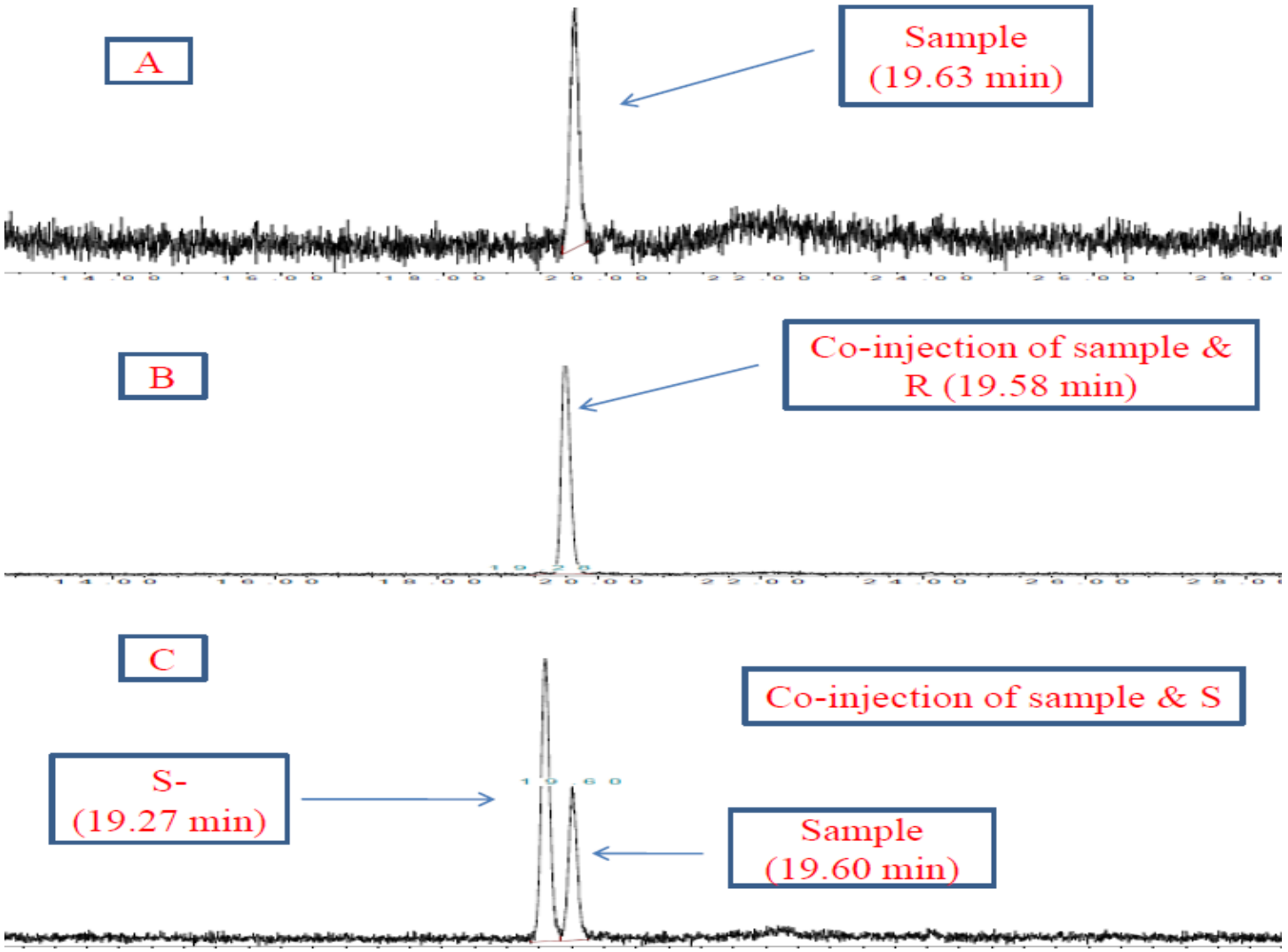

- Supplementary Figure 40 | GC chromatograms of: A) rhododendrosaponins I-III after methanolysis, B) Co-injection of the sample and (R)-methyl 3-hydroxybutanoate, C) Co-injection of the sample and (S)-methyl 3-hydroxybutanoate chromatograms of: A) (R)-methyl 3-hydroxybutanoate, B) (S)-methyl 3-hydroxybutanoate, C) Co-injection of (R) and (S)-methyl 3-hydroxybutanoate.

Compound	R		R_1		R_2
Rhododendrosaponin I	CH_3	CH_2OAc	CH_2OAc	CH_3	β-L-arabinopyranose
Rhododendrosaponin II	CH_3		CH_2OH		L-arabinofuranose
Rhododendrosaponin III	CH_3		CH_2OH		β-L-arabinopyranose

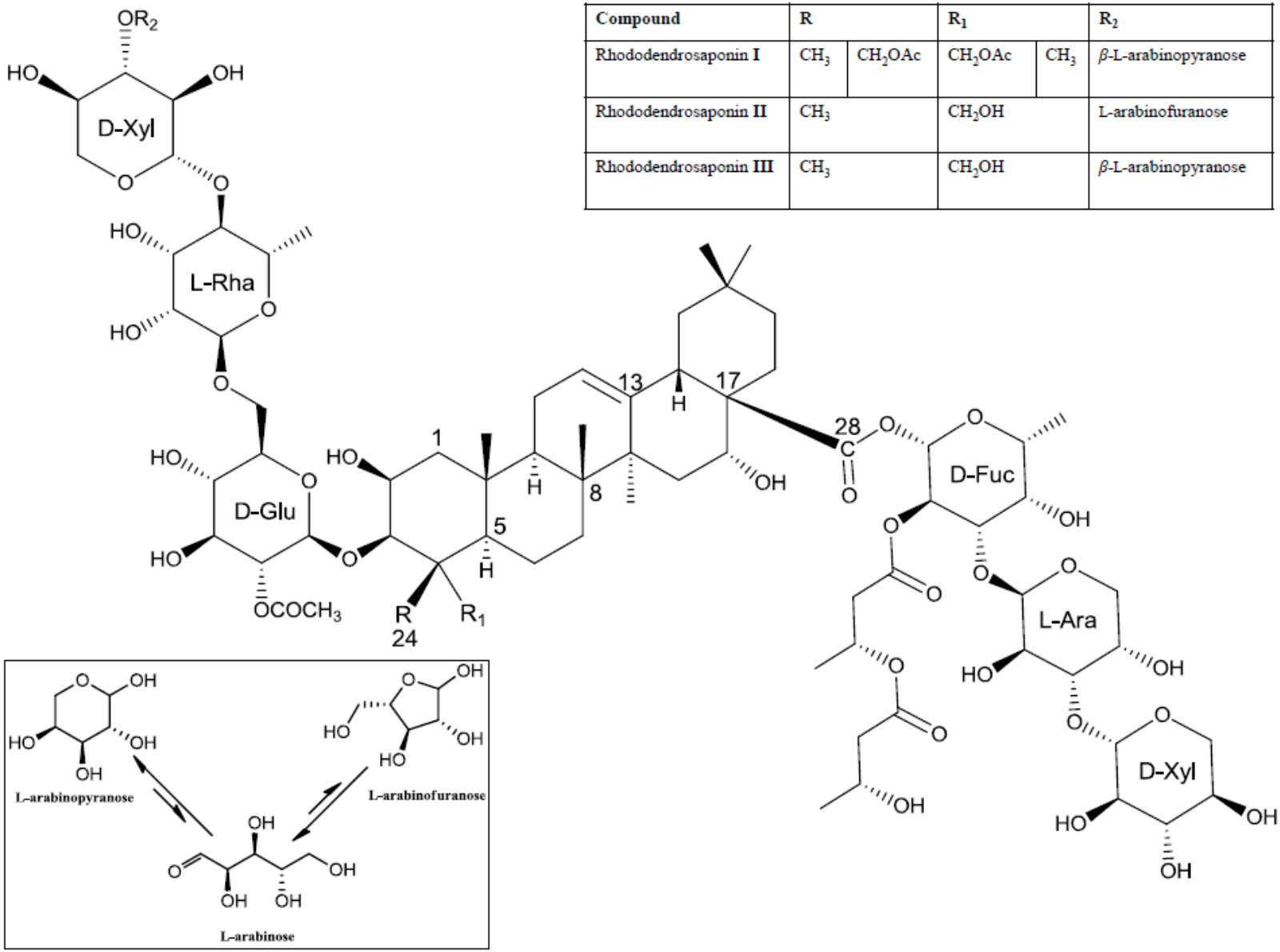

- Supplementary Figure 41 | The structures of rhododendrosaponins I-III based on all available data

Molecular Modeling

- The 3D structure of the major glycoside, rhododendrosaponins **III** was minimized using OPLS_2005 with extended cutoff; Van der Waals of 8.0 K cal/mol, Electrostatic of 20.0 K cal/mol, and H-bond of 4.0 K cal/mol. All stereogenic centers are kept fixed during the calculation. PRCG method was used with 0.05 as a convergence gradient threshold. Mixed torsional/low-mode sampling was used for conformational analysis with 1000 number of steps. PyMol 1.4 was used to generate the 3D surface with element color scheme. Despite the presence of similarity to previously reported natural products, the rarity of the source, the exceptional activity, and the presence of the uncommon Amadori-type isomerism make this group of metabolites unique.

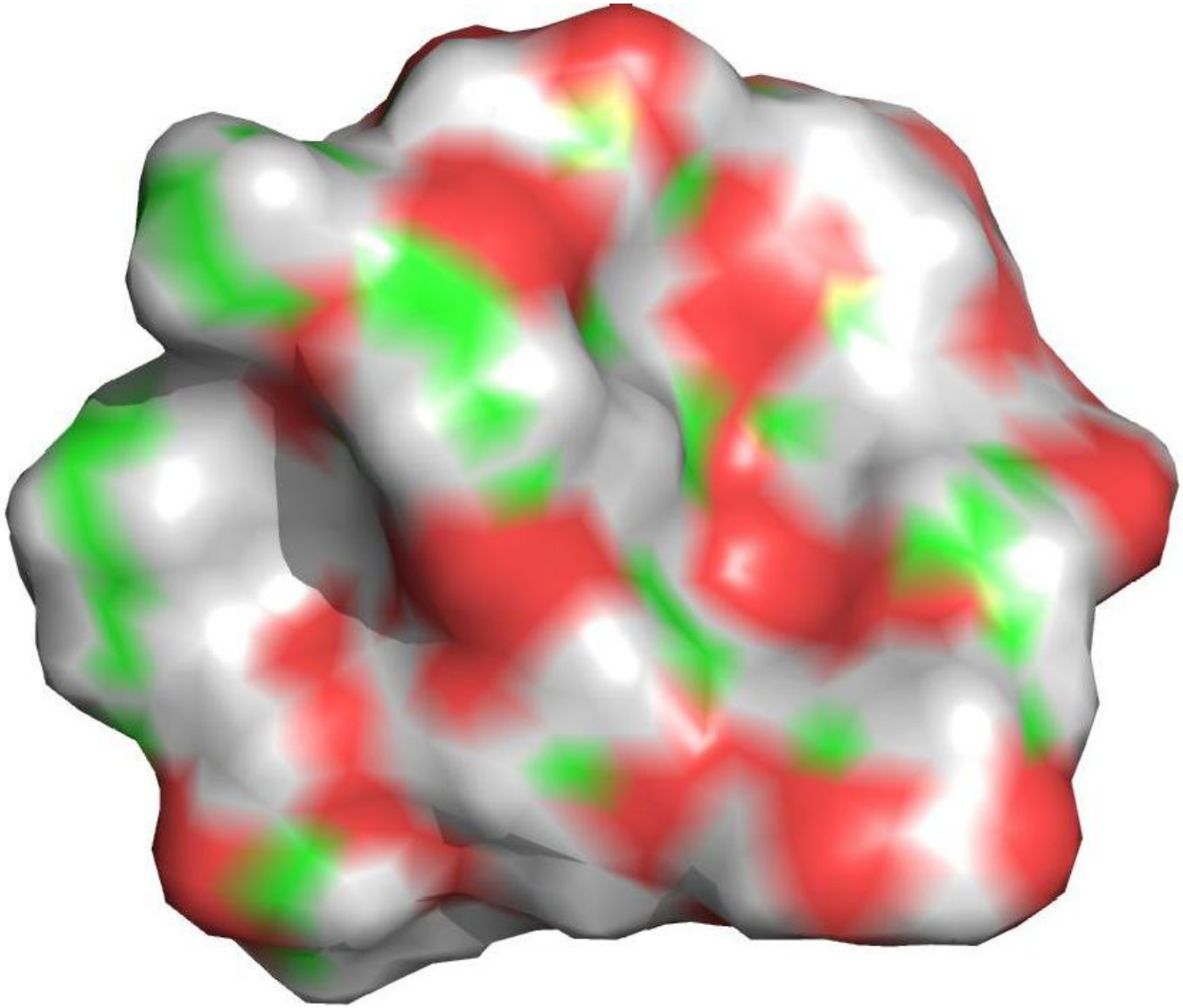

- Supplementary Figure 42 | The minimized 3D structure surface generated by PyMol 1.4 for the major glycoside, rhododendrosaponin III, red represents oxygen while green and grey represent carbon and hydrogen.

HCV activity for the Rhododendrosaponins **I-III**

- Rhododendrosaponins **I-III** were evaluated at six different concentrations for anti-HCV activity and end point determination in Huh-7 replicon Cells. Huh-7 B cells containing HCV genotype 1 replicon RNA were seeded in a 96-well plate at 3,000 cells/well and the compounds were added in dose response at 10, 3, 1, 0.3, 0.1, and 0.03 µg/mL in triplicate immediately after seeding. Following five days incubation (37 °C, 5% CO_2), total cellular RNA was isolated using the Manual Perfect Pure RNA 96 Cell Vac kit from 5 prime. Replicon RNA and an internal Control (TaqMan rRNA control reagent, Applied Biosystems) were amplified in a single step multiple Real Time RT-PCR assay.

- Table 3 | Anti-HCV activity of rhododendrosaponins I-III in Huh-7 replicon cells

Sample Code	Concentration μg/mL	ΔCt HCV	ΔCt rRNA	% Inhibition		EC_{50} μg/mL	EC_{90} μg/mL	CC_{50} μg/mL
				HCV	rRNA			
RS-446	0.3	0.49	0.01	28.89	0.69	0.6	2.3	>2.6
	0.8	1.53	-0.57	65.18	-47.93			
	2.6	4.28	-0.63	94.79	-54.19			
Rhododendrosaponin I	0.03	-0.66	-1.10	-57.78	-113.35	0.2	0.6	7.0
	0.1	-0.22	-0.89	-16.69	-85.39			
	0.3	2.60	-0.44	83.37	-35.22			
	1.0	5.35	-0.85	97.51	-79.51			
	3.0	7.08	-0.21	99.25	-15.35			
	10.0	7.04	6.04	99.23	98.46			
Rhododendrosaponin II	0.03	-0.07	-0.23	-5.20	-16.96	0.2	0.9	7.4
	0.1	-0.08	-0.99	-5.68	-98.19			
	0.3	1.84	-1.18	71.89	-126.52			
	1.0	3.67	-0.97	92.10	-95.02			
	3.0	7.44	0.15	99.41	10.05			
	10.0	7.07	1.96	99.24	74.16			
Rhododendrosaponin III	0.03	-0.63	-1.81	-54.19	-249.27	0.2	0.3	5.3
	0.1	-0.42	-0.98	-33.67	-96.38			
	0.3	3.95	0.59	93.49	33.40			
	1.0	5.36	-0.75	97.53	-67.91			
	3.0	6.88	0.44	99.14	26.05			
	10.0	7.50	6.27	99.44	98.69			

- The antiviral effectiveness of the compounds was calculated by subtracting the threshold RT-PCR cycle of the test compound from the threshold RT-PCR cycle of the non-drug control (ΔCtHCV). A ΔCt of 3.3 equals a 1-log reduction (equal to 90% less starting material) in replicon RNA levels. The cytotoxicity of the compounds was also calculated by using the ΔCt rRNA values. RS-446 (2′-C-Me-C) , was used as the control. To determine EC_{50} and IC_{50} values, ΔCt values were first converted into fractions of starting material and then were used to calculate the percent inhibition. The activity profile clearly revealed significant potency for these metabolites comparable to the recently approved drug Telaprevir (EC_{50} 0.1-0.2 µg/mL) and a therapeutic window warranted to inspire further investigations.

Mass Spectrum Molecular Formula Report

Analysis Info

Analysis Name	J:\MKNa\Na\N77951-6-16-3-4_5_01_11741.d	Acquisition Date	10/4/2007 7:35:13 PM
Method	LCMS-rutin-pos.m	Operator	Administrator
Sample Name	N77951-6-16-3-4	Instrument	micrOTOF 93
Comment			

Acquisition Parameter

Source Type	ESI	Ion Polarity	Positive	Set Corrector Fill	52 V
Scan Range	n/a	Capillary Exit	80.0 V	Set Pulsar Pull	402 V
Scan Begin	50 m/z	Hexapole RF	200.0 V	Set Pulsar Push	402 V
Scan End	3000 m/z	Skimmer 1	50.0 V	Set Reflector	1305 V
		Hexapole 1	21.9 V	Set Flight Tube	9000 V
				Set Detector TOF	2150 V

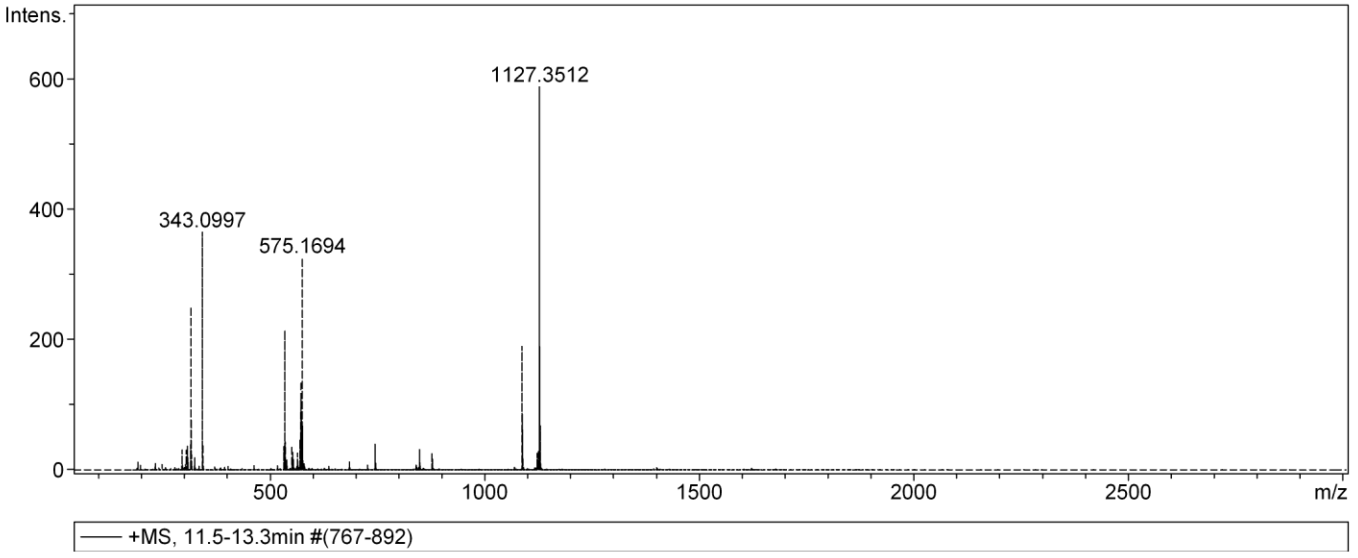

Sum Formula	Sigma	m/z	Err [ppm]	Mean Err [ppm]	rdb	N Rule	e^-
C 26 H 32 Na 1 O 13	0.15	575.1735	7.07	6.98	10.50	ok	even

- Supplementary Figure 43 | LC- HRESIMS Spectrum of Compound IV

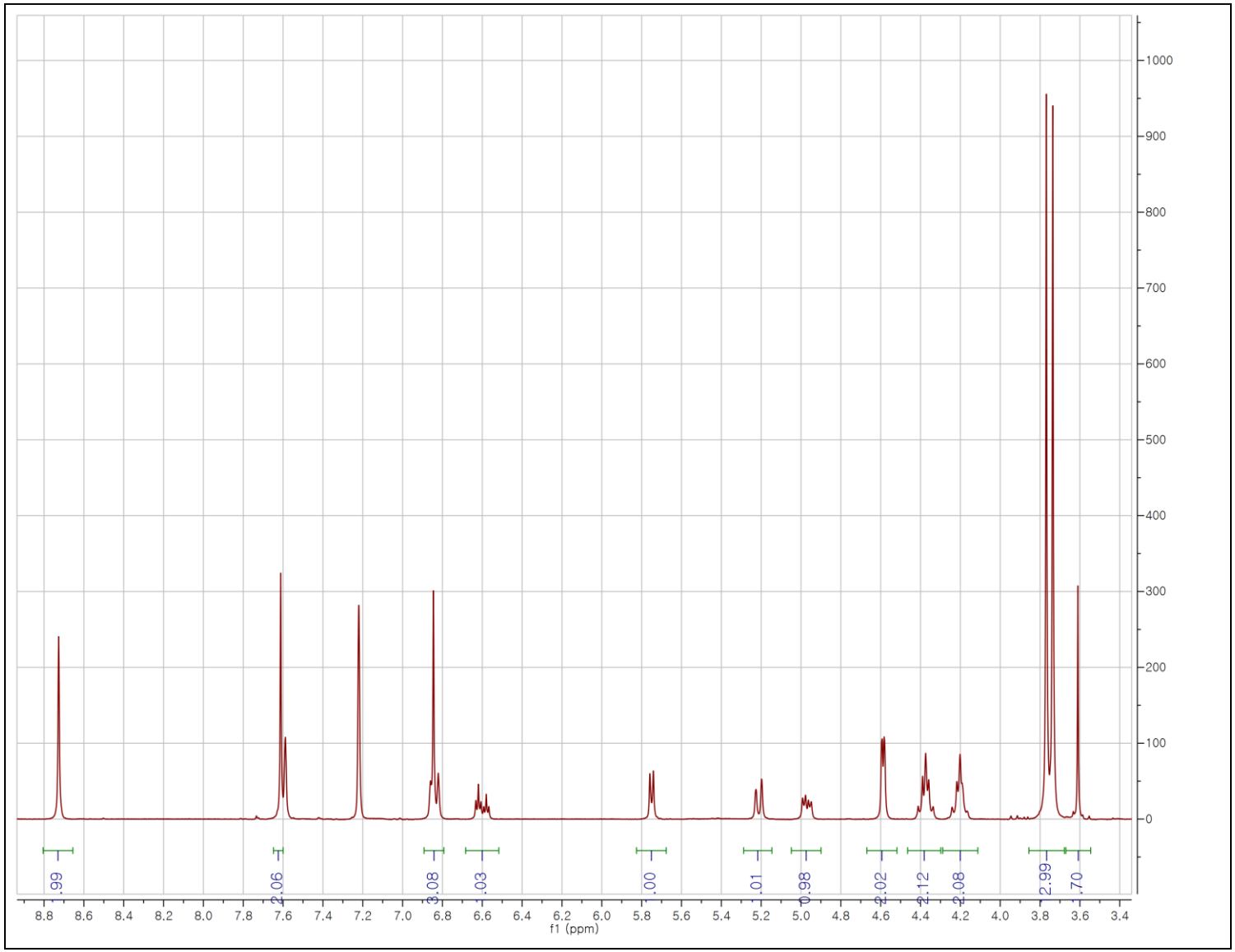

- Supplementary Figure 44 | ^{1}H NMR Spectrum of Compound IV in Pyridine-d_5 (400 MHz)

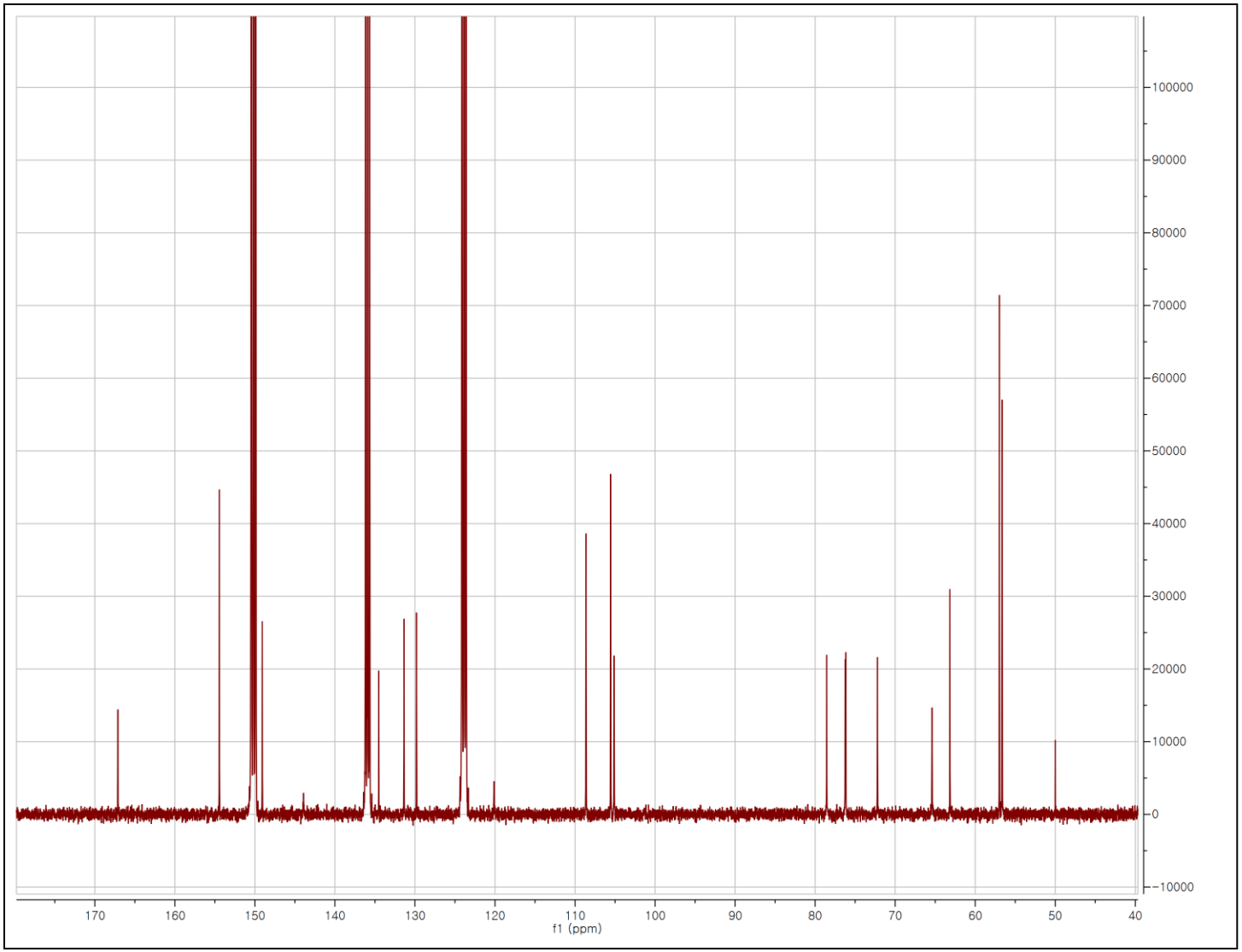

- Supplementary Figure 45 | ^{13}C NMR Spectrum of Compound IV in Pyridine-d_5 (100 MHz)

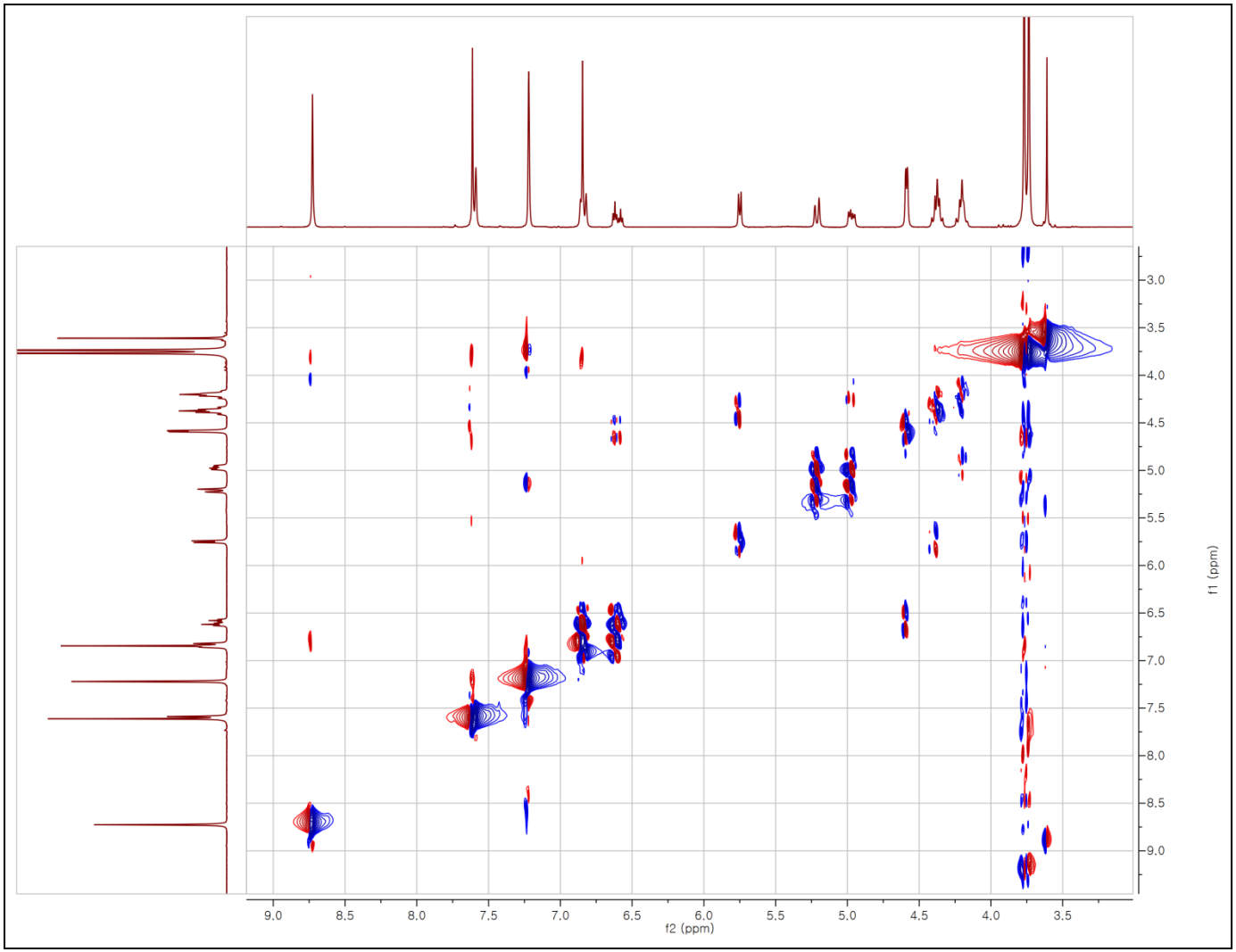

- Supplementary Figure 46 | COSY Spectrum of Compound IV in Pyridine-d_5 (400 MHz)

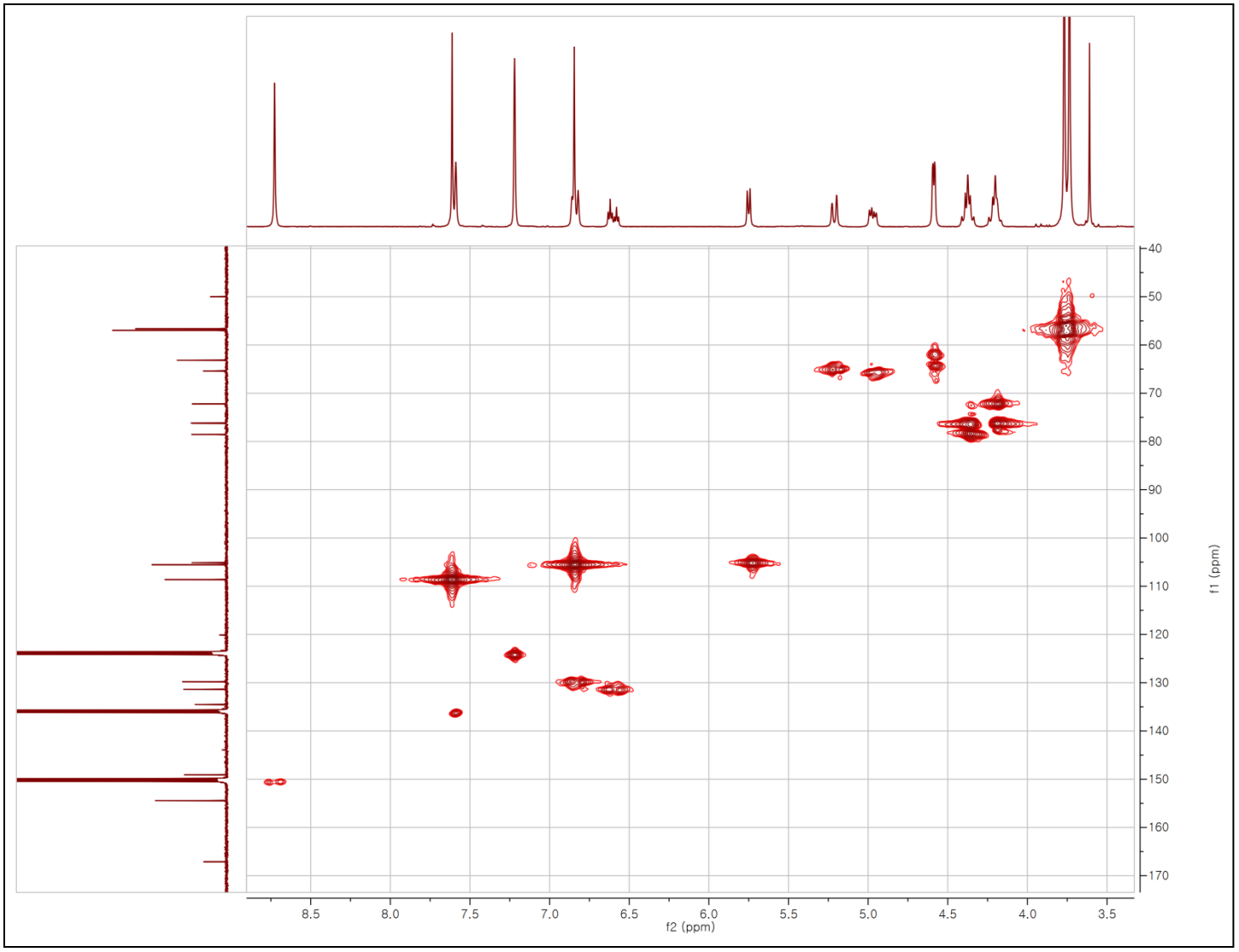

- Supplementary Figure 47 | HMQC Spectrum of Compound IV in Pyridine-d_5 (400 MHz)

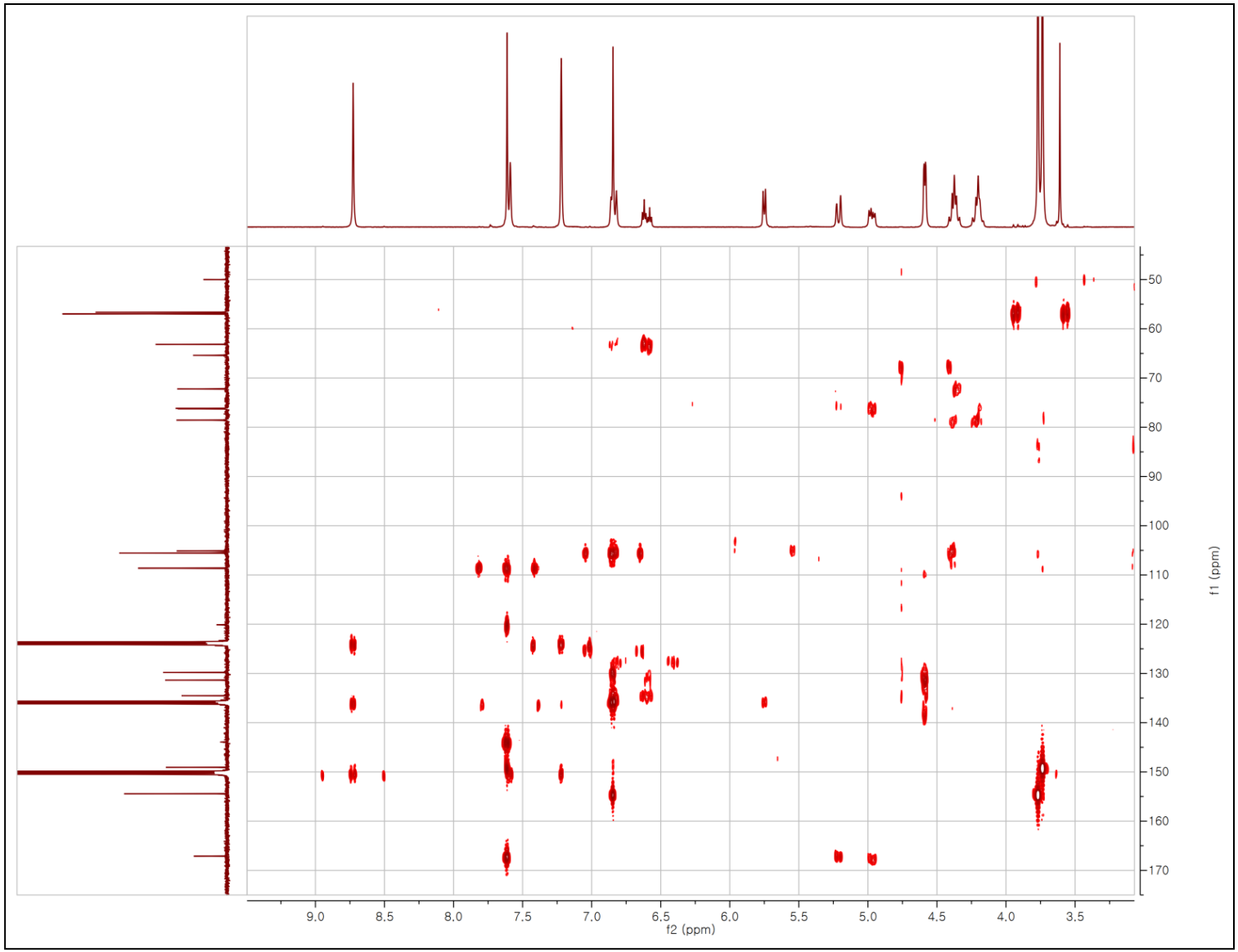

- Supplementary Figure 48 | HMBC Spectrum of Compound IV in Pyridine-d_5 (400 MHz)

Mass Spectrum Molecular Formula Report

Analysis Info

Analysis Name	J:\MKNa\Na\N77951-6-16-5(1)_71_01_11541.d	Acquisition Date	9/25/2007 5:23:04 AM
Method	LCMS-rutin-pos.m	Operator	Administrator
Sample Name	N77951-6-16-5(1)	Instrument	micrOTOF 93
Comment			

Acquisition Parameter

Source Type	ESI	Ion Polarity	Positive	Set Corrector Fill	52 V
Scan Range	n/a	Capillary Exit	80.0 V	Set Pulsar Pull	402 V
Scan Begin	50 m/z	Hexapole RF	200.0 V	Set Pulsar Push	402 V
Scan End	3000 m/z	Skimmer 1	50.0 V	Set Reflector	1305 V
		Hexapole 1	21.9 V	Set Flight Tube	9000 V
				Set Detector TOF	2150 V

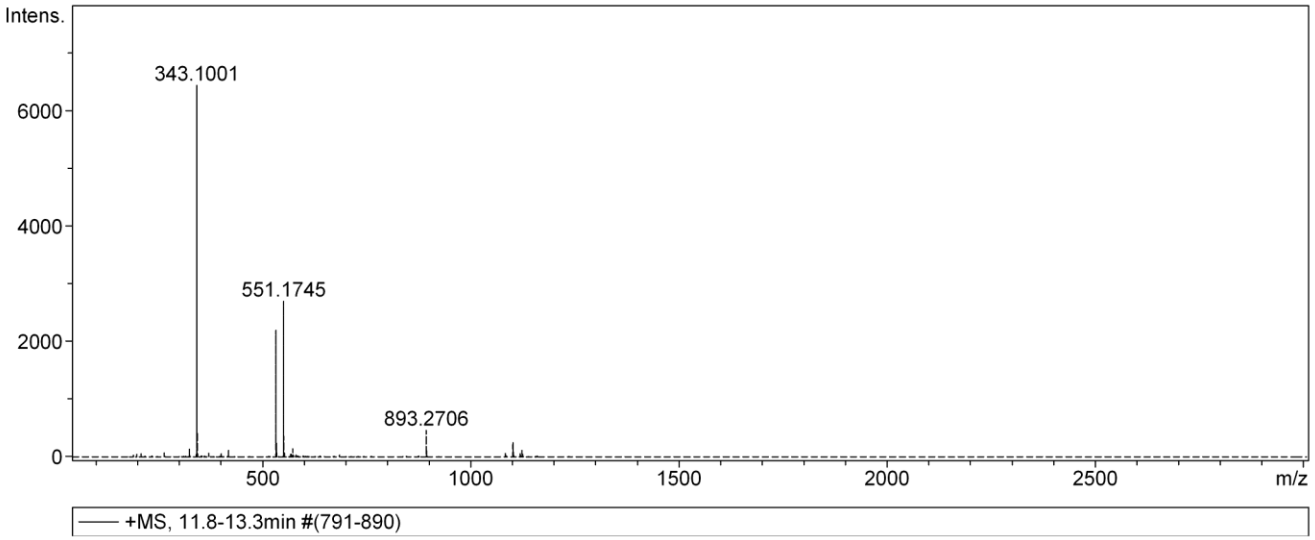

Sum Formula	Sigma	m/z	Err [ppm]	Mean Err [ppm]	rdb	N Rule	e⁻
C 26 H 31 O 13	0.09	551.1759	2.61	2.07	11.50	ok	even

- Supplementary Figure 49 | LC- HRESIMS Spectrum of Compound V

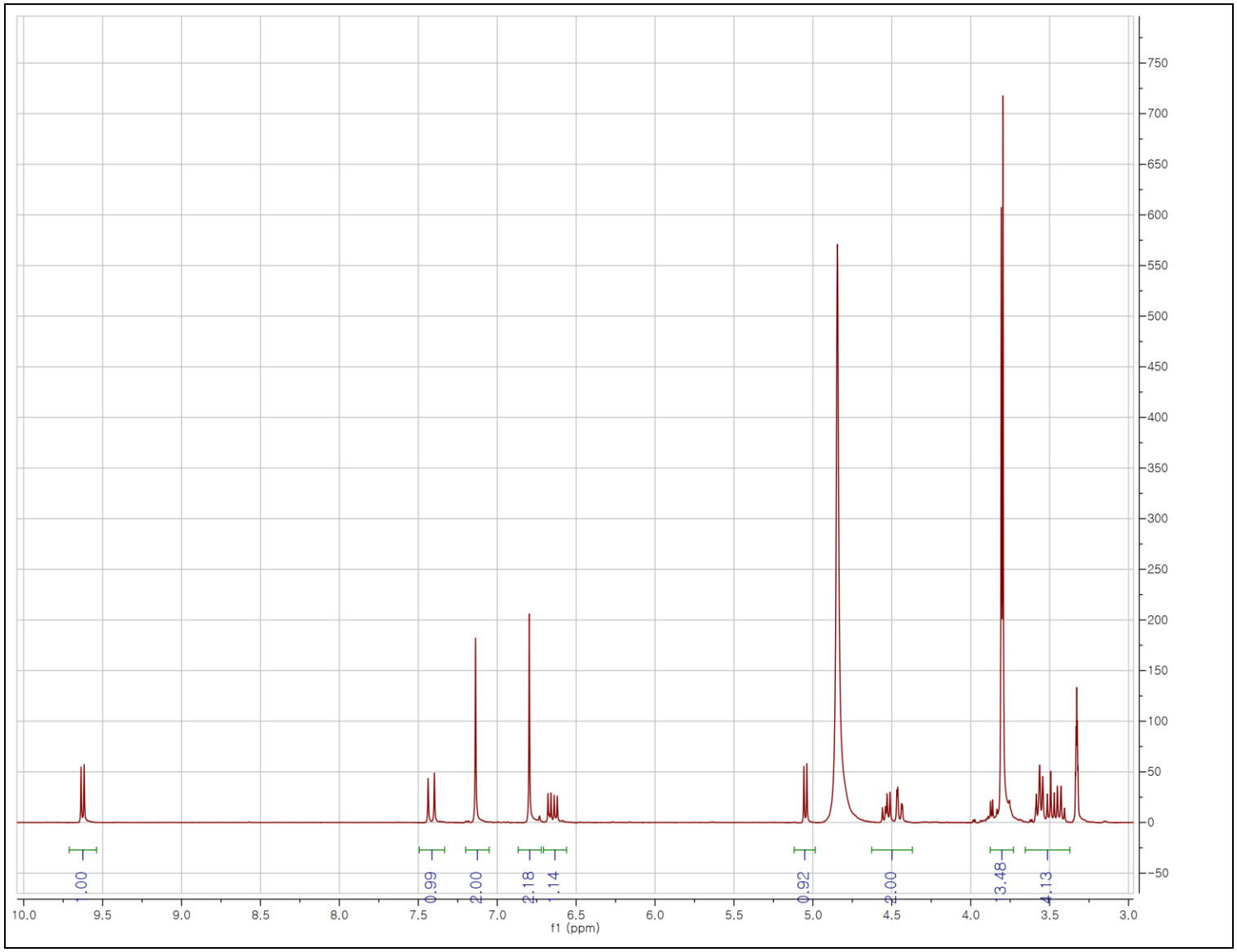

- Supplementary Figure 50 | ^{1}H NMR Spectrum of Compound V in Methanol-d_4 (400 MHz)

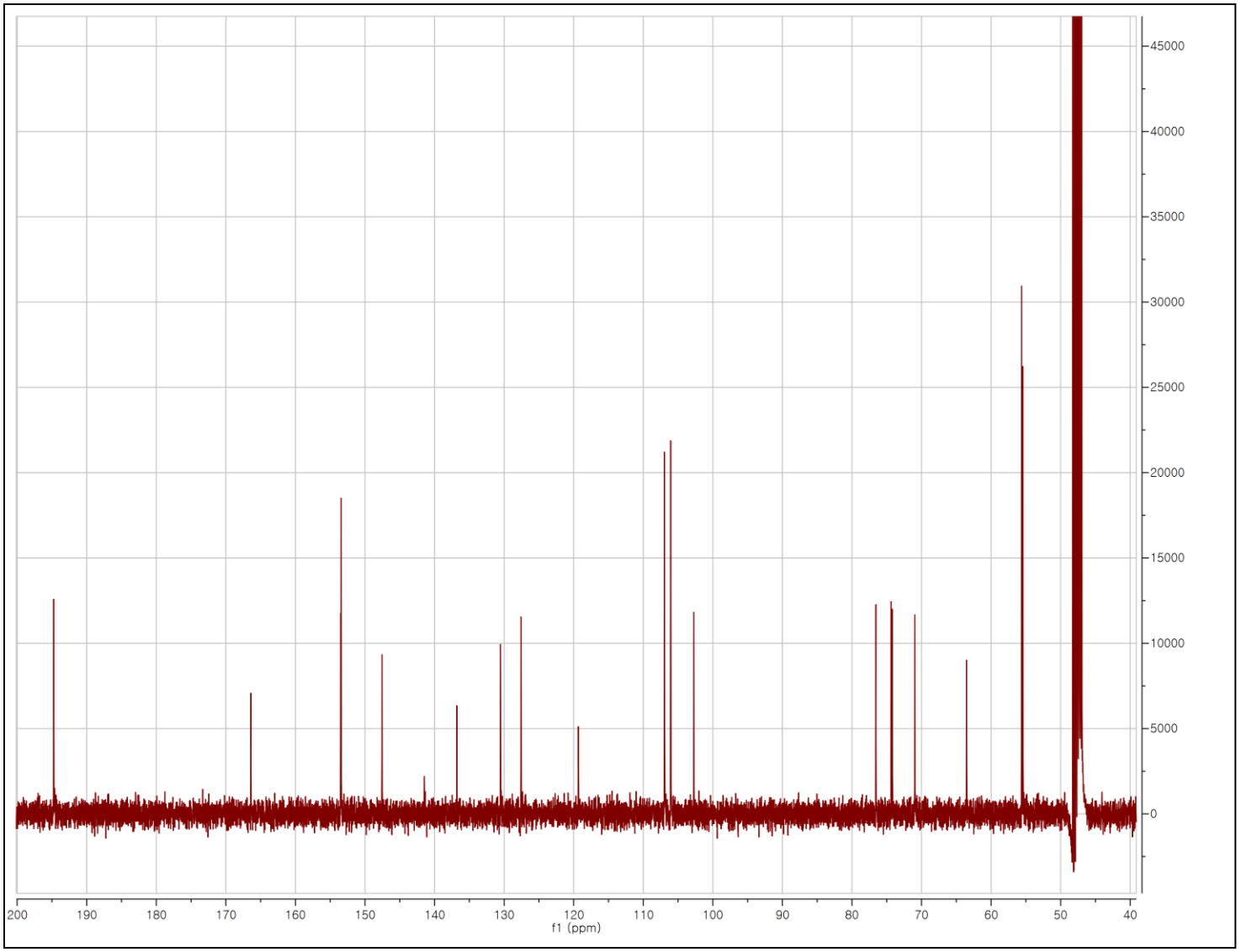

- Supplementary Figure 51 | ^{13}C NMR Spectrum of Compound V in Methanol-d_4 (100 MHz)

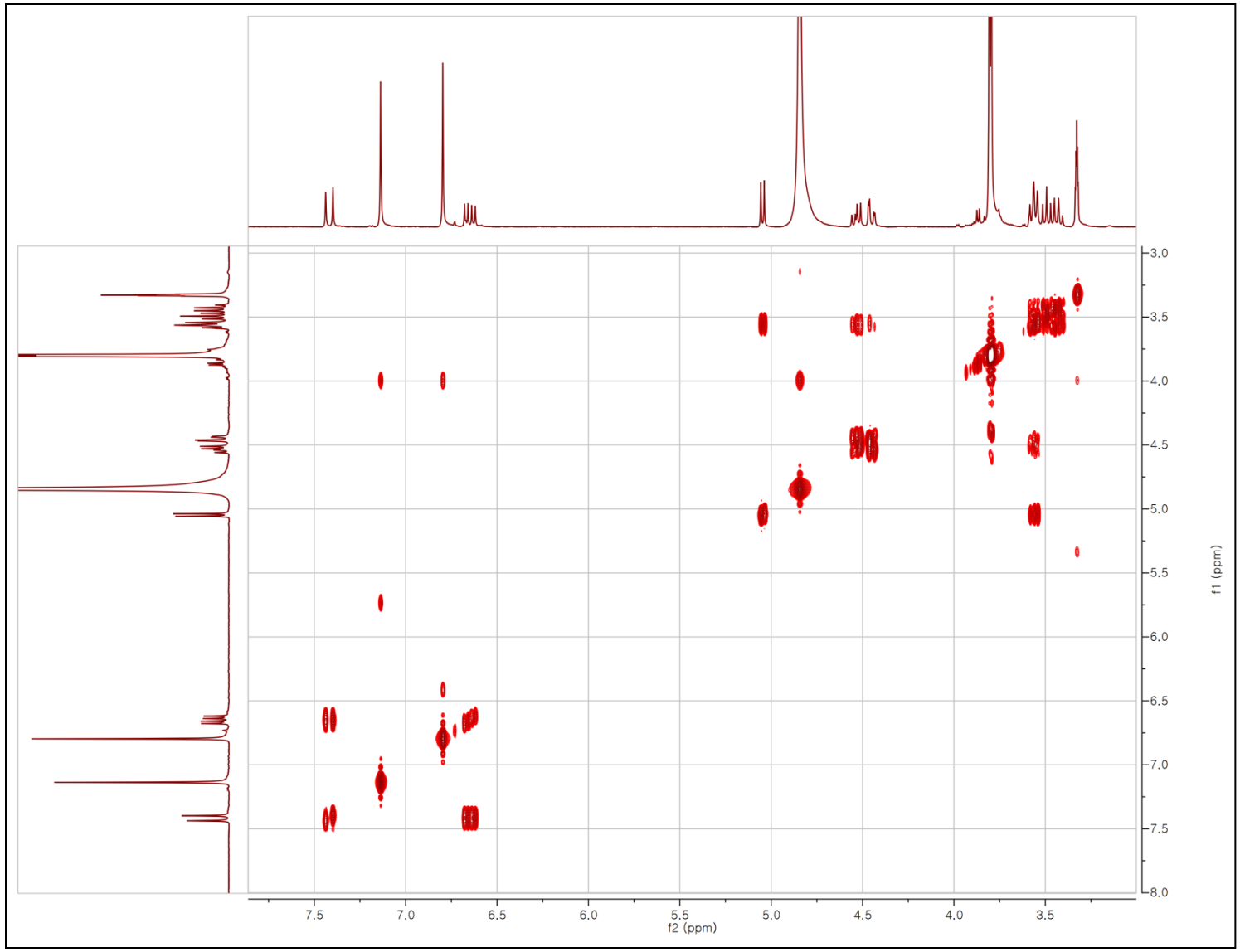

- Supplementary Figure 52 | COSY Spectrum of Compound V in Methanol-d_4 (400 MHz)

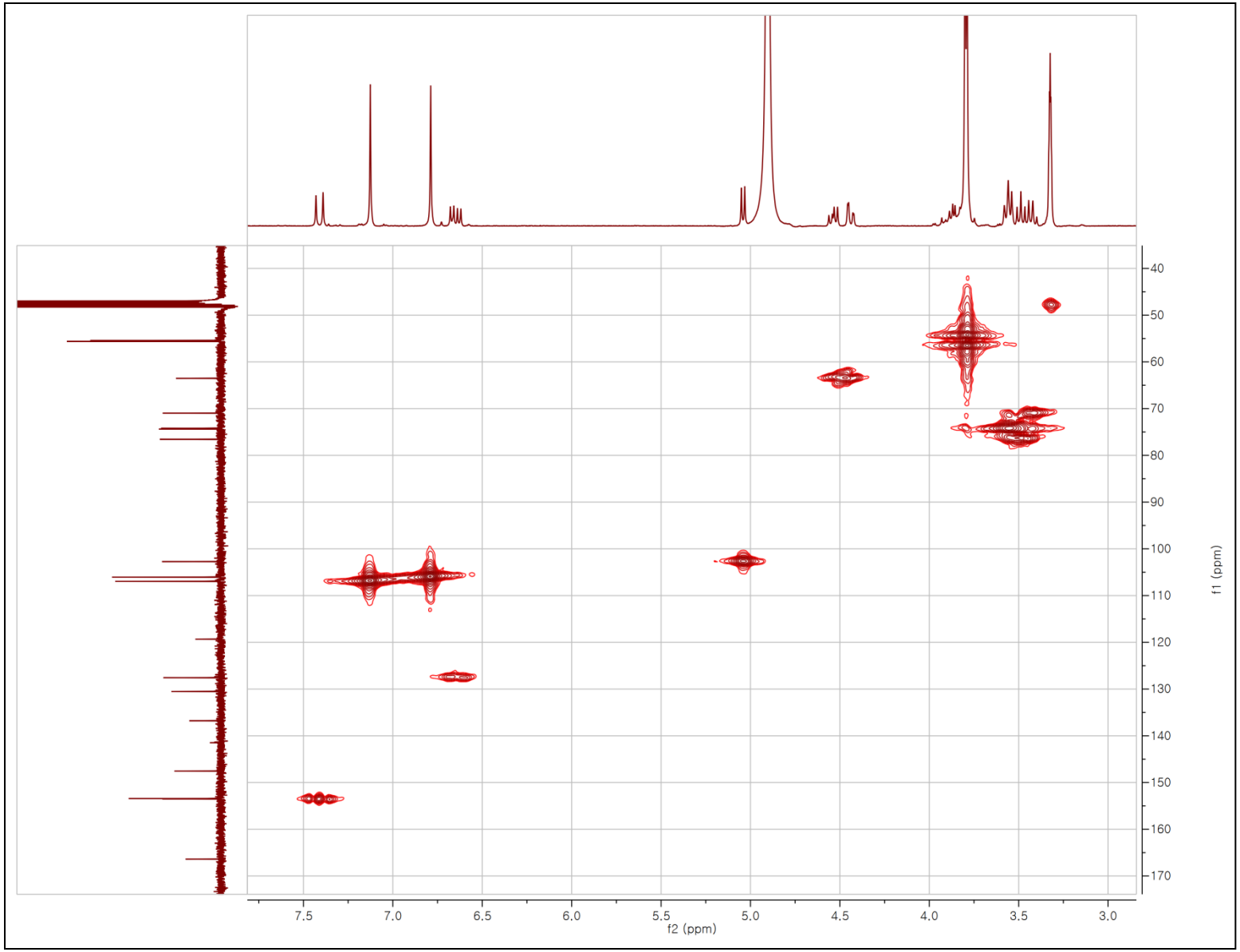

- Supplementary Figure 53 | HMQC Spectrum of Compound V in Methanol-d_4 (400 MHz)

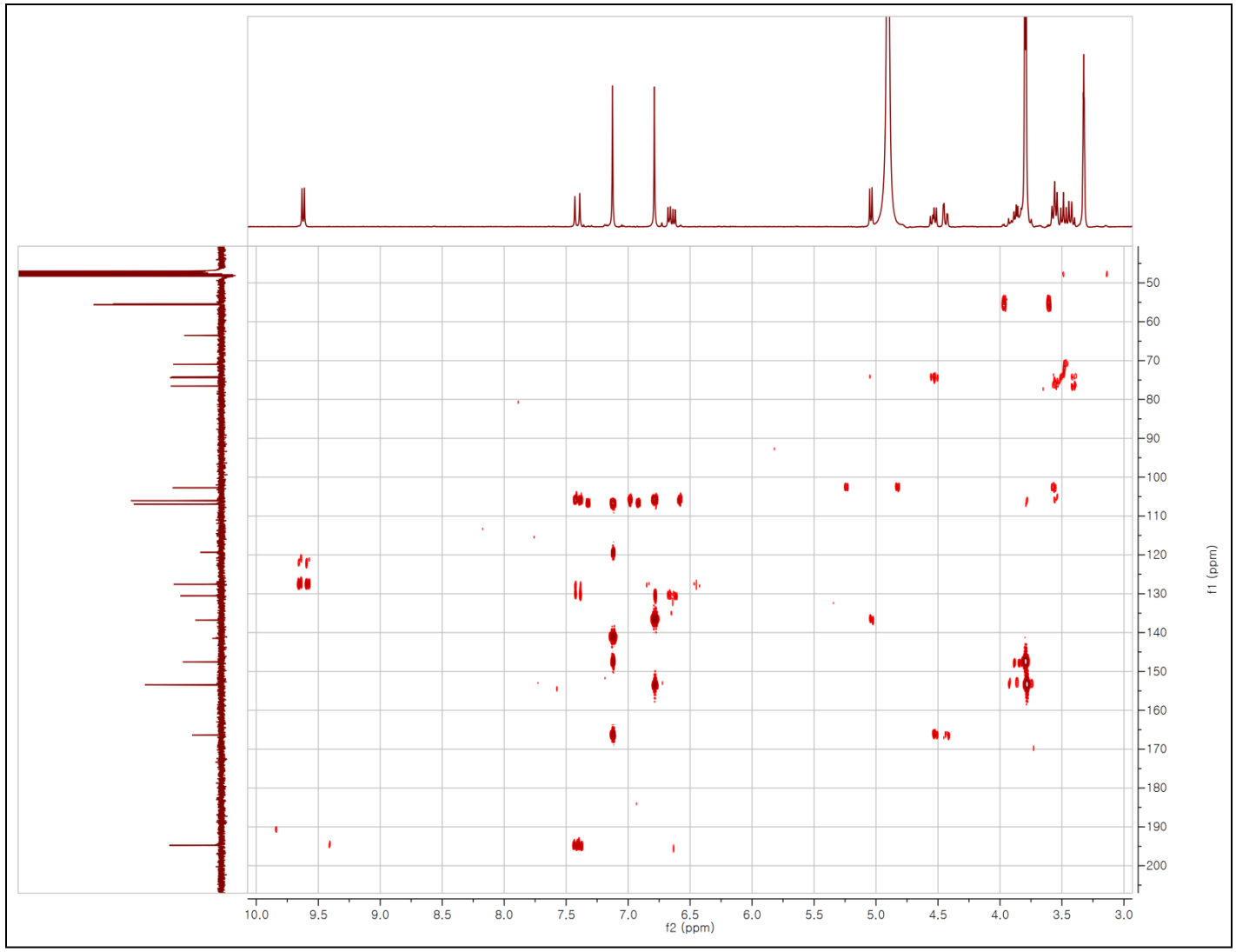

- Supplementary Figure 54 | HMBC Spectrum of Compound V in Methanol-d_4 (400 MHz)

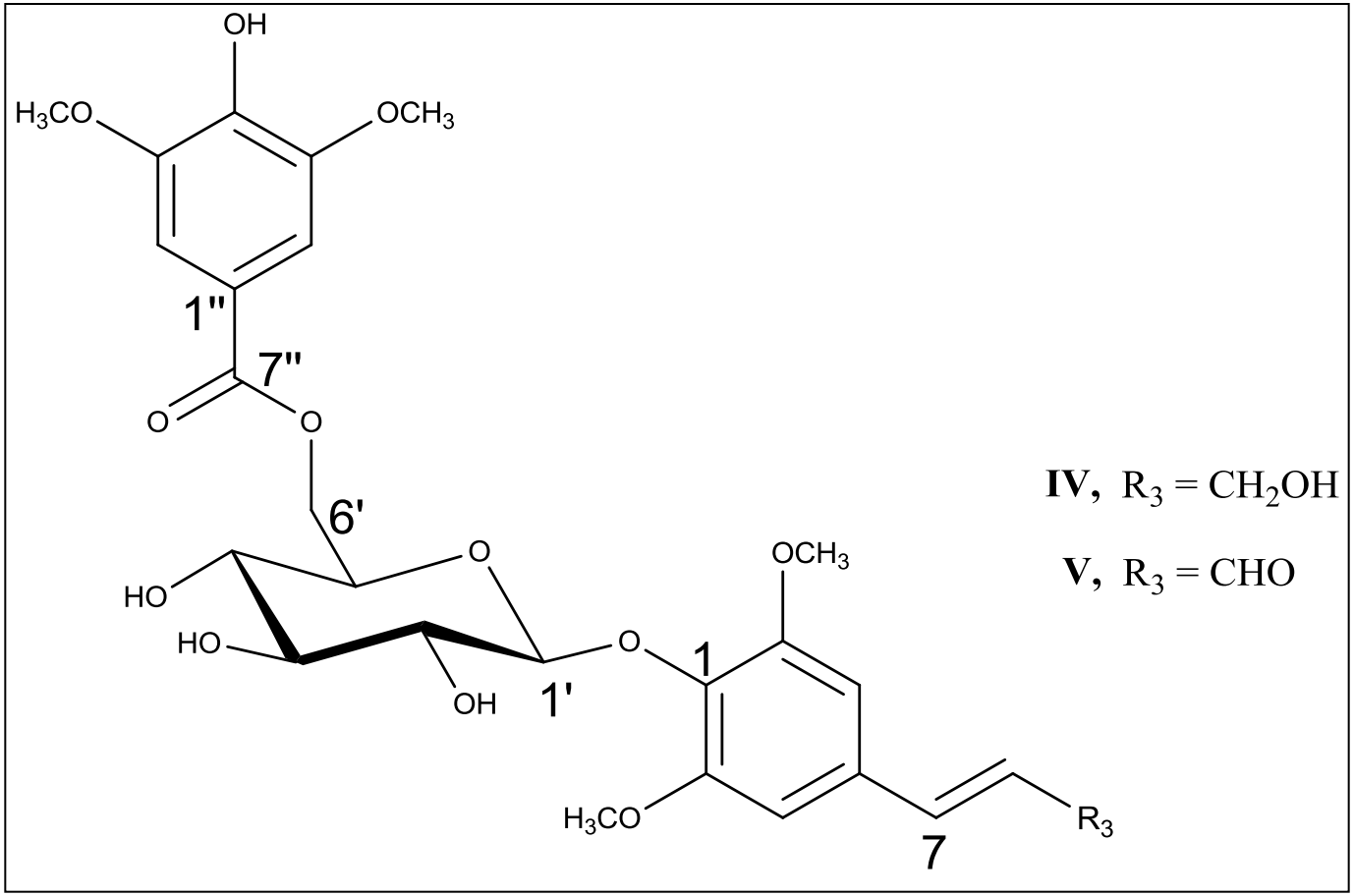

- Supplementary Figure 55 | The proposed structures of IV and V

- Table 3 ㅣ Docking scores of compounds IV and V

Protein / Ligand	1T48	1T49	1T4J
(A) 350 µM	-11.36 (1.07)	-8.42 (1.18)	-7.86 (1.57)
(B) 22 µM	-14.47 (1.02)	-10.65 (1.14)	-9.96 (1.08)
(C) 8 µM	-14.52 (1.28)	-10.92 (0.99)	-9.73 (1.23)
(IV) 81.0 µM	-11.45	-9.13	-9.09
(V) 25.9 µM	-10.46	-8.96	-8.55

Compounds A, B, and C are co-crystalized ligands with 1T48, 1T49 and 1T4J, respectively. Numbers in the parentheses next to docking scores indicate the RMS deviation values. Numbers next to ligand entries show their PTP1B inhibition potency.

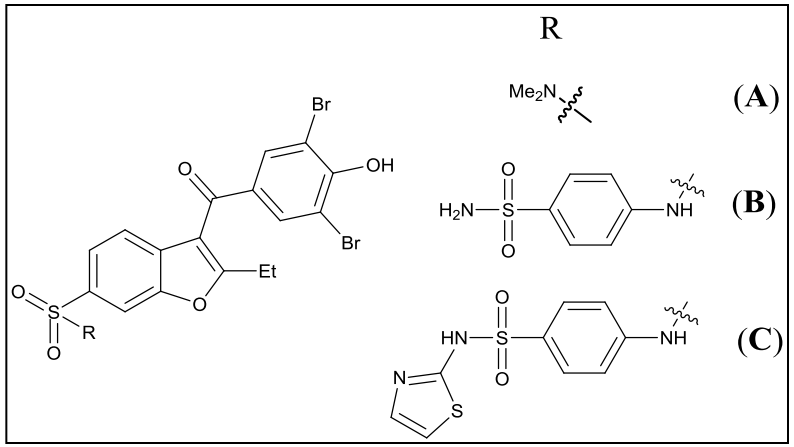

- Supplementary Figure 56 ㅣ The structures of legends A, B, and C

Additional References

1- Reddy, B. A. Digitalis therapy in patients with congestive heart failure. *Int. J. Pharmaceut. Sci. Rev. and Res.* **2010**, *3*, 90-95.

2- Heinrich, M., Lee, T. H. Galanthamine from snowdrop--the development of a modern drug against Alzheimer's disease from local Caucasian knowledge. *J. Ethnopharmacol*. **2004**, *92*, 147-62.

3- Rates, S. M. K. Plants as source of drugs. *Toxicon* **2001**, *39*, 603-613.

4- Ajikumar, P. K., Xiao, W. H., Tyo, K. E. J., Wang, Y., Simeon, F., Leonard, E., Mucha, O., Phon, T. H., Pfeifer, B., Stephanopoulos, G. Isoprenoid pathway optimization for Taxol precursor overproduction in *Escherichia coli*. *Science* **2010**, *330*, 70 – 74.

5- http://www.hepatitis-central.com/; established since 1994, has been dedicated to providing in-depth information for Hepatitis C patients and their families).

6- Stuyver, L. J., Whitaker, T., McBrayer, T. R., Hernandez-Santiago, B. I., Lostia, S., Tharnish, P. M., Ramesh, M., Chu, C. K., Jordan, R., Shi, J., Rachakonda, S., Watanabe, K. A., Otto, M. J., Schinazi, R. F. Ribonucleoside analogue that blocks replication of bovine viral diarrhea and hepatitis C viruses in culture. *Antimicrob. Agents Chemother.* **2003**, *47*, 244-254.

7- Schrödinger Suite 2011 Induced Fit Docking protocol; Glide version 5.7, Schrödinger, LLC, New York, NY, 2011; Prime version 3.0, Schrödinger, LLC, New York, NY, 2011.

8- Schrödinger Suite 2011 Protein Preparation Wizard; Epik version 2.2, Schrödinger, LLC, New York, NY, 2011; Impact version 5.7, Schrödinger, LLC, New York, NY, 2011; Prime version 3.0, Schrödinger, LLC, New York, NY, 2011.

9- Cui, L. et al. Protein tyrosine phosphatase 1B inhibitors from Morus root bark. *Bioorganic & Medicinal Chemistry Letters* **2006**, *16*, 1426-1429.

10- Na, M., Jang, J., Njamen, D., Mbafor, J. T., Fomum, Z. T., Kim, B. Y., Oh, W. K., Ahn, J. S. Protein tyrosine phosphatase-1B inhibitory activity of isoprenylated flavonoids isolated from Erythrina mildbraedii. *J. Nat. Prod*. **2006**, 69, 1572-1576.